REGULATION OF NICHE CELL PLASTICITY

IN THE *DROSOPHILA* TESTIS

by
Leah Greenspan

A dissertation submitted to Johns Hopkins University in conformity with the requirements for the degree of Doctor of Philosophy

Baltimore, Maryland
July, 2018

ABSTRACT

Adult stem cells sustain tissue regeneration by responding to signals from their surrounding microenvironment or niche. Maintenance of stem cells and their niches is tightly regulated to prevent depletion or overgrowth of the stem cell pool. The *Drosophila* testis provides a uniquely accessible genetic system to study the regulation of niches *in vivo*. This niche consists of a cluster of quiescent somatic hub cells that signal to the attached germline and somatic cyst stem cells (CySCs). In several mammalian tissues, injury can cause non-dividing cells to re-enter the cell cycle and repair the tissue, but the mechanisms are not well understood. Recently, we have found that *Drosophila* testis hub cells respond to injury in a similar way. These quiescent cells start to proliferate upon genetic CySC ablation, followed by a change in cell identity. A subset of hub cells convert to somatic stem cells, thus replenishing the lost population. With age, however, these testes acquire ectopic hubs with active stem cells, leading to severe tissue disruption over time.

Here I show that the cell cycle inhibitor and tumor suppressor Retinoblastoma homolog Rbf is required in the hub cells of the *Drosophila* testis to prevent their proliferation and conversion to CySCs. Additionally, continued Rbf loss causes hub cell clusters to split apart and form ectopic hubs, similar to those seen upon CySC ablation. These results suggest that cell cycle inhibitors are normally needed in terminally differentiated niche cells to ensure their proper maintenance. However, how hub cell plasticity is triggered upon injury to the testis still remained unknown. By activating or knocking down various signaling pathways in the hub I discovered that the EGF/MAPK pathway is sufficient to

trigger hub cell proliferation and cell fate conversion. I further show that this pathway becomes activated in the hub upon CySC ablation, and is necessary to replenish lost somatic cyst stem cells after tissue damage. Altogether, this body of work demonstrates that the precise modulation of signals within niche cells, not just the stem cells they support, is necessary to drive tissue regeneration without disease progression.

Thesis Advisor: Erika Matunis, PhD

Thesis Reader: Daniela Drummond-Barbosa, PhD

ACKNOWLEDGMENTS

I would like to start off by thanking my mentor Dr. Erika Matunis. Her scientific expertise and continuous guidance have been instrumental in my success as a graduate student. She has always encouraged me to pursue my own experimental ideas, while providing keen insight when necessary. She has taught to become a rigorous scientist and also an excellent communicator. I am truly appreciative for all the support she has given me over the years and will continue to give me in the future.

I would next like to thank the members of my thesis committee – Dr. Daniela Drummond-Barbosa, Dr. Geraldine Seydoux, and Dr. Andrew Ewald. They all have contributed valuable input into the direction of my research, and have provided advice and support towards my future career goals.

I would like to thank the Matunis lab members for fostering a setting of constant scientific discussion where we could help and learn from each other. In particular I would like to thank Dr. Margaret de Cuevas for her willingness to always lend a hand whether it is editing a paper, thinking through an idea, or helping with an experiment. The support and friendship I received from the Matunis lab members has made graduate school a truly rewarding experience.

In addition, I am grateful to the Biochemistry, Cellular and Molecular Biology (BCMB) program at Johns Hopkins School of Medicine for helping me become a well-rounded

scientist that can approach complex problems from different perspectives. In addition to the course work, this program has provided me with outstanding support and resources.

I would like to thank the fly community for providing stocks and reagents, as well as funding sources that have allowed me to pursue my research.

Finally, I would like to thank my friends and family. The unconditional love and support I receive has helped me to push through the hard times and celebrate the successes. I am extremely grateful for their constant encouragement, which has allowed me to achieve this body of work.

TABLE OF CONTENTS

LIST OF FIGURES

LIST OF TABLES

CHAPTER 1

Genetics of gonadal stem cell renewal

This chapter is a modified version of the manuscript Greenspan LJ, de Cuevas M, Matunis E. (2015). Genetics of Gonadal Stem Cell Renewal. *Annu Rev Cell Dev Biol*. 31: 291-315. Response to Trauma section written by M. de Cuevas.

SUMMARY

Stem cells are necessary for the maintenance of many adult tissues. Signals within the stem cell microenvironment, or niche, regulate the self-renewal and differentiation capability of these cells. Mis-regulation of these signals through mutation or damage can lead to overgrowth or depletion of different stem cell pools. In this chapter we focus on the gonadal stem cell niches of the *Drosophila* testis and ovary, since both contain well-defined niches, as well as the mammalian testis, in which recent techniques have made this a more approachable stem cell system. We discuss the signals that regulate gonadal stem cells in their niches, how these signals decide between self-renewal and differentiation under homeostatic conditions, and how stress conditions, whether from mutations or damage, can cause changes in cell fate and drive stem cell competition.

INTRODUCTION

Stem cells are undifferentiated cells that are important for tissue homeostasis and regeneration through the replacement of lost or damaged cells. Stem cells are capable of producing two types of daughter cells: those that remain stem cells and those that differentiate into more specialized cell types. Maintenance of stem cells is regulated by intrinsic as well as extrinsic signals from the surrounding microenvironment, called the niche. Precise modulation of these signals is vital to ensure proper stem cell number and function. Misregulation of signals resulting from genetic mutations or tissue trauma can cause over- or underrepresentation of one stem cell type versus another, as well as inappropriate changes in cell fate. In this review we focus on gonadal stem cell niches, specifically those in the *Drosophila* testis and ovary and in the mouse testis, and discuss the signals that control the outcome of stem cell divisions under homeostatic conditions. We focus on two topics, stem cell competition and cell fate conversion, for which concepts emerging from studies on gonadal stem cell niches are likely to enhance our understanding of adult stem cells more generally. Understanding the coordination between niche signals, stress, and stem cell dynamics will provide key insight into the mechanisms that drive the progression of diseases such as cancer and allow the development of more effective treatments and preventive care.

GERMLINE STEM CELLS AND THEIR NICHES

The *Drosophila* Testis Niche

An adult *Drosophila* male contains a pair of testes, each composed of a blind-ended tubule with a single stem cell niche anchored to the apical end. The signaling center of

the niche is a cluster of 10--15 densely packed, terminally differentiated somatic cells called hub cells (Hardy et al., 1979). Two types of stem cells adhere to the hub: sperm-producing germline stem cells (GSCs) and somatic cyst stem cells (CySCs). Each GSC typically divides asymmetrically to produce a daughter GSC and a gonialblast, which is displaced from the hub and undergoes four transit amplifying divisions with incomplete cytokinesis, forming a cluster of 16 interconnected spermatogonia (**Figure 1.1A**). As differentiation proceeds, spermatogonia are displaced from the testis apex, maturing into spermatocytes that undergo meiotic divisions to produce 64 haploid spermatids. After spermatid individualization, the mature sperm are released from the testis and stored in the seminal vesicle. For more comprehensive reviews of the testis niche, see de Cuevas & Matunis (2011) and Matunis et al. (2012).

Somatic CySCs contact the hub via long, thin cytoplasmic extensions. Approximately two CySCs fully envelop each GSC, such that direct GSC-GSC contact does not occur (Hardy et al., 1979). Lineage tracing has revealed that CySCs divide asymmetrically to produce differentiating daughters called cyst cells (Gönczy and DiNardo, 1996). Two cyst cells encase each gonialblast, after which they no longer divide but instead elongate to accommodate the dividing spermatogonia (**Figure 1.1A**) (de Cuevas and Matunis, 2011). The cyst cells continue to differentiate throughout spermatogenesis and are ultimately engulfed by epithelial cells at the base of the testis upon spermatid individualization (Fuller, 1993). In addition to serving as a source of somatic support cells, CySCs are also an important part of the GSC niche, as described below. For a comprehensive review of the CySC lineage, see Zoller & Schulz (2012).

Hub cells were first implicated as a source of local signals that regulate stem cell maintenance when the Janus kinase--Signal transducer and activator of transcription (JAK-STAT) pathway was shown to promote self-renewal of both GSCs and CySCs (Kiger et al., 2001; Tulina and Matunis, 2001) (**Figure 1.1B**). However, the downstream targets of this pathway differ in the two cell types, and the effects may also be lineage specific, as STAT activation is thought to promote self-renewal in CySCs and adhesion to the hub in GSCs (Flaherty et al., 2010; Leatherman and DiNardo, 2008; Leatherman and DiNardo, 2010). Hedgehog signaling is also important for promoting the self-renewal of CySCs but not GSCs (Amoyel et al., 2013; Michel et al., 2012; Zhang et al., 2013). This pathway is thought to act in parallel to JAK-STAT signaling to mediate self-renewal, although some of the downstream targets of the two pathways may overlap (Amoyel et al., 2013; Zhang et al., 2013). A third signaling pathway that promotes GSC self-renewal is the Bone Morphogenetic Protein (BMP) pathway. Activation of BMP signaling in GSCs silences transcription of the gene that encodes the differentiation factor Bag-of-marbles (Bam) (Kawase, 2004; Michel et al., 2011). Daughter cells that are displaced from the niche are thought to receive insufficient BMP signaling to repress *bam* expression, leading to *bam* upregulation, which enables them to differentiate properly (Kawase, 2004). In addition to *bam* expression, germ cell differentiation requires signals that result from Epidermal Growth Factor (EGF) signaling within the CySC lineage; without these cyst cell-derived signals, germ cells fail to differentiate (Hudson et al., 2013; Kiger et al., 2000; Lim and Fuller, 2012; Matunis et al., 1997; Schulz et al., 2002; Tran et al., 2000). Understanding how multiple signals are integrated to regulate stem cell

behavior is a major challenge in most stem cell-based tissues and is best approached via genetics in model organisms such as *Drosophila*.

The *Drosophila* Ovarian Niche

In most female mammals, oocytes form only before birth, during fetal development. GSCs are undetectable in adult mouse ovaries, and single-cell lineage tracing has shown unequivocally that the pool of primordial follicles is maintained without input from GSCs (Hanna and Hennebold, 2014; Lei and Spradling, 2013; Zhang et al., 2012). By contrast, the *Drosophila* ovary contains GSCs that remain active and support continuous egg production throughout adulthood. Each ovary is composed of one to two dozen ovarioles, which are the functional units of the ovary and contain chains of developing egg chambers at progressively older stages. The GSCs are located at the anterior tip of each ovariole, in the germarium, where they adhere to the stem cell niche, comprised of terminal filament, cap cells, and a subset of escort cells (**Figure 1.2A**). As in the testis, GSCs typically divide asymmetrically, producing a new GSC and a daughter cystoblast that is displaced from the niche and differentiates. Each cystoblast undergoes four mitotic divisions with incomplete cytokinesis to produce an interconnected 16-cell cyst; one cell within the cyst will traverse meiosis and become an oocyte, whereas the other 15 will become polyploid nurse cells that support oocyte growth (Huynh and St Johnston, 2000; Sahai-Hernandez et al., 2012). At the end of oogenesis, the nurse cells dump their cytoplasm into the oocyte and undergo apoptosis to produce a mature egg (Foley and Cooley, 1998; McCall and Steller, 1998).

As with spermatogenesis, oogenesis is sustained by the cooperative action of GSCs and somatic stem cells, which are called follicle stem cells (FSCs) in the ovary. FSCs produce daughter follicle cells that form a columnar epithelial layer of cells surrounding each germline cyst; the resulting egg chamber buds from the germarium and continues to grow as it matures (**Figure 1.2A**). In contrast to the testis, FSCs reside in a distinct location in the germarium and are not adjacent to GSCs. In addition, their progeny are not quiescent but continue to divide as the cyst grows. For more comprehensive reviews of ovarian stem cells, see Eliazer & Buszczak (2011), Spradling et al. (2011), Sahai-Hernandez et al. (2012), and Slaidina & Lehmann (2014).

The signals that maintain stem cells in the ovary are similar to those that act in the testis (**Figure 1.2B**). In ovarian GSCs, BMP signaling results in transcriptional repression of *bam* (Chen and McKearin, 2003; Song, 2004); as cystoblasts do not receive enough ligand, they begin the differentiation process (Li et al., 2009). JAK-STAT signaling is not directly required in GSCs, but its activation in anterior support cells leads to the production of the BMP ligand Decapentaplegic (Dpp) (Lopez-Onieva et al., 2008; Wang et al., 2008). Additional factors important for GSC self-renewal were recently identified in a large-scale RNA interference (RNAi) screen, and future studies should reveal how these factors are regulated by niche signaling to maintain GSC cell fate (Yan et al., 2014). Although FSCs reside in a distinct environment from the GSCs, the same core signaling pathways regulate both stem cell lineages. Hedgehog, Wingless, BMP, and Epidermal growth factor (EGF) signaling are all required for FSC self-renewal, and the ligands for these signaling pathways are thought to originate from the GSC niche or from adjacent

escort cells (Castanieto et al., 2014; Forbes et al., 1996; Hartman et al., 2010; Kirilly et al., 2005; Song, 2003). Further research is needed to understand how these signaling pathways are coordinated and interact with the GSC niche. For a more in-depth understanding of the signaling pathways that maintain GSCs, see Eliazer & Buszczak (2011); for FSC self-renewal, see Sahai-Hernandez et al. (2012).

The Mammalian Testis Niche

Our understanding of mammalian testis stem cell biology derives largely from studies in mice. In the mouse testis, GSCs [called spermatogonial stem cells (SSCs) in mammals] and their early differentiating progeny reside on the basement membrane inside the seminiferous tubule **(Figure 1.3A**). In contrast to the *Drosophila* testis, where a distinct morphological structure (the hub) marks the niche, SSCs are located along the entire length of the tubule. The nature and arrangement of somatic support cells are also quite different: There is no somatic stem cell population, and the quiescent Sertoli cells that surround the germ cells are large and make contact with multiple germ cells in different stages of development. There are similarities in the behavior of germ cells, however. SSCs and their early progeny divide with incomplete cytokinesis to form clusters of interconnected spermatogonia, which transit into meiotic spermatocytes as they cross the blood-testis barrier to enter the adluminal compartment (Russell, 1978). There, they complete meiosis and elongate to form spermatozoa, which exit the epithelium through the center of the tubule (Oatley and Brinster, 2012). For comprehensive reviews of mouse spermatogenesis, see Oatley & Brinster (2012), Yoshida (2012), and Kanatsu-Shinohara

& Shinohara (2013). For a comparison of rodent and human spermatogenesis, see the review by Hermann et al. (2010).

In *Drosophila*, GSCs can be identified unequivocally by their morphology and location, but this is not true in mammals. In mouse testes, within the population of undifferentiated spermatogonia is a subset of single cells that were long thought to be the SSCs (Tegelenbosch & de Rooij 1993). However, recent studies using lineage tracing and live imaging indicate that the stem cell pool is more heterogeneous, challenging this long-held view (Aloisio et al., 2014; Yoshida, 2012). Because all undifferentiated spermatogonia reside in a single layer on the basement membrane of the seminiferous tubule, they are likely to receive signals from a variety of sources, including adjacent Sertoli cells as well as cells that reside in the interstitial region of the testis, such as Leydig cells, myoid cells, and macrophages (Oatley and Brinster, 2012; Yoshida, 2012). Whether there is heterogeneity in these somatic cell populations remains to be seen. The nerves and capillaries found in the interstitial tissue are also potential sources of systemic signals (Yoshida, 2012). How signals from all of these sources are coordinated to regulate the balance between SSC self-renewal and differentiation remains unclear.

As in *Drosophila*, genetic approaches have uncovered some of the signals that are important for SSC maintenance (**Figure 1.3B**). Other potential regulators have been identified through *in vitro* studies using cultured SSCs. Sertoli cells secrete glial cell line--derived neurotrophic factor (GDNF), which promotes SSC self-renewal, as well as the differentiation factor retinoic acid (Hasegawa and Saga, 2012; Kubota et al., 2004;

Mullaney and Skinner, 1992; Tadokoro et al., 2002). GDNF receptors, GDNF family receptor α 1 (GFRα1) and RET tyrosine kinase, are expressed in both SSCs and early spermatogonia (Meng et al., 2000; Naughton et al., 2006), suggesting that GDNF signaling could function in both cell types (Grisanti et al., 2009; Suzuki et al., 2009). In SSCs, GDNF and fibroblast growth factor 2 (FGF2) activate the phosphoinositide 3-kinase--Akt and mitogen-activated protein kinase (MAPK) pathways (Hasegawa et al., 2013; Kanatsu-Shinohara and Shinohara, 2013; Kubota et al., 2004), which are thought to promote the transcription of genes necessary for stem cell maintenance (Ishii et al., 2012; Oatley et al., 2006; Wu et al., 2010). Activation of the MAPK pathway in Sertoli cells also leads to the upregulation of GDNF production (Hasegawa et al., 2013; Simon et al., 2007), suggesting indirect as well as direct roles for MAPK activation in SSC maintenance. Other extrinsic factors, such as colony stimulating factor 1, leukemia inhibitory factor, and insulin-like growth factor, regulate self-renewal in cultured SSCs (Kubota et al., 2004; Oatley et al., 2009), but further studies are needed to determine their role in stem cell maintenance *in vivo*.

MODES OF GERMLINE STEM CELL SELF-RENEWAL

A defining feature of stem cells is their ability to divide asymmetrically, producing one daughter that remains a stem cell (self-renewal) and one that differentiates. However, studies on stem cells in intact tissues have revealed that individual stem cells are far more plastic than previously thought: they modulate the output of their divisions in response to the needs of the tissue. This plasticity enables tissues to maintain a constant stem cell

population despite damage or loss of stem cells over time. The different modes of stem cell output are described below (**Figure 1.4**).

Division, Differentiation, and Dedifferentiation in Germline Stem Cells

In the *Drosophila* testis and ovary, GSCs usually divide asymmetrically to produce one daughter cell that remains anchored to the niche and one that is displaced from the niche and differentiates. This pattern of division results from the precise orientation of spindles in mitotic GSCs: The spindles are aligned perpendicular to the niche-GSC interface, with one pole anchored near the interface (Yamashita and Fuller, 2008). Several cell components are asymmetrically segregated during these divisions; in the testis, these include centrosomes, certain histones, and even sex chromosomes, although other chromosomes are segregated at random (Tran et al., 2012; Yadlapalli and Yamashita, 2013; Yamashita et al., 2007). Why these asymmetries occur is not known, and they do not have obvious effects on the outcome of stem cell divisions. For example, GSCs lacking centrioles (a main component of centrosomes) still function normally (Riparbelli and Callaini, 2011). Understanding the relationship between asymmetric distribution of histones and the segregation of sex chromosomes could be informative. Occasionally, even in unperturbed wild-type testes, GSCs divide with a symmetric outcome and both daughters either remain at the niche (symmetric renewal) or leave the niche and differentiate (symmetric differentiation) (Salzmann et al., 2013; Sheng and Matunis, 2011). Further studies are needed to determine whether symmetric renewal or differentiation correlates with changes in the segregation of intracellular components.

In the *Drosophila* ovary, one asymmetrically inherited component does correlate with cell fate decisions in dividing GSCs: the machinery that regulates ribosomal RNA (rRNA) transcription (Zhang et al., 2014). Higher levels of this machinery are found in GSCs than in their differentiating daughters, and this unequal distribution correlates with higher levels of rRNA transcription in GSCs. Increasing rRNA transcription in stem cell daughters delays their ability to differentiate; conversely, reducing rRNA transcription promotes differentiation and can rescue *bam* mutant cells, which otherwise fail to differentiate and remain GSC-like. This mode of regulation could be specific for certain proteins that control cell fate decisions, as disrupting rRNA transcription reduces the level of one stem cell factor, the BMP pathway component Mothers against dpp (Mad), but not its binding partner Medea or Histone H2B. Altogether, these data suggest that niche signaling modulates the levels of rRNA transcription in dividing GSCs, which in turn affects cell fate decisions in the daughter cells. A U3snoRNP component that is required for pre-rRNA maturation is also differentially segregated in dividing female GSCs, but whether this asymmetry is important for GSC function is not clear (Fichelson et al., 2009).

Although asymmetric division is the primary mode of GSC division in *Drosophila* gonads, mouse testes are likely to use a different mechanism. Recent studies using live imaging and pulse labeling have revealed that most SSCs divide symmetrically, as indicated by the expression of the GDNF receptor GFRα1. In addition, stem cells can be renewed by fragmentation of interconnected spermatogonia (dedifferentiation), which break apart and move back into the niche to become stem cells (Hara et al., 2014).

However, in 5% of spermatogonial pairs, GFRα1 is asymmetrically distributed, and in many pairs ubiquitin carboxy-terminal hydrolase 1 is enriched in the cell closest to the basement membrane (Grisanti et al., 2009; Lou et al., 2009). The functional significance of these asymmetries is not known. Dedifferentiation of germ cell clusters also occurs in *Drosophila* testes and ovaries, but this happens primarily due to aging or in response to the genetically induced loss of stem cells (Brawley and Matunis, 2004; Cheng et al., 2008; Kai and Spradling, 2004; Sheng et al., 2009).

Neutral Drift Dynamics in Stem Cells

Whether a stem cell remains in the niche or goes on to differentiate is regulated not just by the signals it receives but also by the physical constraints of the niche in which it resides. Niches contain a limited amount of signals and space, and stem cells are constantly competing with each other for niche occupancy (Johnston, 2009). The stem cell population is therefore regulated by the balance between asymmetric divisions, symmetric renewals, and symmetric differentiation, as well as by competition between neighboring stem cells (Klein and Simons, 2011; Sheng and Matunis, 2011; Stine and Matunis, 2013). Lineage tracing has provided insight into the half-lives of stem cells in many tissues: Stem cells are continually lost from the niche and replaced as a result of natural turnover (Fox et al., 2008). In many vertebrate and invertebrate stem cell systems, turnover occurs in a stochastic manner and is termed neutral competition (Baker et al., 2014; Clayton et al., 2007; De Navascués et al., 2012; Doupé et al., 2010; Doupé et al., 2012; Klein and Simons, 2011; Kronen et al., 2014; Lopez-Onieva et al., 2008; Snippert et al., 2010; Stine and Matunis, 2013; Teixeira et al., 2013; Vermeulen et al., 2013). This

neutral drift dynamic occurs in gonadal stem cell niches (Amoyel et al., 2014; Klein et al., 2010; Kronen et al., 2014; Sheng and Matunis, 2011), but whether transient signaling fluctuations control these changes, as seen in the *Drosophila* eye (Losick and Desplan, 2008), remains to be determined. Importantly, the neutral drift dynamics of a stem cell population can be shifted by the acquisition of mutations in stem cells, such that active competition between neighboring cells ensues.

STEM CELL COMPETITION

Mutations within stem cells that tip the balance toward symmetric renewal or symmetric differentiation are the defining feature of stem cell competition. Mutations causing a fitness advantage allow mutant cells to take over the niche and outcompete wild-type stem cells. By contrast, mutations causing a disadvantage lead to mutant cells being lost more quickly from the niche, as a result of either cell death or differentiation (**Figure 1.5A**). While competition can eliminate defective stem cells from the niche, potentially maintaining stem cell fitness, it can also lead to aberrant tissue function. For example, in multiple myeloma and acute myeloid leukemia, cancer stem cells outcompete normal hematopoietic stem cells (Noll et al., 2012). Changes in adhesion, differentiation ability, or proliferation can all affect stem cell competition (**Figure 1.5B**). Thus, understanding these mechanisms is vital for the treatment and prevention of disease as well as for capturing the regenerative capacity of stem cells.

Effects of Adhesion on Stem Cell Competition

Adhesion plays a major role in the regulation of stem cell occupancy within many niches (Chen et al., 2013a). In the *Drosophila* ovary, E-cadherin and its intracellular partner β-

catenin are necessary to form proper adherens junctions. Both proteins localize along the GSC-cap cell junction and the FSC-escort cell junction and anchor GSCs and FSCs to their respective niches (Song and Xie, 2002; Song et al., 2002). Because removal of either protein causes loss of GSCs or FSCs from the niche, these proteins are essential for stem cell maintenance. E-cadherin and β-catenin are also important for niche-stem cell anchorage in the *Drosophila* testis, where they localize to the hub-GSC and hub-CySC interfaces. Reduction of E-cadherin in either stem cell lineage results in the loss of that lineage from the niche, most likely through differentiation (Voog et al., 2008; Yamashita et al., 2003). However, how niche signals coordinate adhesion levels in stem cells to regulate niche occupancy is poorly understood. Recently, the Slit-Roundabout pathway was shown to modulate adhesion in CySCs by regulating E-cadherin (Stine et al., 2014). The ligand Slit is expressed specifically within the hub, and a reduction in levels of the Slit receptor Roundabout 2 in CySCs resulted in their loss from the niche. By contrast, loss of the pathway's downstream effector, Abelson tyrosine kinase, provided CySCs with a competitive advantage. This supports a model in which the Slit-Roundabout pathway attenuates Abelson tyrosine kinase activity, which normally destabilizes β-catenin to allow adherens junction turnover (Stine et al., 2014). The expression of Roundabout 2 in CySCs is also regulated by JAK-STAT signaling, suggesting a mechanism for coordinating niche signaling with modulation of adhesion. As E-cadherin is important for niche-stem cell anchorage in the ovary, it will be interesting to know if the Slit-Roundabout pathway also modulates adhesion in this tissue. Furthermore, Roundabout 4 is expressed in mammalian hematopoietic stem cells and is known to be important for localization to the bone marrow niche; thus, if the same mechanism is

involved in controlling adhesion levels within these cells, it would reveal a conserved function for this pathway (Smith-Berdan et al., 2011).

Integrins are another type of adhesion molecule important for stem cell attachment to niches (Chen et al., 2013a). In the *Drosophila* testis, integrins regulate adhesion of hub cells to the extracellular matrix but not attachment of stem cells to the hub (Lee et al., 2008; Tanentzapf et al., 2007). However, modulation of integrin levels between the two stem cell populations, GSCs and CySCs, can lead to competition for niche occupancy. Integrin levels are regulated by JAK-STAT signaling, and loss of the JAK-STAT signaling suppressor SOCS36E leads to an increase in integrins within CySCs (Issigonis et al., 2009; Singh et al., 2010). This increase in integrins causes the CySCs to adhere better to the hub and consequently push out neighboring GSCs (Issigonis et al., 2009). Increased integrin levels or JAK-STAT signaling in CySCs does not lead to an overrepresentation of these mutant CySCs in the niche, suggesting that SOCS36E could have additional functions (Amoyel et al., 2014).

SSCs in the mouse testis also express integrins, which could mediate their adhesion to the basement membrane of the seminiferous tubule (Shinohara et al., 1999). When SSCs from β1-integrin knockout mice were transplanted into the seminiferous tubules of recipient mice that lacked endogenous germ cells, the SSCs with reduced β1-integrin were unable to attach to the basement membrane but did not have problems with migration to the niche, adhesion to Sertoli cells, or passage through the blood-testis barrier (Kanatsu-Shinohara et al., 2008). Consequently, the mutant SSCs colonized the

recipient testes less successfully than control SSCs, demonstrating that proper attachment to the niche is essential for SSC maintenance.

Stem Cell Proliferation, Differentiation, and Competition

Failure to differentiate or an increase in proliferation can also cause one population of stem cells to outcompete another for space in the niche. In the *Drosophila* ovary, GSCs lacking Bam fail to differentiate and show a competitive advantage over wild-type neighboring GSCs for space within the niche (Jin et al., 2008). The mutant cells display increased levels of E-cadherin at the GSC-cap cell junction as well as increased proliferation, suggesting an indirect link between differentiating factors, adhesion, and division rate (Jin et al., 2008). FSCs lacking the basolateral junction proteins Lethal giant larvae or Discs large also outcompete their wild-type neighbors for niche occupancy (Kronen et al., 2014). These proteins establish polarity in early follicle cell daughters, which is necessary for their differentiation. Thus, a reduction in junction proteins causes defects in differentiation. These defects cause immature daughter cells to accumulate within the niche, increasing the likelihood that mutant FSCs will replace lost FSCs.

Another signaling molecule known to modulate general cell competition is dMyc. This phenomenon is best characterized in the *Drosophila* wing imaginal disc, where knockdown of dMyc in a subset of cells leads to their slow growth and eventually allows wild-type neighbors to take over. By contrast, overexpression of dMyc leads to induction of apoptosis in neighboring cells (De La Cova et al., 2004). Although increasing dMyc levels in GSCs of the *Drosophila* ovary does give them a competitive advantage over

wild-type GSCs, the advantage results from enhanced sensitivity to niche signaling, which allows them to be retained in the niche longer, and not from induction of apoptosis in neighboring cells (Rhiner et al., 2009). Similarly, individual GSCs containing reduced levels of dMyc are eliminated from the niche more quickly than wild-type GSCs. One study looking at the role of dMyc in GSCs showed that it was not essential for GSC competition; this disparate finding could reflect differences in experimental design, choice of loss of function alleles, and/or overexpression methodologies (Jin et al., 2008; Rhiner et al., 2009).

Although failure of stem cells to differentiate can lead to their overrepresentation in the niche, an increase in proliferation rate can also cause a competitive advantage. This is seen in the *Drosophila* testis, in CySCs constitutively expressing either the Hedgehog or Hippo signaling pathways (Amoyel et al., 2014; Michel et al., 2012). Clonal analysis has shown that CySCs homozygous for *patched* or *hippo* mutant alleles, which lead to activation of the Hedgehog or Hippo pathways, respectively, can outcompete both wild-type CySCs and GSCs for niche occupancy. This competition is a result of accelerated proliferation, as seen by an increase in the number of cells in S phase or M phase in the *patched* mutant clones. In addition, the competitive advantage of *patched* and *hippo* mutant clones can be rescued by reducing levels of String, an important inducer of mitosis (Amoyel et al., 2014). In contrast, loss of Hedgehog signaling in *smoothened* mutant CySC clones leads to their rapid loss from the niche, suggesting that mutations that decrease proliferation rates cause a competitive disadvantage. Interestingly, global reduction of Hedgehog signaling leads to a reduced number of CySCs but does not cause

a difference in proliferation rate or a complete loss of the mutant cells (Michel et al., 2012). This suggests that a difference in cell signaling, and its concomitant effect on proliferation rate between two neighboring cells may cause competition, whereas global changes effecting proliferation in all cells may not. Further supporting this idea, CySC clones overexpressing both String and the G1/S phase--promoting factor Cyclin E are capable of outcompeting wild-type CySCs and a portion of GSCs from the niche (Amoyel et al., 2014). However, overexpression of String in all CySCs leads to an increase in CySC proliferation rate but not a loss of GSCs from the niche (Inaba et al., 2011). Together, these studies provide evidence that changes in proliferation rate are a key factor driving stem cell competition and may represent a mechanism leading to cancer initiation. In support of this idea, loss of the tumor suppressor gene *APC* in intestinal stem cell clones in mice and humans is associated with an expanded stem cell population, resulting from an increase in proliferation (Baker et al., 2014; Vermeulen et al., 2013). As loss of this gene can lead to colon cancer, understanding how changes in stem cell dynamics cause competition is important for preventative intervention and the development of effective treatments (Morrissey and Vermeulen, 2014).

Mutations causing a slight advantage in self-renewal without compromising differentiation are thought to impart a competitive advantage to spermatogonial stem cells of the mammalian testis. Although these mutations may lead to an increased division rate, they do not usually affect normal tissue function; instead, they produce mutant sperm that cause congenital disorders in progeny. This is demonstrated by the paternal age effect: older men have a greater chance of fathering children with

developmental defects (Goriely and Wilkie, 2012). This effect is thought to be driven by rare spontaneous activating mutations, primarily in the Ras-mediated signal transduction pathway, which are hypothesized to promote clonal expansion of mutant stem cells with age, thus leading to the accumulation of mutant sperm over time (Goriely and Wilkie, 2012). Although there is evidence indicating an overrepresentation of these mutations in the sperm of older men (Goriely and Wilkie, 2012), little is known about the mechanism of competition, which is thought to occur at the stem cell level. It has also been hypothesized that mutations outside of the Ras signaling pathway can confer similar defects.

Recently, a study looking at mouse SSCs with a specific mutation in Fibroblast Growth Factor Receptor 2 (FGFR2), which causes Apert syndrome, showed that these mutant stem cells had enhanced sensitivity to growth factors, causing an increase in fitness compared with wild-type stem cells (Martin et al., 2014). *In vitro* competition assays, in which the wild-type SSC population and the mutant SSC population contained distinct fluorescent tags and were grown in the same dish, showed that the mutant SSC population could multiply at a faster rate than the wild-type population, but only in low FGF2 conditions. Furthermore, in transplantation assays in which the differentially labeled SSC populations were mixed *in vitro* and then transplanted into busulfan-treated mice depleted of germ cells, the mutant SSCs showed greater stem cell activity and produced more colonies than their wild-type counterparts (Martin et al., 2014). Transplantation assays in which SSCs from older mice were transplanted into younger mice have shown that niche function declines with age (Ryu et al., 2006). Thus, it is

likely that enhanced growth factor sensitivity confers an advantage on mutant SSCs, one that results from changes in their local microenvironment that are caused by aging. This indicates a link between the quality of the niche and the increased self-renewal capacity of stem cells.

A similar link is seen within stem cells of the colon. Tumor suppressor p53 mutants show a competitive advantage only in niches with impaired function resulting from colitis; this environment allows clonal expansion of these mutant cells over time (Vermeulen et al., 2013). This is thought to be how colitis-associated colorectal cancer is initiated. In addition, lower levels of p53 confer a competitive advantage to hematopoietic stem cells under stress conditions (Bondar and Medzhitov, 2010). This overrepresentation of stem cells with low p53 levels can easily lead to a complete loss of p53, resulting in the over-proliferation of these cells and cancer formation. These examples suggest a common mechanism underlying both paternal age effect disorders and cancer. Thus, understanding how niche signaling can bias the symmetric renewal capacity of stem cells is relevant for understanding the underlying causes of a variety of diseases.

RESPONSE TO TRAUMA

An important goal of regenerative medicine is to replace cells that are lost as a result of aging or tissue damage. In tissues with high rates of cell turnover, such as the skin, blood, or intestines, differentiated cells are continuously replaced by the progeny of tissue-specific stem cells, which divide and differentiate to replenish the lost cells. Tissues with low cell turnover may contain reserve or quiescent stem cells that can be stimulated to

divide in response to tissue damage. What happens if stem cells or their niche cells are lost or damaged? As numerous studies have demonstrated, differentiation is not irreversible, and sometimes even fully differentiated cells can be reprogrammed or converted into other cell types to replenish the damaged tissue. Here, we ask how stem cells and their niches respond to trauma, and we review recent studies showing that not just differentiated cells but also stem cells can be regenerated from other cell types.

Differentiated cells can be reprogrammed or converted into other types of cells *in vivo* in two different ways: they can dedifferentiate into stem-like cells that then redifferentiate, or they can transdifferentiate directly into other cell types without first reverting to a stem-like fate (**Figure 1.6**). In plants and some animals, cell fate conversions happen naturally in response to tissue damage; the remarkable ability of hydrozoans, planarians, and salamanders to regenerate amputated body parts is the most striking example of this phenomenon (King and Newmark, 2012). Although adult mammals lack the ability to regenerate entire limbs, recent studies have shown that they too can regenerate missing tissue via cell fate conversions in response to damage or induced changes in genetic output. For example, after toxin-induced ablation of pancreatic β-cells in adult mice, the missing cells can be regenerated by the spontaneous transdifferentiation of pancreatic α-cells (Thorel et al., 2010). New β-cells can also be generated from pancreatic exocrine cells, which can be reprogrammed directly into β-cells by re-expressing a set of embryonic transcription factors (Zhou et al., 2008). In both cases, the regenerated β-cells express insulin and are indistinguishable from endogenous β-cells. Studies such as these

in a wide variety of tissues and organisms continue to challenge established concepts of what it means to be a differentiated cell (Sánchez Alvarado and Yamanaka, 2014).

Germline Stem Cell Regeneration

Recent work has shown that adult stem cells can also be regenerated by cell fate conversions. Dedifferentiation, in addition to replacing stem cells lost through normal tissue turnover, is one mechanism for replacing populations of stem cells that have been lost through tissue damage. In the adult *Drosophila* testis, removal of the stem cell maintenance factor STAT or ectopic expression of the differentiation factor Bam induces rapid loss of GSCs (Brawley and Matunis, 2004; Sheng et al., 2009). When normal signaling is restored, clusters of interconnected spermatogonia break apart into single cells that can migrate into the niche and revert to fully functional stem cells. The same is true in the adult mouse testis: after γ-irradiation or treatment with the drug busulfan, which is preferentially toxic to SSCs and spermatogonia, both transplanted and remaining endogenous spermatogonia have been shown to revert to SSCs and repopulate the niche (Barroca et al., 2009; Hara et al., 2014; Nakagawa et al., 2007). Female GSCs can also be replaced by dedifferentiation; in the adult *Drosophila* ovary, interconnected cyst cells (oogonia) can dedifferentiate to replace GSCs lost after removal of the stem cell maintenance factor Dpp (Kai and Spradling, 2004). In all of these cases, the reverting cells are connected by stable intercellular bridges that must close to allow the formation of individual stem cells. The signals that mediate closure of the bridges and reversion to a less differentiated state are not known; however, as direct contact with niche cells is not essential for these events to occur, other somatic cells may play a role. In *Drosophila*,

testes that contain spermatocytes but no spermatogonia are not able to regenerate GSCs, suggesting that these more differentiated cells are no longer capable of responding to the signals that mediate dedifferentiation. Therefore, past the spermatogonial stage, it is likely that differentiation is indeed irreversible.

Somatic Stem Cell Regeneration

Somatic cells of the gonad may also be capable of dedifferentiating. In the *Drosophila* testis, STAT is required for maintenance of somatic stem cells and GSCs. Somatic stem cells are lost upon removal of STAT, and it is likely that they are replaced by the dedifferentiation of cyst cells when STAT expression is restored, although direct evidence for this hypothesis is lacking. Somatic stem cells in the *Drosophila* testis can also be regenerated from a different and unexpected source: quiescent niche cells. Conditional expression of the proapoptotic gene *grim* in somatic stem cells and early cyst cells associated with spermatogonia results in the complete ablation of these cells from adult testes, whereas germ cells and older cyst cells associated with spermatocytes remain intact (Hétié et al., 2014). When flies are allowed to recover from ablation, their hub cells re-enter the cell cycle, delaminate from the hub, and convert into CySCs, which repopulate the niche and produce daughter cyst cells that are indistinguishable from normal cyst cells. By contrast, older cyst cells do not re-enter the cell cycle and do not appear to contribute to the new population of CySCs. Hub cell conversion to CySCs is seen only in testes that have lost all CySCs and early cyst cells, not in testes that have lost only some of these cells. However, hub cell conversion can be induced even in testes that have lost none of these cells by either ectopic expression of Cyclin D and Cyclin-

dependent kinase 4 in the hub or removal of the transcription factor Escargot or its cofactor, C-terminal binding protein, from hub cells (Hétié et al., 2014; Voog et al., 2014). In these cases, hub cells appear to re-enter the cell cycle before exiting the hub. Mitotic hub cells have never been seen in wild-type adult testes, however, or in testes recovering from CySC loss induced by the removal of STAT in which early cyst cells remain (M. de Cuevas & E. Matunis, unpublished observations). Based on these observations, we speculate that lost CySCs can be regenerated in two ways in adult testes —by dedifferentiation of early cyst cells or by conversion of hub cells—but that hub cell conversion happens only when no early cyst cells remain. Hub cell conversion is not without risks, however. Testes that recover CySCs by hub cell conversion often contain multiple ectopic niches, which could arise from fission of the original hub or from incompletely reprogrammed CySCs that revert to hub cells (Hétié et al., 2014). Whether damage-induced transdifferentiation events are accompanied by uncontrolled niche expansion in mammalian tissues is an important question to ask in future studies.

Germ Cell Fate Conversions

Another intriguing type of stem cell conversion recently documented in the *Drosophila* testis is the sex transformation of male-to-female somatic stem cells (Ma et al., 2014). *chinmo* is a target of the Jak-STAT signaling pathway and encodes a transcription factor required cell-autonomously for CySC self-renewal (Flaherty et al., 2010). Flies carrying a hypomorphic allele of *chinmo*, $chinmo^{ST}$, initially develop what look like wild-type testes, but as the flies age, their cyst cells are gradually replaced by cells that resemble ovarian follicle cells. Lineage tracing experiments and cell type-specific knockdown of Chinmo

suggest that these follicle-like cells are derived from CySCs that fail to maintain their male sex identity when Chinmo levels are reduced, transforming into female somatic stem cells as a result. Chinmo acts in part through the male sex determination factor DoublesexM, which is expressed in wild-type testes but not in *chinmo*ST testes. This work indicates that the sex of somatic stem cells in the adult gonad must be actively maintained and that *chinmo* is required directly for this maintenance in CySCs. Somatic cells in vertebrate gonads must also actively maintain their sex. In adult mouse testes, loss of the transcriptional regulator DMRT1, which is a homolog of Doublesex, causes the transdifferentiation of Sertoli cells to granulosa cells (Matson et al., 2011), and the reciprocal transdifferentiation of granulosa cells to Sertoli cells can be triggered in adult mouse ovaries by loss of FOXL2 (Uhlenhaut et al., 2009). Sex transformations of adult gonads are a naturally occurring phenomenon in some species of fish (Chan 1970). In other species of fish, sex transformations can be experimentally induced, as in medaka, in which *Dmrt1* mutant males develop normal testes that later transform into ovaries (Masuyama et al., 2012), or zebrafish, in which ovaries can retract and functional testis-like organs appear in response to hormone manipulation (Takatsu et al., 2013). Moreover, in several fish species, both oogonia and spermatogonia are capable of reversing sex and giving rise to functional sperm or oocytes, respectively, when transplanted into recipient fish of the opposite sex (Lacerda et al., 2014). Although studies such as these highlight the remarkable sexual plasticity of gonadal cells, whether sex transformations in vertebrates take place in stem cells, differentiated cells, or both remains to be determined.

Besides reversing their sex, germ cells are capable of converting to somatic cells. In the *C. elegans* gonad, removal of the Polycomb repressor complex 2 (PRC2) paired with ectopic expression of transcription factors that specify somatic cell types, such as specific neurons or muscle cells, causes mitotic germ cells to be reprogrammed into those cell types (Patel et al., 2012; Tursun et al., 2011). PRC2 represses gene expression through its activity as a histone 3 lysine 27 methyltransferase and may define a chromatin state in germ cells that prevents them from converting to other cell fates. Therefore, when PRC2 is removed, germ cells become susceptible to reprogramming in the presence of specific somatic transcription factors. Polycomb proteins may also play a role in preventing germ cell reprogramming in the *Drosophila* testis (Eun et al., 2014). Knockdown of the Polycomb group gene *Enhancer of zeste* [*E*(*z*)] in adult testes causes germ cells to express the somatic marker Zfh-1. Here, the function of *E(z)* is non-cell autonomous, as it is required only in cyst lineage cells to prevent germline expression of Zfh-1. Therefore, suppression of Zfh-1 in germ cells must depend on signals from the niche rather than intrinsic factors. It will be interesting to know what happens to other somatic markers in these testes and which cells—stem cells or differentiated cells or both—are misexpressing them.

Lack of Regeneration in Niche Cells

Unlike the stem cells that they support, gonadal niche cells may not be capable of regeneration after damage. Although hub cells in the *Drosophila* testis can re-enter the cell cycle and convert to CySCs in response to CySC ablation, they are apparently not able to replenish other lost hub cells. Conditional expression of proapoptotic genes in hub

cells in adult testes causes some or all hub cells to be ablated, but when flies are allowed to recover from ablation, no new hub cells are generated (P. Hétié & E. Matunis, unpublished observations). Somatic stem cells have been proposed to serve as a source of new hub cells (Voog et al., 2008), but contradictory results (DiNardo et al., 2011) and the inability of hub cells to be restored after ablation suggest that this hypothesis is not correct. Hub cells can also be ablated by knockdown of the novel gene *headcase*, but whether or not lost hub cells can be regenerated after recovery in this case is not known (Resende et al., 2013). Although it lacks the ability to restore itself, the hub is remarkable in its ability to continue supporting stem cells after trauma. After *headcase* knockdown, even single hub cells can continue to support robust populations of germline and somatic stem cells.

PERSPECTIVES

Proper regulation of adhesion, differentiation, proliferation, and cell fate is important for the maintenance of stem cells within the niche. Mutations affecting any of these factors could cause an increase in symmetric differentiation, leading to stem cell exclusion from the niche, or an increase in symmetric renewal, leading to an overrepresentation of stem cells. In addition, damage to the niche can result in the misregulation of local signals, leading to cell fate changes. Although these mechanisms ensure that only the fittest stem cells occupy the niche, they can also have detrimental consequences for tissue function or, in the case of GSCs, progeny development. Thus, niche signaling modulates adhesion, differentiation, proliferation, and cell fate to ensure a constant supply of stem cells that turnover at a steady rate. Further understanding the mechanisms that control these factors

will be essential for the prevention of diseases such as cancer and paternal age effect disorders and may provide targets for future therapies.

Figures

Figure 1.1: The architecture and signaling of the *Drosophila* testis niche. (a) Somatic hub cells (green) signal to attached germline and somatic cyst stem cells (GSCs, orange, and CySCs, blue, respectively). GSCs asymmetrically divide to produce daughter gonialblasts (light orange) that are displaced from the hub and undergo four mitotic divisions with incomplete cytokinesis, producing interconnected spermatogonia (light orange). CySCs divide asymmetrically to produce daughter cyst cells (white); two encase each gonialblast and elongate to accommodate differentiating germ cells throughout spermatogenesis. (b) Hub cells secrete the ligand Unpaired (Upd) activating JAK-STAT signaling in GSCs and CySCs, which is required for their maintenance. The downstream targets of STAT in the GSCs are unknown, but two targets of STAT in the CySCs, *zinc-finger homeodomain protein 1* (*zfh1*) and *chronologically inappropriate morphogenesis* (*chinmo*), are essential for CySC self renewal (Flaherty et al., 2010; Leatherman and Di Nardo, 2008). The ligand Hedgehog, which is secreted from the hub, is also required for CySC but not GSC maintenance. Although its downstream targets are unknown, it may contribute to GSC maintenance by regulating BMP signaling (Zhang et al., 2013). The hub and CySCs both secrete the ligands Decapentaplegic (Dpp) and Glass bottom boat (Gbb), which is thought to be a result of activated STAT or one of its downstream targets (Leatherman and Dinardo, 2010; Michel et al., 2011). Secretion of these ligands activates the Bone Morphogenetic Protein (BMP) signaling pathway in GSCs. Activation of BMP signaling represses the differentiation factor *bag-of-marbles* (*bam*). Four and eight cell spermatogonia do not receive enough BMP signaling to repress *bam* expression and thus up-regulate *bam*, initiating the differentiation process. Daughter cells in each lineage are thought to receive less of the niche signals due to their displacement from the hub. If these niche signals fall below a certain threshold, they can be overridden by the acquisition of new signals that promote differentiation such as those triggered by Epidermal Growth Factor (EGF) signaling within the CySC lineage.

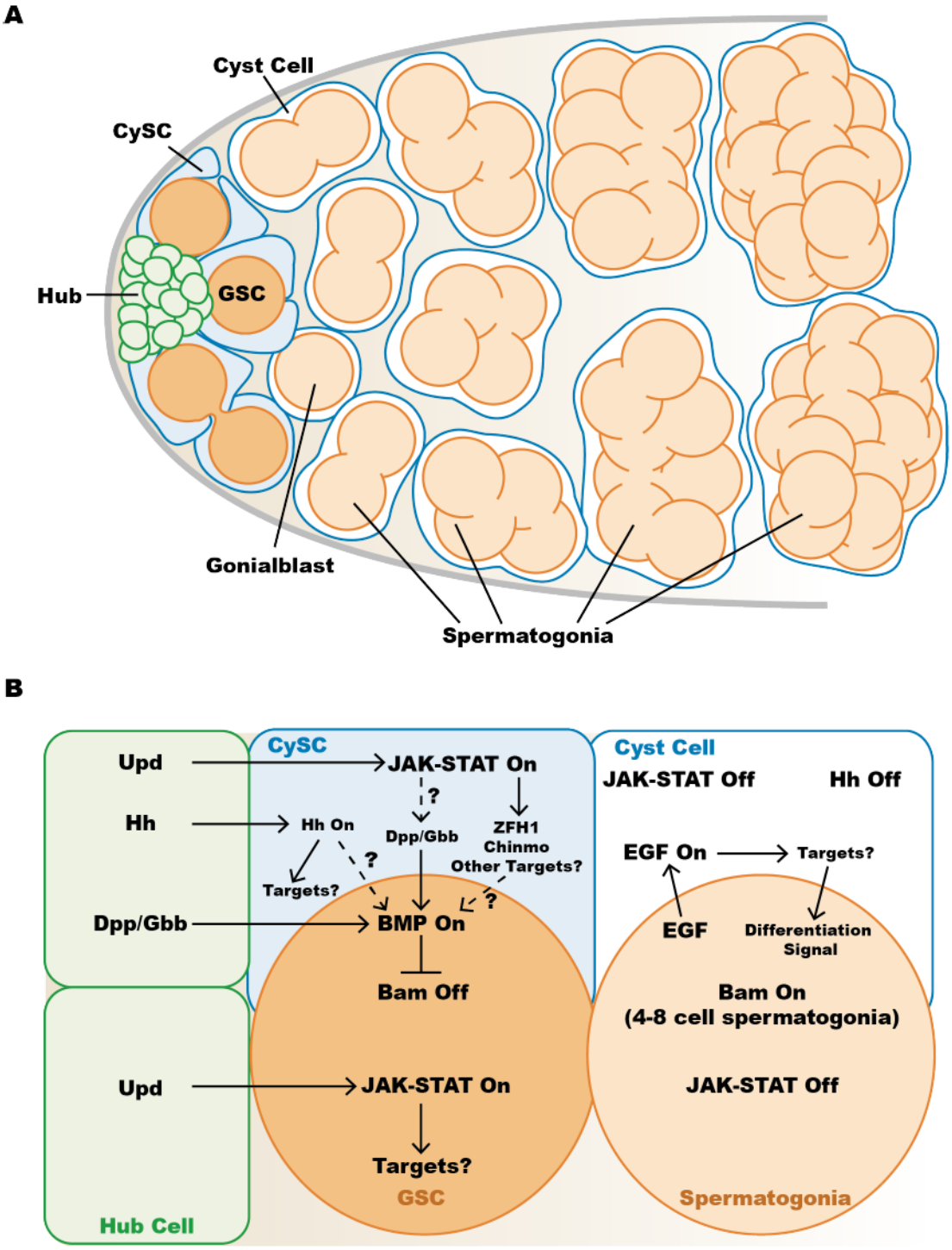
A
Cyst Cell
CySC
Hub
GSC
Gonialblast
Spermatogonia
B
CySC
Upd
JAK-STAT On
?
Hh
Hh On
Dpp/Gbb
ZFH1
Chinmo
Other Targets?
?
Targets?
?
Dpp/Gbb
BMP On
Bam Off
Upd
JAK-STAT On
Targets?
GSC
Hub Cell
Cyst Cell
JAK-STAT Off
Hh Off
EGF On
Targets?
EGF
Differentiation
Signal
Bam On
(4-8 cell spermatogonia)
JAK-STAT Off
Spermatogonia

Figure 1.2: The architecture and signaling of the *Drosophila* ovarian niche. (a) The ovarian niche houses 2-3 GSCs (orange) at the anterior tip of the germarium where they adhere to a group of quiescent somatic cap cells (light green) which themselves are adjacent to quiescent somatic terminal filament cells (green). Each GSC divides asymmetrically to produce a daughter stem cell and a cystoblast that undergoes transit amplification with incomplete cytokinesis to yield sixteen cystocytes (pale orange). As female germ cells differentiate they are displaced posteriorly by the aid of escort cells (Morris and Spradling, 2011). When clusters of cystocytes (cysts) reach the midpoint of the germarium, they become surrounded by follicle cells (white), originating from follicle stem cells (FSCs, Blue). These follicle cells eventually differentiate into a polarized epithelium. One cystocyte becomes the oocyte (yellow), while the remainder become nurse cells. (b) JAK-STAT signaling is activated in the cap cells and possibly the anterior escort cells by the secretion of the ligand Unpaired (Upd) from the terminal filament cells. This leads to the production of the ligand Decapentaplegic (Dpp). Along with Glass bottom boat (Gbb), Dpp triggers a BMP signaling cascade in the GSCs that results in the repression of the differentiation factor *bag-of-marbles* (*bam*). Cystoblasts do not receive enough ligand to activate BMP signaling and thus begin to express *bam* and differentiate. FSCs reside in a distinct environment from the GSCs and activate Hedgehog, Wingless, and BMP signaling pathways, which are necessary for their maintenance. Ligands secreted from the GSC niche are thought to activate these pathways in FSCs.

A

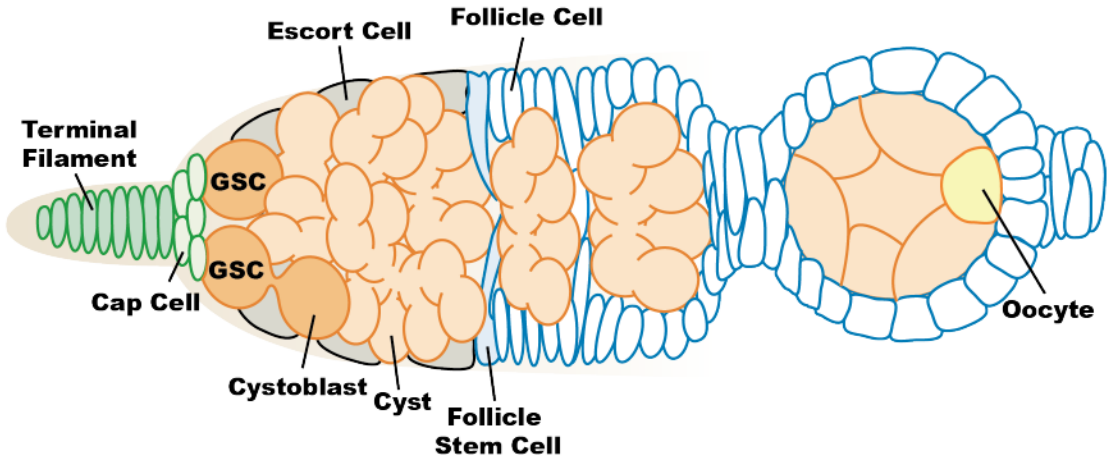
Escort Cell
Follicle Cell
Terminal Filament
GSC
GSC
Cap Cell
Oocyte
Cystoblast
Cyst
Follicle Stem Cell

B

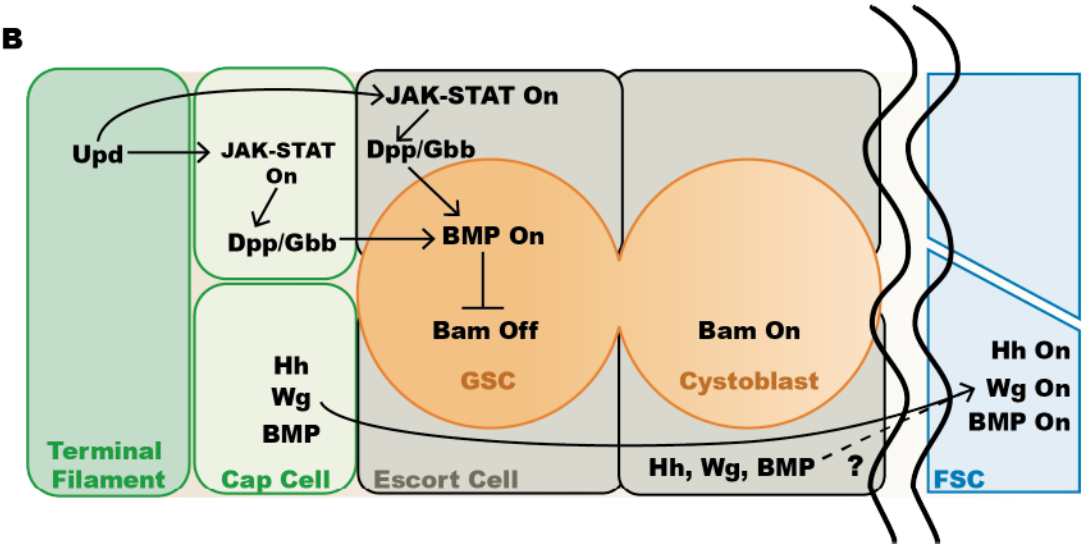
JAK-STAT On
Upd
JAK-STAT On
Dpp/Gbb
Dpp/Gbb
BMP On
Bam Off
GSC
Bam On
Cystoblast
Hh
Wg
BMP
Hh On
Wg On
BMP On
Terminal Filament
Cap Cell
Escort Cell
Hh, Wg, BMP ?
FSC

Figure 1.3: The architecture and signaling of the mammalian testis niche. (a) The seminiferous tubule is bounded by a basement membrane, which separates the site of spermatogenesis from the interstitial space, where Leydig cells, myoid cells, and macrophages reside. Quiescent somatic Sertoli cells adhere to the basal lamina but extend long cytoplasmic processes toward the tubule lumen, simultaneously contacting thousands of germ cells at all stages of differentiation. Sertoli cells meet at specialized tight junctions that comprise the blood-testis-barrier (BTB) and polarize the seminiferous epithelium into basal and adluminal compartments (Oatley and Brinster, 2012). SSCs and spermatogonia reside in a single layer on the basement membrane of the seminiferous tubule where they divide with incomplete cytokinesis to form interconnected cohorts of syncytial germ cells. As germ cells differentiate, they move towards the tubule lumen. (b) Systemically derived gonadotropin follicle-stimulating hormone (FSH) regulates the secretion of the glial cell line-derived neurotrophic factor (GDNF) from Sertoli cells. This ligand, along with the secretion of Fibroblast Growth Factor 2 (FGF2) from Sertoli cells, activates the PI3K-Akt and mitogen activated protein kinase (MAPK) signaling pathways in SSCs and their daughters. Both pathways in turn up-regulate the transcription factors Etv5 and Bcl6b necessary for SSC self-renewal, while GDNF alone induces Oct6 expression (Ishii et al., 2012; Oatley et al., 2006; Wu et al., 2010). Plzf is another important transcription factor required for SSC self-renewal but what regulates its expression is unknown (Buaas et al., 2004; Costoya et al., 2004). Colony Stimulating Factor 1 (CSF1) is secreted from both Leydig and myoid cells, and is thought to regulate maintenance specifically in the stem cells where colony stimulating factor 1 receptor resides (Oatley et al., 2009).

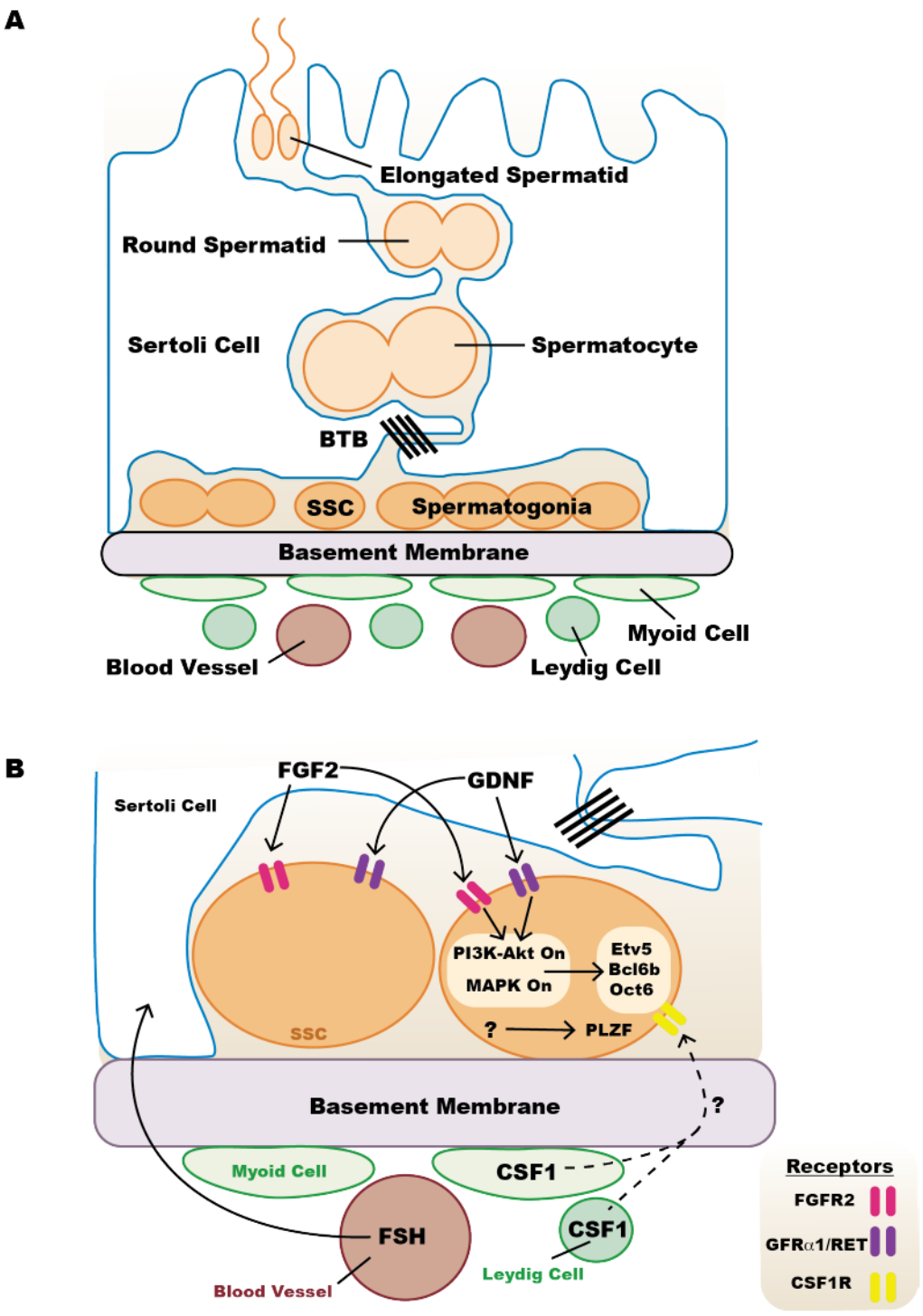
A
Elongated Spermatid
Round Spermatid
Sertoli Cell
Spermatocyte
BTB
SSC
Spermatogonia
Basement Membrane
Myoid Cell
Blood Vessel
Leydig Cell
B
FGF2
GDNF
Sertoli Cell
PI3K-Akt On
MAPK On
Etv5
Bcl6b
Oct6
?
PLZF
SSC
Basement Membrane
?
Myoid Cell
CSF1
FSH
CSF1
Blood Vessel
Leydig Cell
Receptors
FGFR2
GFRα1/RET
CSF1R

Figure 1.4: Modes of stem cell self-renewal. Stem cells can self-renew using various mechanisms. In asymmetric division, one daughter cell remains a stem cell while the other daughter is displaced from the niche and begins to differentiate. In dedifferentiation, interconnected clusters of germ cells break apart and return to the niche where they receive signals that promote a stem cell fate. In symmetric renewal, both daughter cells remain a stem cell attached to the niche. In symmetric differentiation, both daughter cells leave the niche due to differentiation or cell death. During homeostasis, stem cells follow neutral drift dynamics in which the rate of self-renewal equals the rate of differentiation. This ensures that the pool of stem cells in a population remains constant. However, mutations in the stem cells or trauma to the tissue can skew the balance leading to stem cell competition.

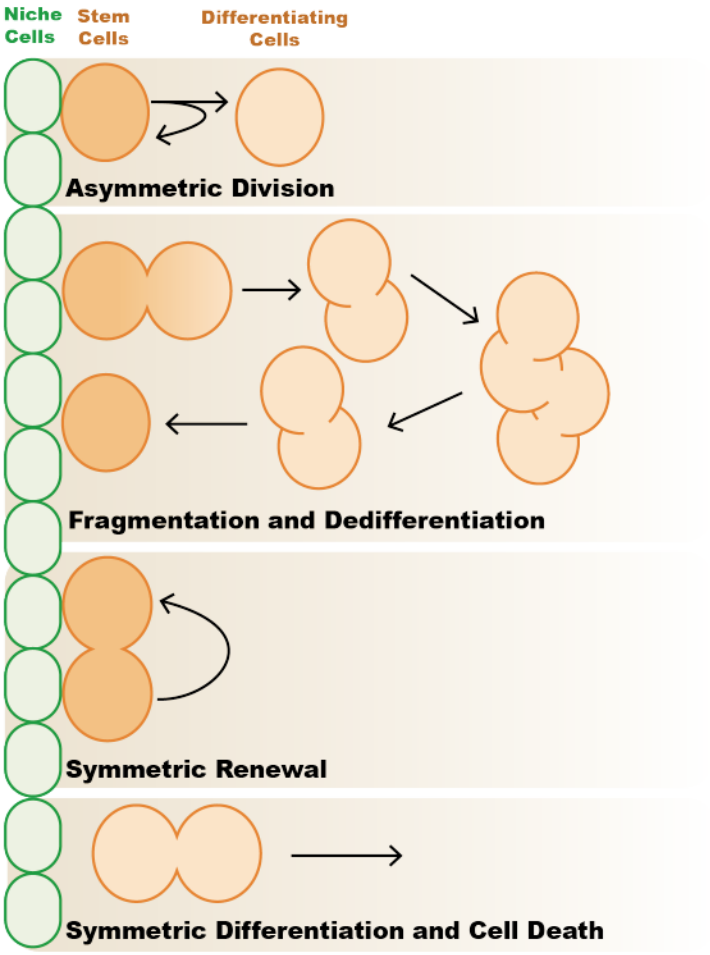
Niche Cells
Stem Cells
Differentiating Cells
Asymmetric Division
Fragmentation and Dedifferentiation
Symmetric Renewal
Symmetric Differentiation and Cell Death

Figure 1.5: Mechanisms of stem cell competition. Niche cells (green), stem cells with a fitness advantage (red) or disadvantage (orange) are indicated. (a) When neutral drift dynamics are skewed, stem cells with a fitness advantage take over the niche while those with a disadvantage are lost from the niche with time. (b) Three different mechanisms can modulate stem cell competition within the niche: adhesion, failure of daughters to differentiate, and different proliferation rates. Stem cells that adhere better to the niche will remain in the niche longer than those that do not. Stem cells that produce daughter cells that fail to differentiate have a greater chance of those daughters staying within the niche and becoming stem cells. Stem cells with a faster proliferation rate will produce more daughters than their neighbors increasing the likelihood that their daughters will remain stem cells.

A

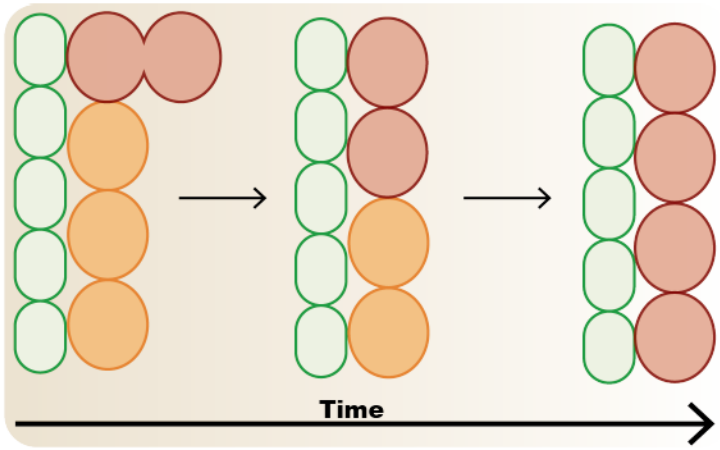

B

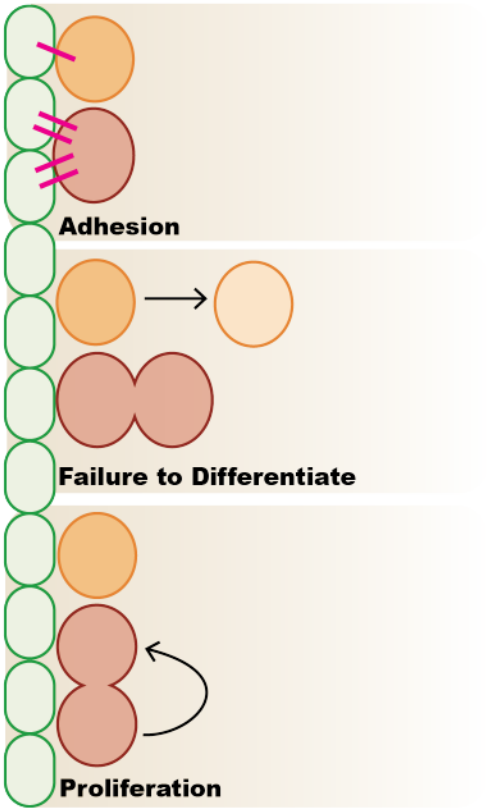

Figure 1.6: Stem cell conversion and regeneration. When stem cells are depleted through mutations or trauma to a tissue, other cells can convert to a stem cell fate to replenish the stem cell pool; stem cells can also convert to other cell types. In dedifferentiation, differentiating cells that have moved away from the niche can revert into stem cells and repopulate the niche. In niche cell conversion, quiescent niche cells can re-enter the cell cycle and convert into somatic stem cells, as in the *Drosophila* testis. In sex transformation, male somatic stem cells can convert to female somatic stem cells, as in *chinmo*ST mutant *Drosophila* testes.

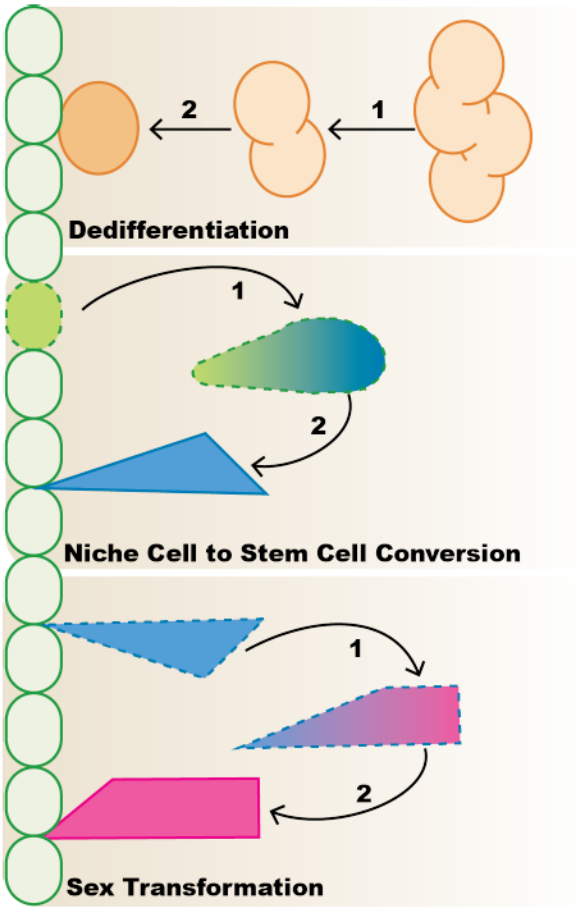
2
1
Dedifferentiation
1
2
Niche Cell to Stem Cell Conversion
1
2
Sex Transformation

CHAPTER 2

Retinoblastoma intrinsically regulates niche cell quiescence, identity, and niche number in the adult *Drosophila* testis

This chapter is a modified version of the manuscript Greenspan LJ and Matunis EL. (2018). Retinoblastoma intrinsically regulates niche cell quiescence, identity, and niche number in the adult *Drosophila* testis. *Cell Rep*, in revision.

Summary

Homeostasis in adult tissues depends on the precise regulation of stem cells and their surrounding microenvironments, or niches. Here we show that the cell cycle inhibitor and tumor suppressor Retinoblastoma (RB) is a critical regulator of niche cells in the *Drosophila* testis. The testis contains a single niche, composed of somatic hub cells, that signals to adjacent germline and somatic stem cells. Hub cells are normally quiescent, but knockdown of the RB homolog Rbf in these cells causes them to proliferate and convert to somatic stem cells. Over time mutant hub cell clusters enlarge and split apart, forming ectopic hubs surrounded by active stem cells. Furthermore, we show that Rbf's ability to restrict niche number depends on the transcription factors E2F and Escargot, and the adhesion molecule E-cadherin. Together this work reveals how precise modulation of niche cells, not only the stem cells they support, can drive regeneration and disease.

Introduction

Stem cells maintain homeostasis within many adult tissues by producing both new stem cells (self-renewal) as well as daughter cells that differentiate (Greenspan et al., 2015). Signals from the surrounding microenvironment where the stem cells reside, called the niche, are vital for promoting stem cell maintenance (Greenspan et al., 2015; Ohlstein et al., 2004). Uncovering how niches regulate stem cells is key to harnessing the regenerative capacity of stem cells for therapeutic purposes after damage. In addition, mis-regulation of cell signaling within stem cell niches can lead to tumor growth and cancer metastases (Dagogo-Jack and Shaw, 2018), underscoring the need for better understanding niche function.

The *Drosophila* testis provides an ideal model system to study stem cell regulation *in vivo* since it contains a well-defined niche where the cell types are easily identified and manipulated genetically. This niche consists of a cluster of quiescent somatic hub cells that signal to the attached germline stem cells (GSCs) and somatic cyst stem cells (CySCs) (**Figure 2.1A**) (Hardy et al., 1979; Kiger et al., 2001). Damage to this niche reveals an unexpected degree of cellular plasticity. Recently we found that genetic ablation of all somatic cyst stem cells induces hub cells to exit quiescence and begin mitotic divisions (Hétié et al., 2014). Surprisingly, this ablation event also leads to the cell fate conversion, or transdifferentiation, of hub cells to CySCs. This change in cell fate is accompanied by the formation of new niches throughout the testis, characterized by the presence of multiple hubs each supporting active stem cells. However, it is still not known if hub cell quiescence and fate must be actively maintained. In addition, the

molecular regulators and cellular behaviors that drive these phenotypes have not been characterized.

The *Drosophila* Retinoblastoma homolog Retinoblastoma-family protein (Rbf) is a key cell cycle regulator that inhibits cell cycle progression by binding and repressing the cell cycle activator E2F and whose activity is controlled through phosphorylation from Cyclins (Sutcliffe et al., 2003). Rbf is known to negatively regulate cell proliferation in many cell types and is a tumor suppressor gene that is down regulated in many cancers (Cheung and Rando, 2013; Dyson, 2016). Here we show a novel role for Rbf in its cell autonomous requirement for maintaining quiescence in terminally differentiated hub cells, and its necessity for hub cell fate. Loss of Rbf in hub cells leads to the activation of E2F driving hub cell proliferation and conversion of hub cells to cyst lineage cells. Rbf also has unexpected effects on this model stem cell system: extended Rbf loss in hub cells causes ectopic niche formation within the testis. Live imaging and lineage tracing reveal that this process is driven by fission of the original hub. Therefore, loss of Rbf in hub cells leads to an increase in the stem cell population via two means: cell-autonomously through the direct conversion of hub cells to stem cells, and non-autonomously through the expansion of the niche. Together our results suggest a mechanism in which cell cycle factors regulate hub cell quiescence and plasticity, and demonstrate how the modulation of niche cells, as opposed to the stem cells they support, can drive regeneration and disease.

Results

Rbf is required to maintain hub cell quiescence

Since hub cell proliferation is one of the first phenotypes observed upon recovery from CySC ablation, we hypothesized that cell cycle inhibitors might play an active role in intrinsically maintaining hub cell quiescence. Retinoblastoma (RB) is a known cell cycle regulator in many mammalian stem cell populations. Loss of RB in frequently dividing spermatogonial stem cells leads to a depletion of the stem cell pool, while loss of RB in the quiescent support cells (Sertoli cells) that contribute to the testis niche leads to Sertoli cell proliferation and dysfunction causing a failure in sperm development (Hu et al., 2013; Rotgers et al., 2014). In the *Drosophila* testis, Rbf is normally expressed broadly, and is detected in all of the cells within the testis apex. These cells include the terminally differentiated hub cells, germ cells, and cyst lineage cells (**Figure S2.1A-A'**). To determine if this cell cycle inhibitor is necessary for the maintenance of hub cell quiescence we used the E132Gal4-UAS-TubGal80^{ts} system, from now on termed E132^{ts}, to conditionally knockdown Rbf specifically in adult hub cells. A complete loss of Rbf protein specifically within the hub, confirmed by immunostaining adult testes with anti-Rbf antisera (**Figure S2.1B-C'**), was observed in E132^{ts}>Rbf-RNAi flies raised at the permissive temperature of 18°C and shifted to 29°C for 7 days to induce RNAi knockdown. To determine if hub cells lacking Rbf can proliferate, we immunostained testes for the mitotic marker Phospho-histone H3 (PH3). PH3 positive hub cells were seen in 26% (n=19/73) and 20% (n=20/101) of testes with Rbf knocked down in the hub ($p<0.0001$, Rbf RNAi A and B respectively) (**Figure 2.1B-D**), compared to E132^{ts}>GFP-RNAi control testes in which we never saw PH3 positive hub cells (n=0/90). To extend

these findings, hub cells lacking Rbf were assessed for incorporation of the thymidine analog ethynyl deoxyuridine (EdU), which labels cells undergoing DNA replication. EdU positive hub cells were seen in 88% (n=23/26) and 60% (n=27/45) of testes expressing two independent Rbf RNAi lines for 7 days (Figure 1B-D), confirming that these hub cells are progressing through the cell cycle. We rarely saw EdU positive hub cells in $E132^{ts}$>GFP-RNAi control testes (n=2/28). In comparison, low levels of S phase labeling have been reported in other studies of wild-type testes (Voog et al., 2008), suggesting that sometimes hub cells may undergo replication. However, ploidy measurements of hub cells (**Figure S2.1I**) suggest that most hub cells are normally diploid. We conclude that in contrast to wild-type hub cells, which are quiescent, hub cells lacking Rbf enter both S and M phase of the cell cycle.

Since hub cells divide in hubs lacking Rbf, we expected the hub cell clusters to increase in size. To assess this, hub volume was measured using 3D reconstructions of testes expressing a bright cytoplasmic GFP transgene in hub cells. Within three days, hub specific knockdown of Rbf led to a significantly larger hub volume than control testes expressing only GFP (**Figure S2.1D-E, H**). Hub volumes continued to increase at 7 and 14 days post induction (**Figure S2.1H**). Additionally, hub cells appeared to spread along the basement membrane of the tissue and protrude into the center of the testis, creating a neck that connected the two sections in some testes, while hubs in control testes remained unchanged (**Figure S2.1F-G**). Altogether these data indicate that Rbf is required in hub cells to actively maintain their quiescent state, and loss of Rbf leads to hub cell proliferation and subsequent enlargement of the hub.

Loss of Rbf in hub cells causes conversion to cyst lineage cells

Since CySC ablation causes loss of hub cell quiescence and drives hub cell to CySC conversion (Hétié et al., 2014), we next asked if loss of Rbf could also change hub cell identity. To assess the fate of hub cells upon Rbf knockdown, the Gal4 Technique for Real-time and Clonal Expression (G-TRACE) (Evans et al., 2009) was used to track hub cells lacking Rbf over time. This lineage tracing system uses a red fluorescent protein (RFP) to mark current Gal4 expression and a green fluorescent protein (GFP) to track cells that originate from the Gal4 expressing cells. When combined with a hub specific Gal4 driver, hub cells expressing this system will appear yellow while cells derived from hub cells that have changed fate will lose RFP expression and retain GFP expression, appearing green. $E132^{ts}$>G-TRACE, Rbf-RNAi flies were shifted to 29°C for 7 days to simultaneously induce marking and Rbf knockdown specifically in hub cells. Testes from these flies frequently had green cells dispersed throughout the niche outside of the hub cell cluster (78%, n=70/90 testes), indicating they had lost their hub cell identity (**Figure 2.2B,D**). In comparison, control testes expressing G-TRACE alone contained yellow hub cells (RFP^+GFP^+) that remained confined to the apical tip of the testis (**Figure 2.2A,C**). As expected based on prior studies using the G-TRACE system in the *Drosophila* testis (Voog et al., 2014), a few green cells were occasionally seen outside of the hub cluster in control testes (25%, n=21/85 testes). This background marking could be due to incomplete repression of Gal4 by Gal80 during part of development or due to effects of the hub-Gal4 driver itself. Importantly, significantly more testes contain green (hub derived) cells outside the original hub cluster when Rbf is knocked down in hub

cells ($p<0.0001$, **Table S2.1**). This indicates that Rbf is required to maintain hub cell fate.

To verify that Rbf knockdown causes hub cells to leave the hub cluster and lose their identity, a second lineage-tracing reporter was used with a different drug inducible hub-specific driver (GS2295-Gal4). Using this system, 21% (n=8/38) of testes lacking Rbf in hub cells showed conversion of hub cells (as indicated by GFP marked cells outside of the hub cell cluster) by 21 days post induction (**Figure S2.2B,D**). In contrast, GFP marked cells were not detected outside of the hub in testes from lineage traced controls (n=0/64 testes) (**Figure S2.2A,C and Table S2.1**). Together with the G-TRACE lineage tracing, these data indicate that Rbf is necessary to maintain hub cell identity.

To determine the identity of lineage-traced cells arising upon hub-specific Rbf knockdown, we immunostained testes with hub, cyst lineage, and germ cell markers. Traced cells close to the hub cluster expressed the CySC marker Zinc Finger Homeodomain 1 (ZFH1, S2B) suggesting that these cells converted into somatic stem cells. These cells also expressed the general cyst lineage marker Traffic Jam (Tj, **Figure 2.2D and Figure S2.2D**), but lacked the hub specific marker Fasciclin III (Fas III, **Figure 2.2F and Figure S2.2B,D**). Traced cells were seen flanking germ cells but did not express the germ cell marker Vasa (**Figure S2.3B**) suggesting they had converted from hub cells to cyst cells. When Rbf was continuously knocked down in hub cells for a longer period of time (14 days), traced cells were seen away from the hub cluster undergoing further differentiation as indicated by expression of the late cyst lineage

marker Eyes Absent (Eya, **Figure 2.2F**). These cells also maintained their male sex identity as staining for the female somatic cell markers Castor and Cut showed no expression in testes with Rbf knocked down in the hub (data not shown). These results indicate that upon Rbf loss, a subset of hub cells convert to CySCs and progress through the cyst lineage differentiation process.

However, converted hub cells did show some aberrant behaviors compared to normal cyst cells. In wild-type testes the only proliferating somatic cells are the somatic cyst stem cells next to the hub (**Figure S2.3C and S2.4A**) (Gönczy and DiNardo, 1996; Inaba et al., 2011). In contrast, traced hub cells were seen proliferating both next to and more than two cell diameters away from the hub (**Figure S2.3D**). This observation suggests that Rbf may also be required for cyst cell quiescence in the adult testis, as has been recently shown to occur in the *Drosophila* larval testis (Dominado et al., 2016). Therefore we speculated that Rbf levels might not be restored in converted cyst cells fast enough to keep them quiescent. To directly address whether Rbf promotes adult cyst cell quiescence, Rbf was knocked down specifically in cyst cells but not CySCs using the EyaGal4 driver (Ma et al., 2014). Loss of Rbf specifically in cyst cells led to an expansion of TJ-positive cells throughout the testis, and these cells were capable of dividing away from the hub, compared to controls, which only showed proliferating somatic cells within two cell diameters from the hub (**Figure S2.4A-B**). Rbf knockdown in cyst cells also led to a non-autonomous expansion of undifferentiated germ cells throughout the adult testis as indicated by the TJ-negative DAPI bright nuclei (**Figure S2.4A-B**), consistent with previous reports in the larval testis (Dominado et al., 2016).

Interestingly, the CySC marker ZFH1 remained restricted to the apex in testes lacking Rbf in the cyst cells (**Figure S2.4C-D**), suggesting that dividing cyst cells did not revert to a stem cell like state. Altogether, these data suggest that Rbf is required in cyst cells to maintain their quiescence but not their differentiation state, demonstrating a contrast to its role in hub cells.

Live imaging reveals dynamics of hub cell conversion *in vivo*

The G-TRACE lineage tracing system (Evans et al., 2009) combined with our established techniques for live imaging (Greenspan and Matunis, 2017; Sheng and Matunis, 2011), affords us the opportunity to visualize how and from where within the hub cell fate conversion occurs *in vivo*. Testes co-expressing Rbf RNAi and the G-TRACE system in hub cells for 10 days were imaged live for 12-18 hours. As we expected based on our fixed images, hub cells were seen dividing in most testes (n=18/27 testes, **Movie S2.1**) within different regions of the hub cluster, including the portion along the basement membrane, within the protrusion, and in the neck connecting these two sections. However, cell division did not correlate with those cells that converted to a cyst lineage fate since daughter cells could be seen remaining in the hub cluster throughout the duration of the movie after division (**Movie S2.1**). Live imaging further revealed that these hub cells are very dynamic. Hub cells could be seen moving between different regions of the hub cluster (n=18/27 testes, data not shown) as well as leaving the hub cell cluster entirely (n=15/27 testes), mostly from the basement membrane but occasionally from the neck and protrusion (**Movie S2.1**). Since a change in hub identity is indicated by loss of red fluorescence signal, we asked whether the cells that migrated away from

the hub cluster lost their hub cell fate. To answer this question a subset of hub cells were analyzed to determine their loss of fluorescence over time (**Figure 2.3A-B, Movie S2.3**). Hub cells with Rbf knocked down could be seen exhibiting three different behaviors throughout the course of the movie. Some cells maintained their RFP expression and stayed within the hub cluster, some cells started to lose their RFP expression but stayed within the hub cluster, and a third category lost most of their RFP expression and migrated away from the main hub cluster (**Figure 2.3C**). Linear regression analysis showed a significant correlation between a hub cell's displacement and its loss of RFP expression, meaning that cells that migrated the farthest from their original position tended to lose the most fluorescence (**Figure 2.3C**). In contrast to hub cells lacking Rbf, hub cells in control testes expressing the G-TRACE system alone were never seen dividing or leaving the main hub cluster during live imaging (n=0/6 testes). In addition, no correlation was seen between RFP expression levels and displacement amongst hub cells expressing G-TRACE alone in control testes, since these cells did not lose RFP expression or migrate far from their original position (**Figure 2.3C, Movie S2.2**). Together this live imaging data reveals that upon Rbf loss some hub cells start to lose their hub identity before migrating away, further supporting the conclusion that Rbf is required for hub cell fate.

During our live imaging of hubs lacking Rbf we occasionally observed cells dying within the hub or being extruded from the hub first then shrinking, eventually losing fluorescence (**Figure 2.3A-B, Movie 2.2**). This observation, together with the previous findings that Retinoblastoma is known to inhibit apoptosis in certain tissues (DeGregori

et al., 1997; Dyson, 2016; Tanaka-Matakatsu et al., 2009), prompted us to assay for expression of the cleaved caspase Dcp1, which marks dying somatic cells in the testis (Hasan et al., 2015; Yacobi-Sharon et al., 2013). Dcp1-positive hub cells were occasionally seen when Rbf was specifically knocked down in hub cells (n=9/44 and n=3/53 testes for Rbf RNAi A and B respectively, **Figure 2.3D-F**), but undetectable in hubs of GFP RNAi control testes (n=0/61 testes). This finding indicates that Rbf is not only required to maintain hub cell quiescence and fate, but also to prevent hub cell apoptosis. However, the level of apoptosis that occurs upon Rbf knockdown must be minimal compared to the level of cell proliferation, since overall hub size increases with time upon Rbf knockdown.

Rbf acts through E2F to maintain hub cell quiescence and fate

Rbf is known to inhibit the cell cycle by binding to the transcriptional activator E2F and preventing its activity. Upon hyper-phosphorylation by Cyclin D/Cdk4, Rbf releases E2F allowing it to transcribe its target genes, many of which drive cell cycle progression (Dyson, 2016). However, Rbf is also known to have E2F-independent roles (Korenjak et al., 2012). Since knockdown of Rbf alone leads to cell cycle activation, we hypothesized that knockdown of Rbf and E2F simultaneously in hub cells could be sufficient to prevent hub cell proliferation. To ask whether Rbf acts through E2F to regulate hub cell quiescence and fate, we simultaneously removed Rbf and E2F specifically in hub cells for 14 days and assessed their proliferation status using the mitotic marker PH3. Testes lacking both Rbf and E2F in hub cells showed a complete rescue of hub size, and proliferating hub cells were undetectable (n=0/42 testes, **Figure 2.4D and Table 2.1**).

For comparison, Rbf knockdown alone yielded dividing hub cells in 52% of testes (n= 29/56, **Figure 2.4A and Table 2.1**). To ensure this rescue was specific to E2F, flies expressing Rbf RNAi and a generic RNAi (GFP RNAi) still showed proliferating hub cells similar to Rbf RNAi alone (n=4/15, **Table 2.1**). As expected, E2F knockdown alone showed no hub cell proliferation phenotype, since hub cells are normally quiescent (**Figure 2.4C and Table 2.1**). Together these data indicate that Rbf acts through E2F to maintain hub cell quiescence. Since testes lacking both Rbf and E2F in hub cells contain hubs that are phenotypically indistinguishable from wild-type hubs this suggests that loss of E2F is sufficient to suppress both hub cell proliferation and the hub to cyst lineage conversion phenotype induced by Rbf knockdown alone. If conversion were still occurring without proliferation, we would expect a loss of hub cells over time, which is not seen.

Esg overexpression does not rescue hub cell quiescence upon Rbf knockdown

To identify genes that could be acting downstream of E2F we considered the Snail family transcription factor Escargot (Esg), since loss of Esg in hub cells causes hub cell to cyst lineage conversion (Voog et al., 2014) but not excessive hub cell proliferation. Instead, this conversion causes a loss of hub cells over time, leading to testes completely lacking hubs. In contrast, testes lacking Rbf in hub cells develop increasingly larger hubs with time as well as hub cell to cyst lineage conversion. Thus we hypothesized that Esg is working downstream of or in a parallel pathway to Rbf/E2F to regulate quiescence. To test this hypothesis we overexpressed Esg specifically in hub cells while simultaneously knocking down Rbf in the hub, and assayed testes for hub cell proliferation. Mitotic

(PH3-marked) hub cells were detected in 35% of testes expressing Esg and Rbf RNAi simultaneously (n=17/48, **Figure 2.4F**), which was not statistically different from the 22% seen with Rbf RNAi alone (n=18/83, **Table 2.1**). This result indicates that overexpression of Esg is not sufficient to suppress the hub cell proliferation phenotype induced by loss of Rbf, and thus suggests that Esg does not play a role in regulating hub cell quiescence.

Loss of Rbf in hub cells results in ectopic niche formation

While more than half of testes that have undergone CySC ablation are able to recover their cyst cells after damage, many (42%) of these recovering testes contain multiple niches, rather than the single niche found in wild-type testes (Hétié et al., 2014). Since mis-regulated niche formation may underlie cancer metastases (Greaves et al., 2006) and Retinoblastoma is known to be down regulated in many forms of cancer (Dyson, 2016), we asked if knockdown of Rbf in hub cells for 14 days is sufficient to drive ectopic niche formation. Ectopic hubs were identified as clusters of Fas III positive cells no longer connected to any other cluster of hub cells. Ectopic hubs were detected in 18% (n=15/85) and 25% (n=29/117) of testes with Rbf knocked down in the hub compared to GFP RNAi controls which always contained a single hub (n=0/61) (**Figure 2.5A-C, Table 2.1**). Ectopic hubs expressed multiple hub markers including Fas III, Armadillo, Hedgehog, and Unpaired (**Figure 2.5A-F and Figure S2.5A-D**). In addition, ectopic hubs were surrounded by both germline stem cells, as indicated by Vasa-positive cells with a dot fusome, and cyst stem cells, as demonstrated by ZFH1 staining (**Figure 2.5D-F**). Furthermore, the stem cell marker Stat92E was also expressed in cells surrounding the

ectopic hubs **(Figure S2.5E-G**). Together these data indicate that each ectopic hub is in fact an ectopic stem cell niche, which are phenotypically indistinguishable from the ectopic niches that form upon CySC ablation (Hétié et al., 2014). Therefore, Rbf is necessary to prevent ectopic hub formation, and loss of Rbf in the hub can cause multiple functional niches to form within the testis.

Knockdown of E2F, over-expression of Esg, or over-expression of E-cadherin prevents ectopic hub formation

Since Rbf is required to prevent ectopic hub formation, we next wanted to ask whether the same downstream components that influence quiescence and changes in fate also regulate ectopic hub formation. Therefore we simultaneously removed Rbf and E2F specifically in hub cells by RNAi knockdown for 14 days ($E132^{ts}$> Rbf-RNAi, E2F RNAi) and assayed for ectopic hubs using the hub marker Fas III. We saw a complete rescue of the ectopic hub phenotype (n=0/42 testes with ectopic hubs, **Figure 2.6D, Table 2.1**) compared to Rbf knockdown alone or Rbf knockdown combined with a generic GFP RNAi (n=15/85 or n=5/19 respectively, **Figure 2.6A, Table 2.1**). As expected, E2F knockdown alone did not cause ectopic hub formation (n=0/53 testes with ectopic hubs, **Figure 2.6C, Table 2.1**). These results suggest that Rbf acts through E2F to prevent ectopic hub formation. Since Esg may work downstream of Rbf/E2F to regulate hub cell to cyst stem cell conversion, we next asked if Esg plays a role in the formation of multiple hubs. We saw a significant rescue in ectopic hub formation when Esg was overexpressed simultaneously with Rbf knockdown in hub cells (n=1/48, **Figure 2.6F, Table 2.1**). This rescue was surprising since loss of Esg alone in hub cells is not

sufficient to cause ectopic hub formation (Voog et al., 2014 and data not shown). As expected, ectopic hubs were never seen when Esg was overexpressed in hub cells (n=0/35 testes with ectopic hubs, **Figure 2.6E, Table 2.1**), since Esg is normally expressed in the hub (Hétié et al., 2014; Voog et al., 2014). Together these data indicate that both loss of Esg, which has been shown to regulate cell adhesion, and activation of E2F targets, such as those that stimulate cell proliferation, are necessary for the formation of ectopic niches.

Since the adherens junction molecule E-cadherin is positively regulated by Escargot in the *Drosophila* trachea (Tanaka-Matakatsu et al., 1996) and a loss of E-cadherin is seen when Escargot is knocked down in the hub (Voog et al., 2014), we wanted to determine if E-cadherin expression was altered in hub cells upon Rbf knockdown. To determine E-cadherin expression levels, testes with Rbf knocked down in hub cells for 7 days were immunostained with E-cadherin antisera and protein levels assessed by fluorescence intensity. A significant reduction in the levels of E-cadherin expression was seen throughout the entire hub in testes where Rbf had been knocked down specifically in hub cells compared to GFP RNAi controls (**Figure S2.6**), suggesting that Rbf can regulate levels of E-cadherin mediated adhesion. To next test the role that cell adhesion plays in the formation of ectopic hubs, E-cadherin was overexpressed simultaneously with Rbf RNAi knockdown in hub cells for 14 days. This simultaneous expression yielded a significant suppression of ectopic hub formation (n=2/73, **Figure 2.6H and Table 2.1**). These testes still contained enlarged hubs with dividing hub cells (**Table 2.1**) suggesting that proliferation alone is not sufficient to drive ectopic hub formation. As expected,

multiple hubs were never seen when E-cadherin alone was over-expressed in the hub (**Figure 2.6G and Table 2.1**). These data further support the model that adhesion must be down-regulated in hub cells upon Rbf knockdown in order for ectopic niches to form, and that up-regulating adhesion molecules is sufficient to suppress their formation.

Ectopic niches can form through splitting of the original hub

The formation of new stem cell niches may be useful for regenerating tissue after injury but its mis-regulation could lead to cancer (Greaves et al., 2006). Because *de novo* niche formation is challenging to study *in vivo*, we wanted to better characterize the cellular aspects of ectopic hub formation upon Rbf knockdown. Theoretically, new niches could occur in two ways: the original hub could split apart (niche fission) as seen in intestinal crypts (Withers and Elkind, 1970), or individual cells could move out of the hub and establish new niches (seeding). To test if either possibility was occurring, *Drosophila* testes expressing GFP specifically in the hub were imaged live for 12-18 hours after 13 days of Rbf knockdown. Clusters of hub cells were seen both spreading across the periphery of the testis along the basement membrane and protruding towards the center of the testis as previously seen in our fixed images (**Figure S2.1G**). This dichotomy in behavior sometimes drove clusters of hub cells far enough apart to occasionally cause a single cluster of hub cells to split in to two clusters (**Movie S2.4**). Fixing and immunostaining testes for the hub marker Fas III after live imaging confirmed that the membranes of these multiple hub cell clusters were no longer connected (data not shown), verifying that ectopic hubs can arise from fission of the original hub. While this result does not rule out the seeding mechanism, live imaging of testes expressing Rbf

RNAi and the G-TRACE system in hub cells for 10 days (described above) did not show re-expression of the hub cell driver in cells leaving the hub, as indicated by loss of RFP expression. This observation suggests that converted hub cells and their progeny are most likely not involved in the formation of new hubs. Altogether these data support a model that ectopic niches form due to fission of an enlarged hub, and not the seeding of cells leaving the hub.

Discussion

In many tissues, stem cells have the ability to self renew through either asymmetric or symmetric divisions. However, upon damage, other mechanisms may be required to replenish the lost stem cells in order to maintain homeostasis, as has been demonstrated in the crypt base columnar stem cells of the mouse intestinal niche (Beumer and Clevers, 2016). In the *Drosophila* testis, two additional modes of regeneration have been discovered. Dedifferentiation of spermatogonia allows for germline stem cells to be replenished after loss (Brawley and Matunis, 2004), while direct conversion of niche cells to cyst stem cells regenerates the somatic stem cell population after ablation (Hétié et al., 2014). These studies provide vital insight into cellular plasticity helping to advance regenerative therapies for tissue repair. However, un-regulated cellular regeneration can cause cells to over-proliferate, leading to cancer. Thus, understanding the mechanisms that underlie such processes is key to providing tissue regeneration therapies without inducing undesirable and unintended side effects.

The tumor suppressor Retinoblastoma (RB) is mutated in many forms of cancer driving cellular over-proliferation (Burkhart and Sage, 2008). While RB is best known for its role in cell cycle control, many studies have shown additional functions for RB in regulating endoreplication, apoptosis, genome stability, and cellular differentiation (Calo et al., 2010; Cayirlioglu et al., 2003; Coschi et al., 2014; DeGregori et al., 1997; Dyson, 2016; Tanaka-Matakatsu et al., 2009; Thomas et al., 2001). Although we have previously shown that overexpression of Cyclin D/ Cyclin dependent kinase 4 (Cdk4) is sufficient to induce hub cell divisions and cell fate conversion in the *Drosophila* testis (Hétié et al., 2014), here we show that the RB homolog Retinoblastoma family like protein (Rbf) is required to actively promote hub cell quiescence and identity. Therefore this is the first molecule we have identified that acts under normal conditions, as opposed to damaged conditions, to maintain the terminally differentiated state of hub cells. Loss of Rbf in hub cells causes hub cells to proliferate and convert to CySCs, which we show is mediated through the activity of Rbf's canonical binding partner E2F. This newly uncovered function of Rbf suggests that Rbf can regulate cell fate. Upon Rbf knockdown in the hub, some cells maintain their hub cell fate, as evidenced by the appearance of hub cells upon prolonged Rbf knockdown, while other cells convert to a cyst lineage fate. Why this is the case is an intriguing question for future studies. Since hub cells could be seen starting to lose hub identity while still within the cluster (**Fig. 2.3A-C, Movie S2.1, and Movie S2.3**) it is most likely not autocrine signaling from hub cells that maintain their identity. One possibility could be that the rate of proliferation is greater than the rate of conversion allowing for some hub cells to remain hub cells while others do not. And perhaps in the case of Escargot knockdown in hub cells (Voog et al., 2014), the rate of proliferation is

too slow for any hub cells to be maintained so all convert to cyst lineage cells. Another possibility could be that the hub cells are more heterogeneous than initially thought and only a subset of hub cells are capable of maintaining their identity. Little is currently known about hub cell heterogeneity, but *in situ* hybridization to whole testes for transcripts from the *magu* gene suggests this possibility (Zheng et al., 2011). Single cell sequencing of hub cells would provide great insight into the diversity of this cell population.

In addition to being required in hub cells, we show that Rbf is required to regulate somatic cyst cell quiescence but not stem cell fate. Loss of Rbf in cyst cells causes them to proliferate away from the hub but does not cause these cells to express stem cell markers. This finding suggests that even within the same tissue, Rbf can have different functions within varying somatic cell types. This result is surprising since both hub cells and cyst cells are derived from a common pool of somatic gonadal precursor cells in the *Drosophila* embryo (Le Bras and Van Doren, 2006).

Besides regulating niche cell quiescence and fate, here we show that Rbf plays a role in regulating niche number in the *Drosophila* testis. Prolonged loss of Rbf in hub cells causes hub cells to form functional ectopic niches. Multiple direct or indirect downstream targets of E2F play a role in controlling this process since overexpression of either the transcription factor Escargot or the adhesion molecule E-cadherin is sufficient to suppress ectopic hub formation but not hub cell proliferation. These findings lead to the intriguing question of what is minimally required to build a new niche. While niche

fission is known to occur within the mammalian intestinal crypt during postnatal development (Maskens and Dujardin-Loits, 1981), regeneration after damage (Cairnie and Millen, 1975; Wright and Al-Nafussi, 1982), and upon mutation of the Wnt signaling pathway regulator APC (Wasan et al., 1998), little is known about the mechanisms that drive these processes. Our fixed and live imaging of Rbf knockdown in hub cells of the *Drosophila* testis suggests that a combination of niche cell proliferation with a loss of cell-cell adhesion can lead to the splitting of the hub causing niche fission. Since crypt fission may play a role in the propagation of cancerous cells within the mammalian intestine (Greaves et al., 2006), better understanding the mechanisms that drive this process will provide vital therapeutic targets.

Great heterogeneity is often observed between the cells that comprise a single human tumor. This heterogeneity can arise from genomic instability within a cell population (Carter et al., 2006), or due to environmental cues driving vast changes in cellular morphology, proliferation, gene expression, and other cellular processes (Dagogo-Jack and Shaw, 2018; Marusyk and Polyak, 2010). Here we show that loss of the tumor suppressor gene Rbf in the hub cells of the *Drosophila* testis can lead to an excess of many different cell types within the tissue through non-autonomous and autonomous means. Increasing niche cell number allows for more germline and cyst stem cells to be maintained, presumably due to an increase in the physical size of the niche, niche signals, or both. In addition, Rbf knockdown in the hub leads to the increase of cyst lineage cells due to the conversion of hub cells to CySCs. Both the non-autonomous and autonomous affects lead to an increase in stem cell number, which consequently leads to an increase

in early-differentiated daughters, thus driving an expansion of different cell populations within the tissue. Furthermore, the formation of ectopic niches within the testis leads to stem cells residing in aberrant locations, demonstrating how a mutation in a particular cell type (in this case, specifically within niche cells) can drive many different phenotypes. Thus understanding the cell or origin for many cancers may provide better insight into how certain cancers progress. Future studies dissecting whether quiescent stromal support cells contribute to cancer more generally, and whether Rbf family members act in multiple niches will further illuminate the role of niche cells, and not just the stem cells they support, in tissue regeneration and disease progression.

Materials and Methods

Drosophila husbandry and strains

Flies were raised on a standard yeast/molasses medium (1212.5mL water, 14.7mL agar, 20.4g yeast, 81.8g cornmeal, 109.1ml molasses, 10.9mL tegosept, 3.4mL propionic acid, 0.4mL phosphoric acid/ per tray of 100 vials) supplemented with dry yeast at 18°C unless otherwise indicated. Male flies between 0-5 days of age were used for all experiments and subject to different conditions as noted within the text, figures, legends, and methods. The following stocks were used EyaA3-Gal4 (from S. DiNardo laboratory), hsflp/hsflp; tub>CD2>GAL4, UAS-GFP/CyO (from B. Ohlstein laboratory), ywhsFlp/ywhsFlp; UAS-esg/CyO; UAS-LacZ/TM2 (from A. Tomlinson laboratory), HH-Lacz/TM3,Sb (from K. Vani laboratory), and UAS-Shg/UAS-Shg (also known as E-cad) (from J.P. Vincent laboratory). Other stocks were from the Bloomington Drosophila Stock Center (BDSC). For a complete list of strains see the key resource table.

Transgene Induction

Heat induction: Flies containing a temperature sensitive TubGal80 were grown at the permissive temperature 18°C and shifted to the non-permissive temperature 29°C for either 3, 7, or 14 days as indicated to induce transgene expression of RNAi lines or over-expression lines.

Drug induction: RU486 powder was dissolved in 200 proof ethyl alcohol to make a 50mg/mL stock solution stored at -20°C. For *GS2295-Gal4* induction, 0-5 day old flies raised at 25°C were placed in vials with filter paper soaked in 125µL of 2mg/mL of

RU486 in apple juice and 2.5µL green food coloring. Flies were transferred to fresh drug/apple juice vials daily for 3 days at 25°C. Flies were checked for green-dyed guts to ensure drug consumption, then transferred to a standard yeast/molasses food for 18 days at 25°C prior to dissecting, fixing, and immunostaining.

In vivo EDU labeling (Leatherman and Di Nardo, 2008)

For *in vivo* labeling of cells undergoing S phase, flies were dissected in Schneider's *Drosophila* medium then testes still in their cuticles transferred to a glass dissection dish with 500µL of 10µM EDU in Schneider's *Drosophila* medium for 20 minutes at room temperature. After soaking, testes were immediately transferred to a microtube with fixation solution (4% paraformaldehyde in 1X PBS with 0.1% Trition X-100) for 25 minutes at room temperature on a nutator. Testes were then washed in 1X PBX (1X PBS with 0.1% Trition X-100) followed by incubation in 250µL of the ClickIT reaction cocktail (2.5µL EDU buffer additive diluted in 22.5µL of dH_20, 25µL 10X reaction buffer diluted in 190µL of dH_20 with 10µL 100mM $CuSO_4$, and 0.625 µL Alexa fluor azide 555) as per the kit's instructions for 30 minutes to visualize EDU. After the reaction, testes were washed in 1X PBX, blocked, and stained as described below.

Dissection and Immunohistochemistry (Matunis et al., 1997)

Dissection: Flies were anesthetized using CO_2 then dissected with the cuticle still surrounding the testes in 1X Becker Ringer's solution (111 mM NaCl, 1.88 mM KCl, 64 µM NaH_2PO_4, 816 µM $CaCl_2$, 2.38 mM $NaHCO_3$) (Ashburner, 1989) and transferred immediately to fixation solution (4% paraformaldehyde in 1X PBS with 0.1% Trition X-100) for 22 minutes at room temperature on a nutator.

Immunohistochemistry: All washes were conducted using 1X PBX (1X PBS with 0.1% Trition X-100) except the final wash before adding mounting media in which 1X PBS was used. Testes were blocked overnight at 4°C in 1X PBX with 3% BSA, 0.02% NaN_3, and 2% goat or donkey serum. Antisera was diluted in 1X PBX with 3% BSA and 0.02% NaN_3. Testes were immunostained in primary antisera overnight at 4°C with the exception of mouse anti-Eyes Absent which was incubated at 4°C for three days and rabbit anti-STAT92E which was incubated at 4°C for one day and room temperature for one day. Secondary antibodies were diluted in 1X PBX containing 3% BSA and 0.02% NaN_3 and testes incubated overnight at 4°C. The nuclear counterstain 4,6-diamidino-2-phenylindole (DAPI) (Millapore/Sigma) was added to most secondary antibody dilutions at a final concentration of 1μg/mL. All testes were mounted in Vectashield antifade mounting medium (Vector Laboratories).

All polyclonal antibodies were stored in a 1:2 dilution at -20°C, and all monoclonal antibodies were stored at 4°C except for mouse anti-Phospho-Histone H3 and mouse anti- β-Galactosidase which were stored at -20°C in a 1:2 glycerol dilution. Antisera was used at the following final concentrations: mouse anti-Fasciclin III (1:50), mouse anti-Phospho-Histone H3 (1:400), guinea pig anti-Traffic Jam (1:20,000), rabbit anti-Vasa (1:200), mouse anti-Rbf (1:10), chick anti-GFP (1:10000), rabbit anti-dsRed (1:10000, goat anti-dsRed (1:500), mouse anti-Discs Large (1:50), mouse anti-Eyes Absent (1:10), mouse anti-Armadillo (1:50), guniea pig anti-Zfh1 (1:1000), rabbit anti-cleaved *Drosophila* Dcp1 (1:200), mouse anti-hu-li tai shao (1B1) (1:50), mouse anti- β-

Galactosidase (1:1000), rabbit anti-Stat92E (1:1000), rat anti-DE-cadherin (1:20), rabbit anti-Castor (1:50), mouse anti-Cut (1:20).

All Fluor 488 secondary antibodies were used at a final concentration of 1:400. All other secondary antibodies were used at a final concentration of 1:200.

Lineage Tracing

In the following genotypes, expression of the Gal4 driver caused permanent expression of GFP in hub cells and their descendants. Marked cells were detected by immunostaining. Testes with GFP cells outside the confines of the hub cluster that no longer expressed hub markers were considered positive for converting cells. The hub cluster was defined as either hub-Gal4 expressing cells marked by RFP for lineage tracing using the G-TRACE system, or Fasciclin III positive cells for lineage tracing using the alternative marking system. To trace hub cells after Rbf knockdown, *E132Gal4/Y; UAS-GTRACE/+; TubGal80^{ts}/UAS-Rbf RNAi* flies were raised at 18°C and 0-5 day old males shifted to 29°C for 7 or 14 days as indicated. *E132Gal4/Y; UAS-GTRACE/+; TubGal80^{ts}/+* flies lacking Rbf RNAi were processed in parallel to control for age and temperature. For the alternative lineage tracing method, *GS2295-Gal4/Tub>CD2>Gal4,UAS-GFP; UAS-Flp/UAS-Rbf RNAi* flies were raised at 25°C and 0-5 day old males fed RU486 for 3 days then allowed to recover for 18 days at 25°C as described above. *GS2295-Gal4/Tub>CD2>Gal4,UAS-GFP; UAS-Flp/+* flies lacking Rbf RNAi were processed in parallel to control for age, temperature, and drug consumption.

Extended Live Imaging (Greenspan and Matunis, 2017)

Flies were dissected in 1X Becker Ringer's solution (111 mM NaCl, 1.88 mM KCl, 64 μM NaH_2PO_4, 816 μM $CaCl_2$, 2.38 mM $NaHCO_3$) (Ashburner, 1989) and testes completely removed from the cuticle and separated from the accessory glands. Testes were mounted on a 35mm glass bottom dish with a 10mm microwell (MatTek Corporation). Imaging dishes were coated with 200μL of 1mg/mL of poly-L-lysine dissolved in 0.1M Trizma buffer pH 8.5 for at least one hour then rinsed with sterile dH_20 prior to testis mounting. Testes were cultured in either 500μL or 1000μL of Schneider's *Drosophila* medium pH 7 or Shields and Sang M3 Insect medium supplemented with 15% fetal bovine serum (v/v), 0.5X penicillin/streptomycin, and 0.2mg/mL insulin from bovine pancreas dissolved in acidified water. Live images were acquired using a Zeiss LSM 780 microscope. Up to nine different positions per dish were imaged using a programmable *xy* stage. Images were acquired in 25 or 10 minutes intervals for up to 18 hours. Z stacks ranging 30μm with 1.25μm steps were acquired for each time point. Only testes that contained a strong fluorescent signal and minimal sample drift in the *x*, *y*, and *z* planes throughout the movie were included for analysis. Samples whose hub cells were too far away from the coverslip to follow individual cellular behaviors, or those testes with a lot of movement due to muscle sheath contraction were excluded. After completion of live imaging, culture media was removed from the imaging dish and testes fixed and stained directly in the dish as described above.

Microscopy and Image Analysis

Image acquisition: Fixed images were obtained using either a Zeiss LSM 5 Pascal equipped with a 63x oil immersion objective, 405nm diode, 488nm ArKr, and 543nm HeNe lasers with digital zoom or a Zeiss LSM 700 (JHU SOM microscope facility)

equipped with a 63x oil immersion objective, 405nm diode, 488nm solid-state, 561nm solid-state, and 639nm diode lasers with digital zoom. A Zeiss LSM 780 microscope (JHU SOM microscope facility) equipped with a 63x oil immersion objective, 405nm diode, 488nm Ar, 561 solid-state, and 639 diode lasers with digital zoom was used to acquire all live imaging, fixed images taken from those samples imaged in real time, and those used to measure hub volume. Images were acquired using either Zeiss LSM or Zen software. All Z stacks through the testis tissue had a step size of 1.25μm except for Z stack used in ploidy and E-cadherin fluorescence measurements in which a 0.5μm step size was used.

Image processing: Images acquired using Zeiss LSM or Zen software were processed using Fiji or IMARIS software. Brightness for individual channels from single confocal slices was enhanced using Fiji, then each channel overlaid to form a merged image. All 3D reconstructions were created in IMARIS using acquired Z stacks and the volume tool to create a composite image. Brightness for individual channels was also enhanced within the IMARIS software.

Quantification and Statistical Analysis

Hub cell proliferation quantification

To quantify hub cell divisions, testes were subject to EDU labeling to label cells in S phase (as described above) and/or immunostained with the mitotic marker Phospho-Histone H3. Testes with EDU and/or PH3 marked cells within the confines of the hub cluster were considered positive for dividing hub cells. The hub cluster was defined as

those cells marked by the hub membrane marker Fasciclin III. Testes that had no EDU incorporation throughout the entire tissue were excluded.

Apoptosis quantification

To quantify dying hub cells, testes were immunostained with the apoptotic marker cleaved *Drosophila* Dcp1, and the hub cluster indicated by the hub membrane marker Fasciclin III. Since some Dcp1 labeling could be seen in non-dying cells, dying hub cells were considered only those cells within the confines of the hub cluster in which Dcp1 labeled the entire cell. These cells tended to be smaller in size due to cell shrinking upon apoptosis activation.

Ectopic hub quantification

To quantify ectopic hubs, testes were immunostained with the hub membrane marker Fasciclin III. Z stacks were acquired to include the entire hub range. Hub clusters whose membranes were no longer connected in any Z planes were considered separate hubs. Testes with more than one hub cluster were considered positive for ectopic hubs.

Hub volume measurement

To determine hub volume upon Rbf knockdown, Z stacks of fixed testes whose hub cells expressed a bright cytosplasmic GFP and Rbf RNAi for 3, 7, or 14 days as indicated were acquired to include the entire hub range. Sibling flies that did not express Rbf RNAi were used to control for age and temperature. A surface rendering of the entire hub was generated using the surface tool with default parameters within IMARIS software. To

generate the surface rendering, only a segment of the testis with the hub, as indicated by the GFP channel, was included. A surface area detail level of 0.25μm was utilized with an absolute intensity that contained at least 10 voxels. The GFP fluorescence intensity threshold was adjusted for each surface rendering so that the entire hub was included within the object but bounded by Fasciclin III membrane staining. GFP expression outside the Fasciclin III bounds was considered to be converting hub cells and was excluded from hub volume measurements. Once the surface rendering was created, the volume could be automatically measured using the statistics tab.

Live cell tracking and fluorescence intensity measurements

To track cell behavior over the course of the movie, individual hub cells were randomly selected from 5 GTRACE only control movies and 7 GTRACE; Rbf RNAi movies where flies had been shifted to 29°C for 10 days prior to live imaging. Only movies acquired with 16 bits at 10min time point intervals were utilized for fluorescence quantification and testes that had too much sample drift in the *x*, *y*, or *z* planes were excluded. Cells were tracked manually using the Spots tool within IMARIS software. Hub cell diameter was set at 4μm for the XY plane and 4μm for the Z plane. Cells were tracked using the red channel only, by manually clicking on the cell at the first and last time point. Fluorescence intensity and the X, Y and Z coordinates were automatically measured for the first and last time points using the Spots function. For each cell, percent of red fluorescence intensity remaining was calculated using the following formula:
% loss = 1 + (fluorescence at last time point – fluorescence at first time point)/ fluorescence at first time point. Displacement was calculated using the following

formula: $d = \sqrt{((x_2-x_1)^2 + (y_2-y_1)^2 + (z_2-z_1)^2)}$. Since some movies were longer in time than others each measurement was calculated for the last common time point T91. For distance values of hub cells after CySC ablation, hub cells were tracked as described above for every time point and distance automatically calculated in IMARIS.

E-cadherin fluorescence intensity measurements

To measure levels of E-cadherin expression, testes were immunostained with E-cadherin and DAPI. Z stacks with a 0.5μm step size were acquired to include the entire hub range. Fluorescence signal was acquired at the same gain in the linear range for all samples. Fluorescence intensity was measured using FIJI software. All stacks containing the hub were merged into a single summed slice and Ecadherin fluorescence intensity was measured by drawing an object around the entire hub and using the measure feature. The corrected total cell fluorescence (CTCF) was then calculated by taking the integrated density and subtracting the area times the mean of 3 fluorescence background readings. The CTCF for E-cadherin fluorescence was then normalized over the CTCF for the DAPI channel, which was calculated in the same manner. The normalized E-cadherin fluorescence measurements were compared for testes expressing Rbf RNAi in their hub cells to those expressing GFP RNAi in their hub cells for 7 days.

Ploidy Measurements

To determine the normal ploidy of hub cells, CTCF measurements were calculated, as described above, for the DAPI channel of control testes (testes from flies expressing GFP RNAi in their hub cells for 7 days). The CTCF measurement for the entire hub was then

divided by the number of hub cells within each hub to determine the CTCF DAPI reading per hub cell. CTCF DAPI measurements of hub cells were then divided by the mean CTCF DAPI measurement of all sperm cells measured to determine ploidy. To measure DAPI fluorescence of sperm cells, seminal vesicles were opened up to allow sperm to be mounted on the same slide as testes. Z stacks with a 0.5μm step size were acquired to include many sperm. Stacks containing many sperm were merged into a single summed slice. To measure the DAPI fluorescence of multiple sperm at a time a ROI map was generated in FIJI with a threshold of 4626 - 65535. Only entire sperm that were in the field of view were measured. CTCF DAPI measurements were then calculated for each sperm.

Statistical Analysis

For all quantifications, *n* represents the number of testes analyzed. Statistical significance was expressed as P values and determined using a Fisher's exact test for most measurements except hub volume, E-cadherin fluorescence measurements in which an unpaired t test with Welch's correction was used. Linear regression analysis was used to compare displacement of hub cells over time to the percent of red fluorescence remaining. All statistical tests were run using PRISM 6 software. (*) denotes $p<0.05$, (**) denotes $p<0.01$, (***) denotes $p<0.001$, and (****) denotes $p<0.0001$ and (*ns*) denotes values that were not significant. Error bars represent standard deviation.

Bar graphs and tables indicate the percent of testes with a certain phenotype out of all the testes analyzed with that genotype. Scatterplots show raw data of the entire distribution of values observed with the average reported as a horizontal black line and bars

representing the standard deviation above and below the average. XY graph shows individual hub cells for each genotype plotted as displacement versus percent red fluorescence remaining. Linear regression lines were generated for each genotype based on the calculated R^2 values.

Figures

Figure 2.1: Hub cells lose quiescence upon knockdown of Rbf. (A) Schematic of *Drosophila* testis stem cell niche, which contains a specialized microenvironment that consists of somatic hub cells (green) that signal to the attached germline stem cells (GSCs, dark gray) and somatic cyst stem cells (CySCs, dark blue). Differentiating spermatogonia (light gray) are enveloped by cyst cells (light blue), and are displaced from the testis apex. (B) Bar graph showing the percent of testes containing dividing hub cells as measured by either EDU incorporation indicating cells in S phase (red bars) or phospho-histone H3 staining (PH3) indicating cells in mitosis (green bars). Two independent UAS-RNAi lines, labeled A or B accordingly, were expressed with an E132Gal4;;TubGal80^{ts} driver to control knockdown of Rbf specifically in the hub. Testes expressing either RNAi line showed a significant difference in EDU incorporation and PH3 staining in hub cells when compared to a UAS-GFP RNAi control. (C-D) Single confocal sections through the testis apex immunostained for EDU (S phase cells, red), Fas III (hub, membranous green), PH3 (mitotic cells, nuclear green), TJ (cyst lineage, white) and DAPI (nuclei, blue). Merged and single channel images are shown. Flies were shifted to 29°C for 7 days to induce RNAi knockdown. See also Figure S2.1. (C-C’’’) Control testes showed no EDU incorporation or PH3 staining within cells of the hub cell cluster (white outline). (D-D’’’) Loss of Rbf in hub cells using Rbf RNAi leads to hub cell divisions as seen by EDU incorporation (yellow arrowheads) and PH3 staining (yellow arrows) within the hub (white outlines). Scale bars represent 20μm. Fisher’s exact test, ****$p<0.0001$, *$p<0.05$, n.s., not significant.

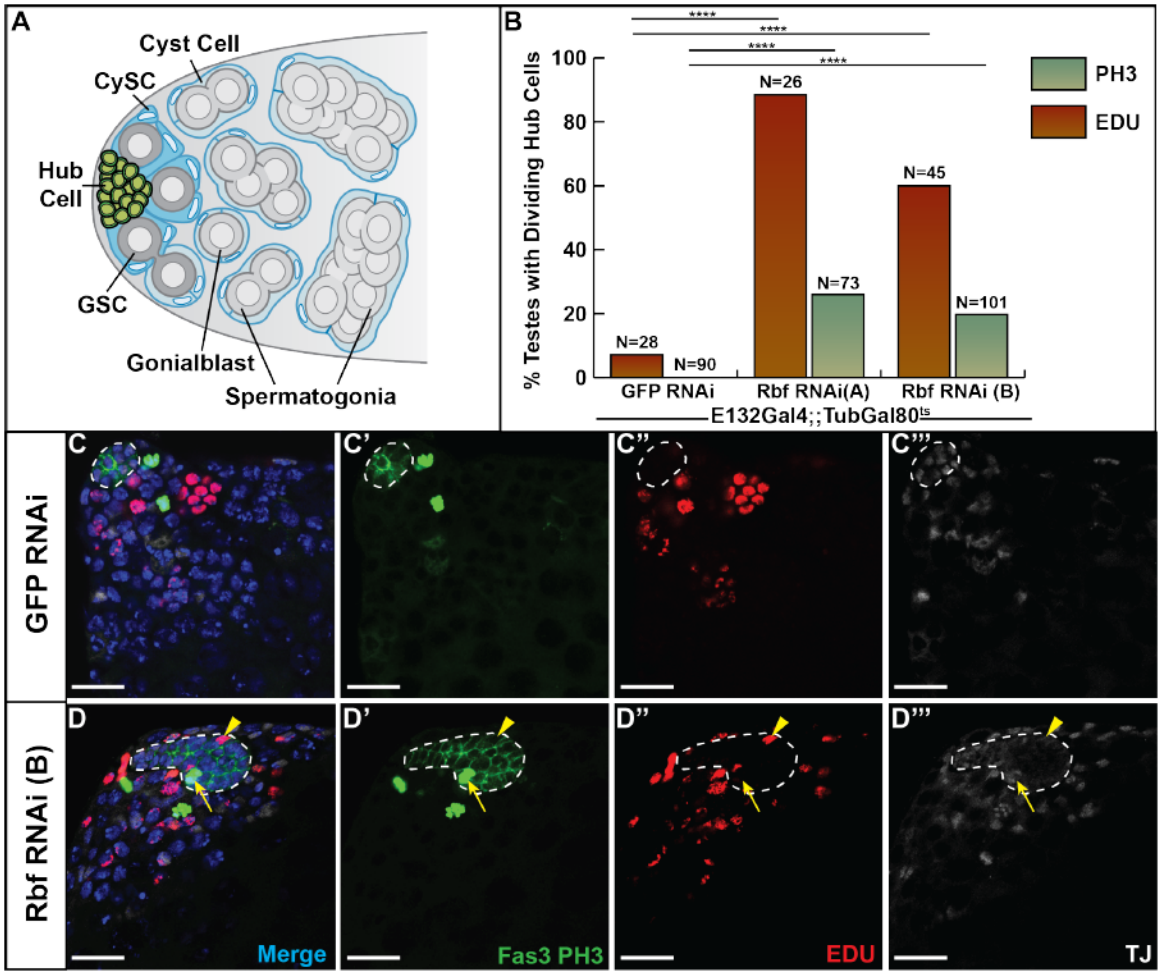
A
Cyst Cell
CySC
Hub Cell
GSC
Gonialblast
Spermatogonia
B
% Testes with Dividing Hub Cells
100
80
60
40
20
0
****
****
****
****
N=28
N=90
N=26
N=73
N=45
N=101
PH3
EDU
GFP RNAi
Rbf RNAi(A)
Rbf RNAi (B)
E132Gal4;;TubGal80ts
GFP RNAi
Rbf RNAi (B)
C
C'
C''
C'''
D
D'
D''
D'''
Merge
Fas3 PH3
EDU
TJ

Figure 2.2: Hub cells convert to cyst lineage cells upon Rbf knockdown. (A-F) Single confocal sections through the testis apex marked with the G-TRACE lineage tracing system using the hub specific driver E132-Gal4 with a temperature sensitive TubGal80. G-TRACE only control testes are shown in A, C, E, while G-TRACE testes with Rbf knocked down in the hub are shown in B, D, F. Marking and RNAi induction occurred for 7 days (A-D) or 14 days (E-F) at 29°C. Testes are immunostained for dsRed (Gal4 expressing hub cells, red), GFP (hub cells and cells derived from hub cells, green), DAPI (nuclei, blue), and either Dlg (cell membranes, white, A-B), TJ (cyst lineage, white, C-D), or Fas III and Eya (hub membrane and late cyst cells respectively, white, E-F). Merged and single channels are shown. See also Table S1 for conversion quantification. See also Figures S2.2-S2.4, and Movies S2.1-S2.3. (A-A''') Hub cells (white asterisk) are seen in a confined area at the apical tip of the control testis. These cells express the hub-GAL4 driver allowing for continuous expression of both RFP and GFP causing cells to appear yellow. (B-B''') Rbf knockdown causes hub cell conversion. Cells within the main hub cluster (white asterisk) still express the hub-GAL4 driver and appear yellow. Cells originating from the hub that have migrated away from the main hub cluster have lost their hub cell identity (yellow arrowheads) and appear only green. (C-C''') Cyst lineage cells (TJ, white) do not express either RFP or GFP and thus are not derived from converting hub cells in control testes. (D-D''') Upon Rbf knockdown, hub derived traced cells (RFP^-GFP^+) express the cyst lineage marker TJ (yellow arrowheads) indicating these cells have changed their cell fate. TJ positive cells not derived from the hub (RFP^-GFP^-) are also seen (yellow arrow). See also Figure S3. (E-E') Late cyst cells are unmarked (RFP^-GFP^-), express Eya (nuclear white, yellow arrow), and are seen far away from the hub (white asterisk) in control testes. (F-F') Upon Rbf knockdown, some converted hub cells (RFP^-GFP^+) that are far away from the hub (white asterisk) are seen expressing the late cyst marker Eya (nuclear white, yellow arrowheads), indicating they can progress through cyst lineage differentiation. Unmarked (RFP^-GFP^-) late cyst cells (Eya^+) are also seen (yellow arrow). Some marked cells (RFP^-GFP^+) do not express Eya

(white arrowhead) suggesting these cells have lost hub fate but have not yet acquired later cyst cell fate. Scale bars represent 20μm.

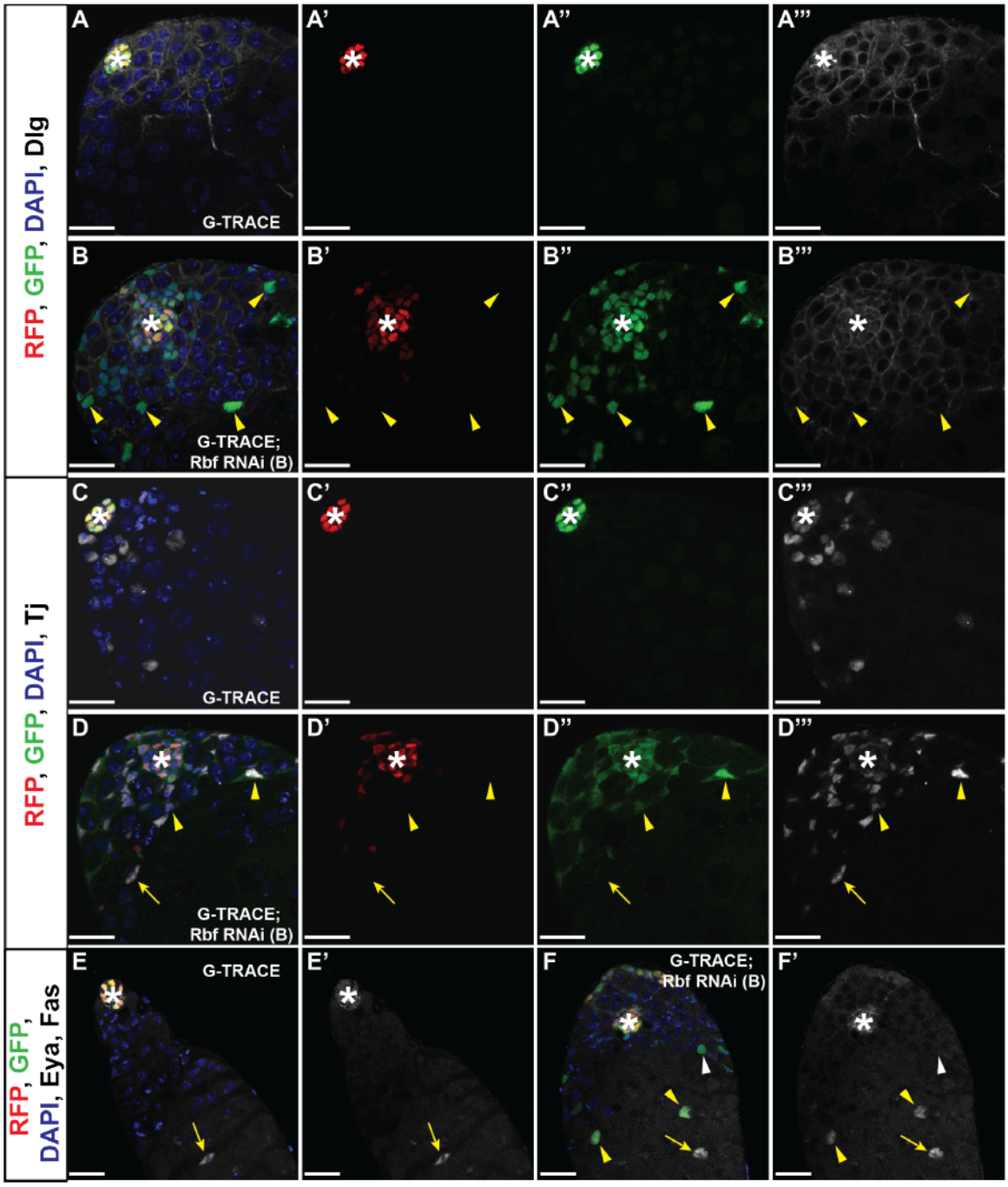

Figure 2.3: Live and fixed imaging of testes with Rbf knocked down in the hub shows migration of converting hub cells and hub cell death.

(A-B) Still frames from live images of testes expressing G-TRACE and Rbf RNAi specifically in the hub for 10 days at 29°C using the E132Gal4;;TubGal80^{ts} driver. Testes were imaged live for approximately 15 hours with images acquired every ten minutes. Images show red channel only. (A) Timeframe 1 shows three hub cells marked by grey circles that have already left the main hub cluster. (B) By the last timeframe (T91), the hub cell marked 1 has undergone cell death as seen through the condensation of its DNA. The other two marked hub cells (2 and 3) have traveled farther from the main hub cluster and have lost red fluorescent expression indicating they are no longer hub cells. (C) Dot plot depicting the displacement from T1 to T91 versus the percentage of red fluorescence expression remaining at T91 compared to T1. Green dots show individual hub cells from control testes expressing G-TRACE only (n=15), while red dots show individual hub cells from testes expressing G-TRACE and Rbf RNAi in the hub (n=42). Linear regression analysis shows a significant correlation (R^2=0.33, $p<0.0001$) between the displacement of a hub cell and the amount of fluorescence it loses in testes where Rbf has been knocked down. Control testes show no such correlation (R^2=0.04, ns). See also Movies S2.2-S2.3. (D-F) Single confocal sections through the testis apex fixed and immunostained for cleaved caspase Dcp1 (dying cells, red), Fas III (hub, membranous green), and DAPI (nuclei, blue). Hubs are outlined in white. (D'-F') Red channel only. Flies were shifted to 29°C for 7 days to induce RNAi knockdown using the E132Gal4;;TubGal80^{ts} driver. (D-D') Dying cells can be seen within control testes (white arrowhead) but are never seen within the hub. (E-F') Rbf knockdown in hub cells causes hub cell apoptosis as indicated by shrinking hub cells that are marked with Dcp1 throughout the entire cell (yellow arrowheads). Scale bars for A-B represent 15μm. Scale bars for D-E' represent 10μm.

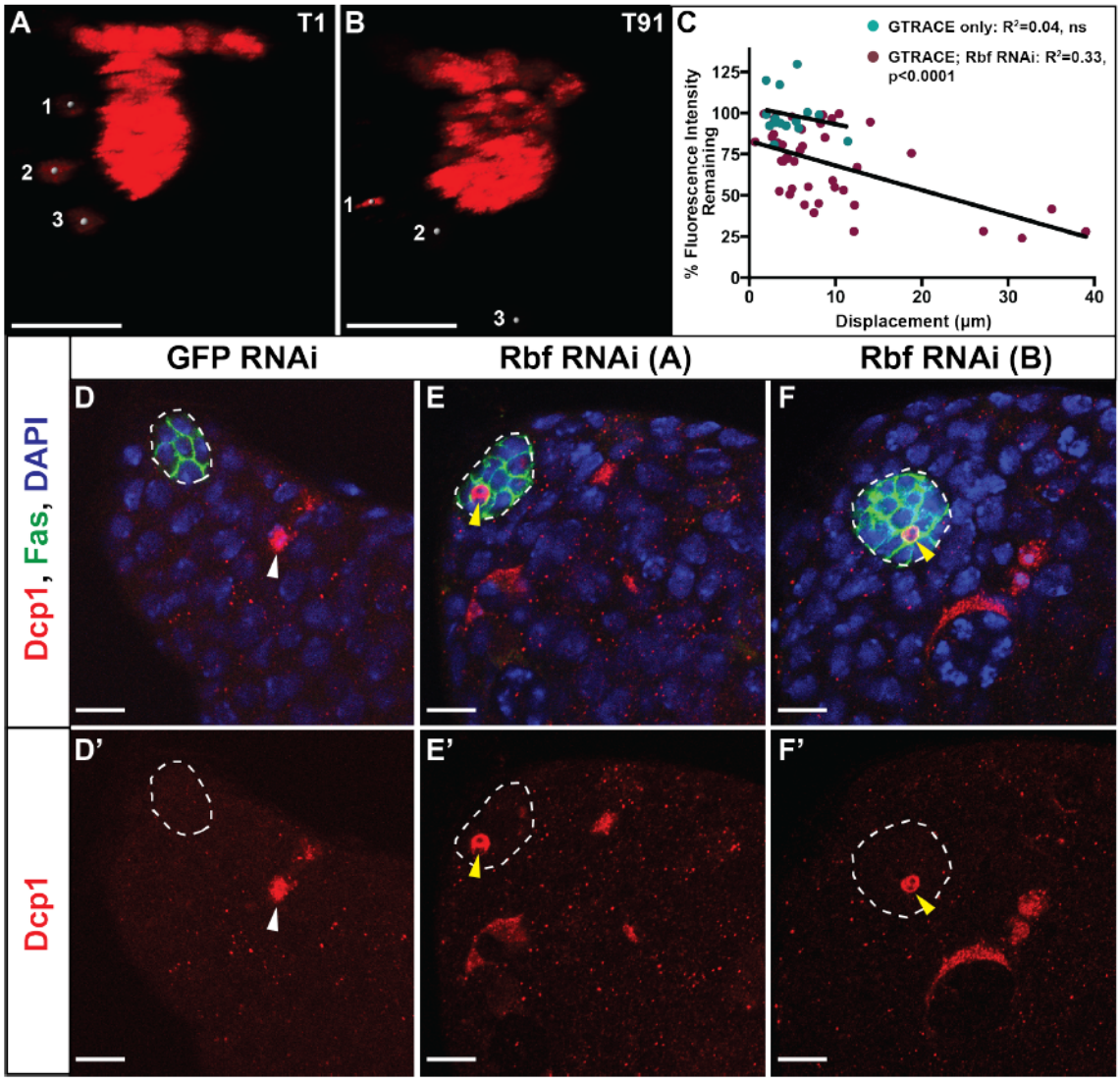
A
T1
1
2
3
B
T91
1
2
3
C
GTRACE only: R²=0.04, ns
GTRACE; Rbf RNAi: R²=0.33, p<0.0001
% Fluorescence Intensity Remaining
125
100
75
50
25
0
0
10
20
30
40
Displacement (μm)
GFP RNAi
Rbf RNAi (A)
Rbf RNAi (B)
Dcp1, Fas, DAPI
D
E
F
Dcp1
D'
E'
F'

Figure 2.4: E2F knockdown but not Esg over-expression suppresses hub cell proliferation caused by Rbf knockdown. (A-F) Single confocal sections through the testis apex immunostained for Vasa (germ cells, red), Fas III (hub, membranous green), PH3 (mitotic cells, nuclear green), and DAPI (nuclei, blue). Hubs are outlined in white. Flies were shifted to 29°C for 14 days to induce RNAi knockdown using the E132Gal4;;TubGal80^{ts} driver. (A-B) Testes with Rbf knocked down in the hub have extensive hub cell proliferation indicated by PH3 marked hub cells (yellow arrowheads) leading to an enlargement of the hub. (C and E) Knockdown of E2F (C) or over-expression of Esg (E) individually in the hub does not induce hub cell divisions as indicated by the absence of PH3 in hub cells. Note that the hub size also appears normal. (D) Knockdown of both E2F and Rbf in the hub suppresses hub cell proliferation as indicated by an absence of PH3 in the hub. Hub size appears normal. (F) Overexpression of Esg in the hub does not suppress the proliferation phenotype caused by Rbf knockdown. An enlarged hub with PH3 marked hub cells (yellow arrow) is still detected. Scale bars represent 20μm. See also Table 2.1 for proliferation quantifications.

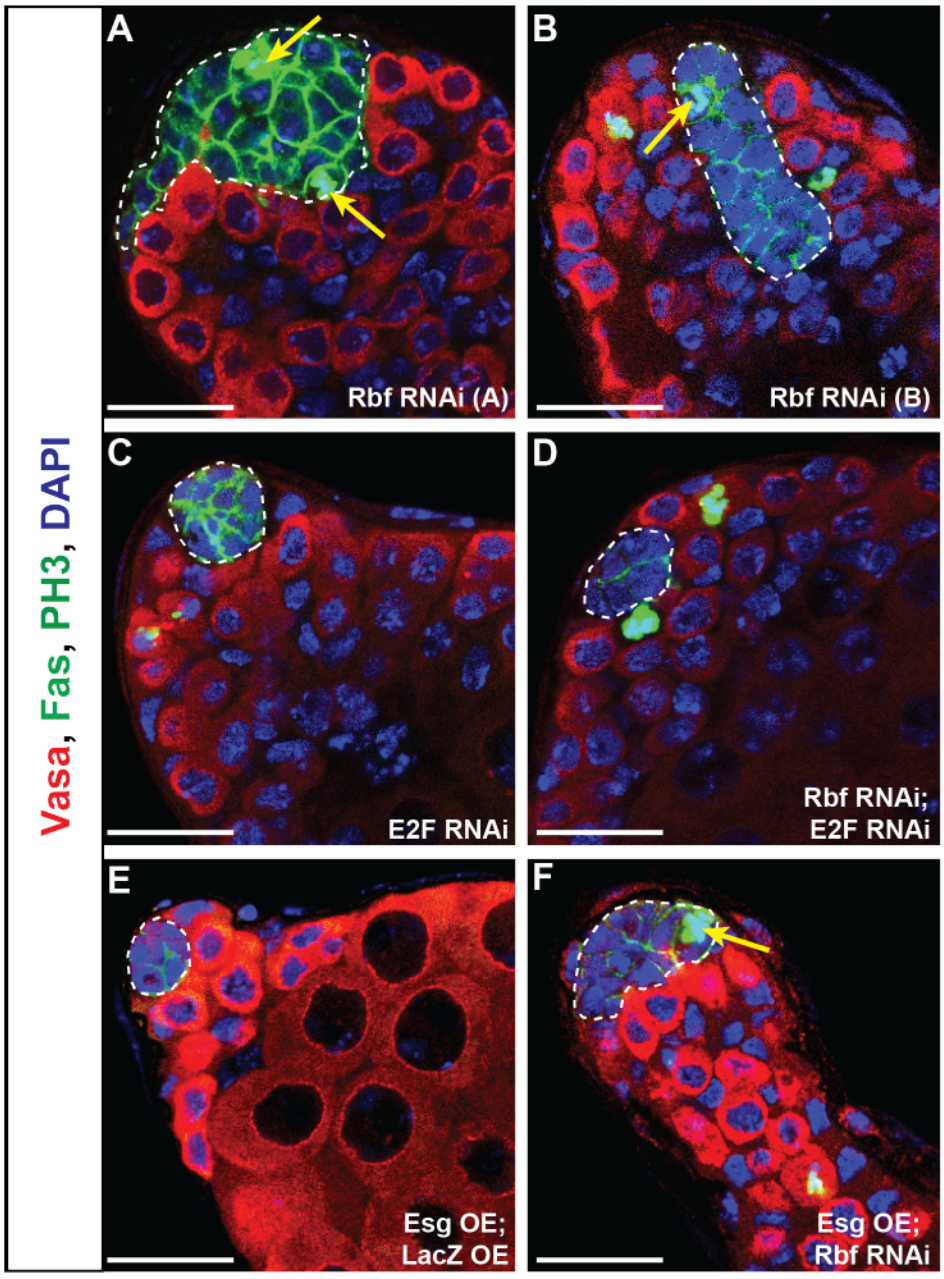
Vasa, Fas, PH3, DAPI
A
Rbf RNAi (A)
B
Rbf RNAi (B)
C
E2F RNAi
D
Rbf RNAi;
E2F RNAi
E
Esg OE;
LacZ OE
F
Esg OE;
Rbf RNAi

Figure 2.5: Loss of Rbf in hub cells causes ectopic niche formation.

(A-C) Single confocal sections through the testis apex immunostained with Fas III (hub, membranous green), PH3 (mitotic cells, nuclear green), and DAPI (nuclei, blue). RNAi was induced for 14 days at 29°C using the E132Gal4;;TubGal80^{ts} driver. Control testes expressing GFP RNAi in hubs cells (A) contain only a single hub (white outline), while those testes expressing Rbf RNAi in hub cells (B-C) contain multiple hubs. See also Movie S2.4. (D-F'') Single confocal sections through the testis apex immunostained with Armadillo (hub, membranous white), 1B1 (fusome, white), ZFH1 (CySCs, green), Vasa (germ cells, red) and DAPI (nuclei, blue). (D'-F') Green channel only. (D''-F'') White channel only. RNAi was induced for 14 days at 29°C using the E132Gal4;;TubGal80^{ts} driver. Control testes (D) contain a single hub surrounded by both CySCs (yellow arrows) and GSCs represented by red cells with a dot fusome (yellow arrowheads). Testes with Rbf knocked down in the hub (E-F'') contain multiple hubs (white outlines) scattered throughout the testis apex, each with CySCs (yellow arrows) and GSCs (yellow arrowheads). Scale bars represent 20μm. See also Figure S2.5 and Movie S2.4.

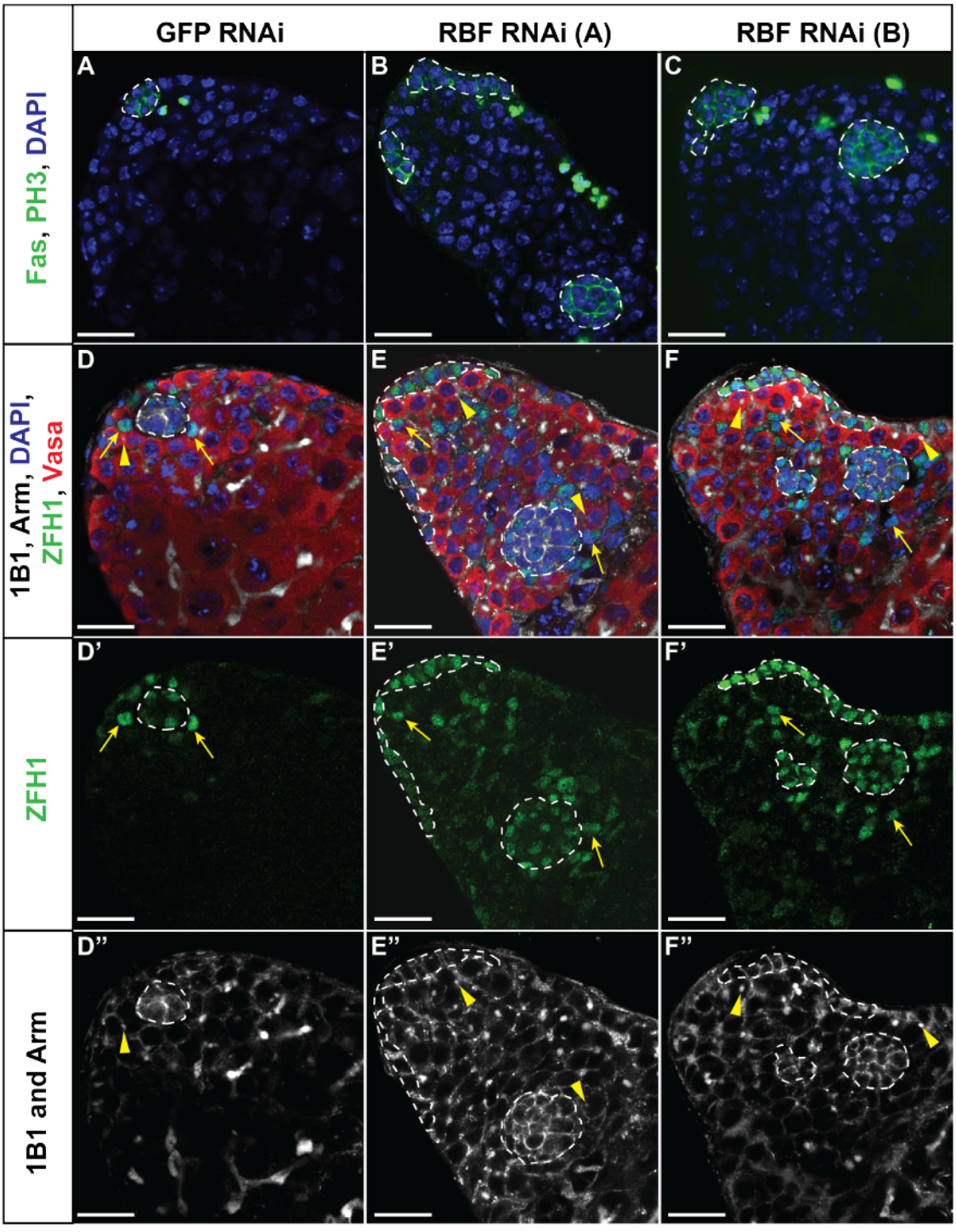
GFP RNAi
RBF RNAi (A)
RBF RNAi (B)
Fas, PH3, DAPI
1B1, Arm, DAPI, ZFH1, Vasa
ZFH1
1B1 and Arm
A
B
C
D
E
F
D'
E'
F'
D''
E''
F''

Figure 2.6: E2F knockdown, Esg overexpression, or Shg overexpression suppresses ectopic hub formation upon Rbf knockdown.

(A-H) Single confocal sections through the testis apex immunostained for Vasa (germ cells, red), ZFH1 (CySCs, green), Fas III (hub, membranous white), PH3 (mitotic cells, nuclear white), and DAPI (nuclei, blue). Hubs are outlined in white. RNAi was induced for 14 days at 29°C using the E132Gal4;;TubGal80^{ts} driver. Only a single hub at the apical end of the testis is detected when E2F is knocked down (C) Esg is overexpressed (E) or Shg is overexpressed (G) individually in hub cells. In contrast, induction of Rbf RNAi (A and B) in hub cells can induce ectopic hub formation as indicated by multiple Fas III positive hub clusters that are not connected (white outlines with yellow arrows). Expression of two RNAis simultaneously does not dilute the strength of the knockdown as ectopic hubs are still seen when Rbf and GFP are knocked down in conjunction (A). E2F knockdown (D), Esg overexpression (F), or Shg overexpression (H) is sufficient to prevent multiple hubs from forming upon Rbf knockdown as only a single hub (white outline) is seen in these testes. Note that upon Rbf knockdown, E2F knockdown in the hub (D) restores normal hub size while overexpression of Esg or Shg (F and H respectively) does not. These testes contain a single enlarged hub. Scale bars represent 20μm. See also Table 2.1 for ectopic hub quantifications and Figure S2.6 for E-cadherin fluorescence quantification.

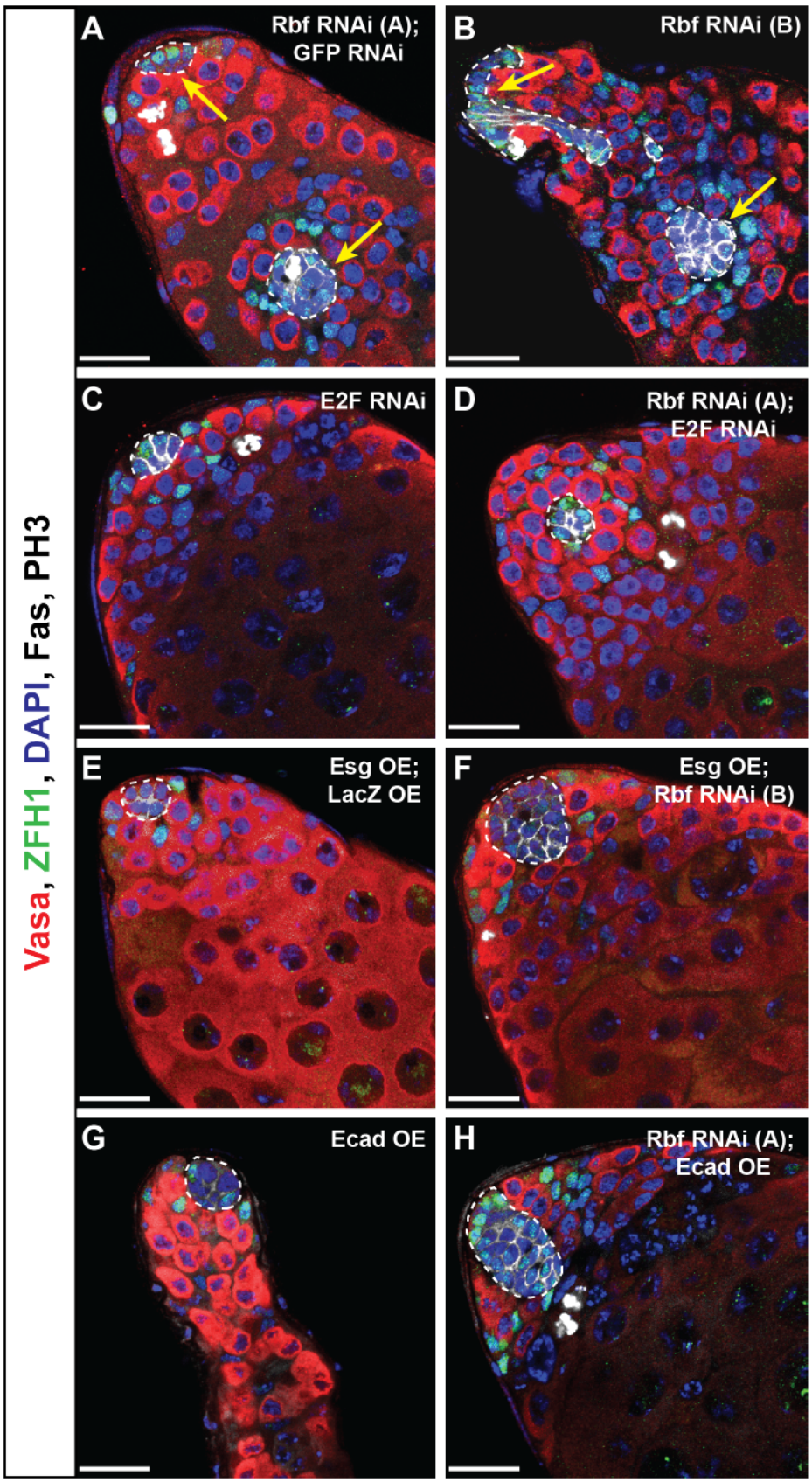
Vasa, ZFH1, DAPI, Fas, PH3
A
Rbf RNAi (A);
GFP RNAi
B
Rbf RNAi (B)
C
E2F RNAi
D
Rbf RNAi (A);
E2F RNAi
E
Esg OE;
LacZ OE
F
Esg OE;
Rbf RNAi (B)
G
Ecad OE
H
Rbf RNAi (A);
Ecad OE

Tables

Table 2.1: Rescue of Rbf knockdown phenotypes

Genotype: E132Gal4;; TubGal80^{ts}	% Testes with PH3+ Hub Cells	% Testes with Multiple Hubs
UAS-GFP RNAi	0% (n=0/30)	0% (n=0/61)
UAS-Rbf RNAi (A)	52% (n=29/56)[a,d,****]	18% (n=15/85)[a,d,***]
UAS-Rbf RNAi (A); UAS-GFP RNAi	27% (n=4/15)[a,d,*]	26% (n=5/19)[a,d,***]
UAS-Rbf RNAi (B)	22% (n= 8/83)[a,d,**]	25% (n=29/117)[a,d,****]
UAS-E2F RNAi	0% (n=0/53)[a,d,**ns**]	0% (n=0/53)[a,d,**ns**]
UAS-Rbf RNAi (A); UAS-E2F RNAi	0% (n=0/42)[b,d,**]	0% (n=0/42)[b,d,**]
UAS-Esg; UAS-LacZ	0% (n=0/35)[a,d,**ns**]	0% (n=0/35)[a,d,**ns**]
UAS-Esg; UAS-Rbf RNAi (B)	35% (n=17/48)[c,d,**ns**]	2% (n=1/48)[c,d,***]
UAS-Ecad	0% (n=0/98)[a,d,**ns**]	0% (n=0/98)[a,d,**ns**]
UAS-Rbf RNAi (A); UAS-Ecad	26% (n=19/73)[b,d,**ns**]	3% (n=2/73)[b,d,**]

[a] Compared with UAS-GFP RNAi
[b] Compared with UAS-Rbf RNAi (A); UAS-GFP RNAi
[c] Compared with UAS-Rbf RNAi (B)
[d] Fisher's Exact Test, *p<0.05, **p<0.01, ***p<0.001, ****p<0.0001, ns=not significant

Supplemental Information

Figure S2.1: Rbf knockdown in hub cells causes loss of Rbf protein and enlargement of the hub. (A-C) Single confocal sections through the testis apex immunostained for Rbf (green), Vasa (germ cells, red), and DAPI (nuclei, blue). Hubs are outlined in white. (A'-C') Green channel only. Flies were shifted to 29°C for 7 days to induce RNAi knockdown using the E132Gal4;;TubGal80^{ts} driver. (A-A') Rbf protein is expressed in germline stem cells (yellow arrowhead) and differentiating germ cells (white arrowhead) as well as cyst stem cells (yellow arrow) and cyst cells (white arrow) in control testes. Lower levels of Rbf protein are seen in hub cells (white outline). (B-C') Expression of Rbf RNAi in hub cells leads to loss of Rbf protein specifically in the hub, but not in germ cells or cyst lineage cells. (D-H) Max projection of testes immunostained for GFP (hub, green), TJ (cyst lineage, red), and DAPI (nuclei, blue) with 3D reconstructed hubs. Flies were shifted to 29°C for 3, 7, or 14 days to induce Rbf RNAi using the E132Gal4;;TubGal80^{ts} driver. (H) Column graph showing hub volume of 3D reconstructed hubs in control or Rbf knockdown hubs. The longer Rbf is knocked down in hub cells, the larger the hub volume becomes compared to control hubs. (I) Ploidy measurement of hub cells per testis measured by DAPI fluorescence of hub cells compared to DAPI fluorescence of sperm cells. On average the DNA content of hub cells was 1.83 times that of sperm cells suggesting that these cells are normally diploid. Scale bars represent 10μm (A-C) or 30μm (D-G). Error bars indicate mean volume with standard deviation. Unpaired t test with Welch's correction, ****$p<0.0001$, ***$p<0.001$.

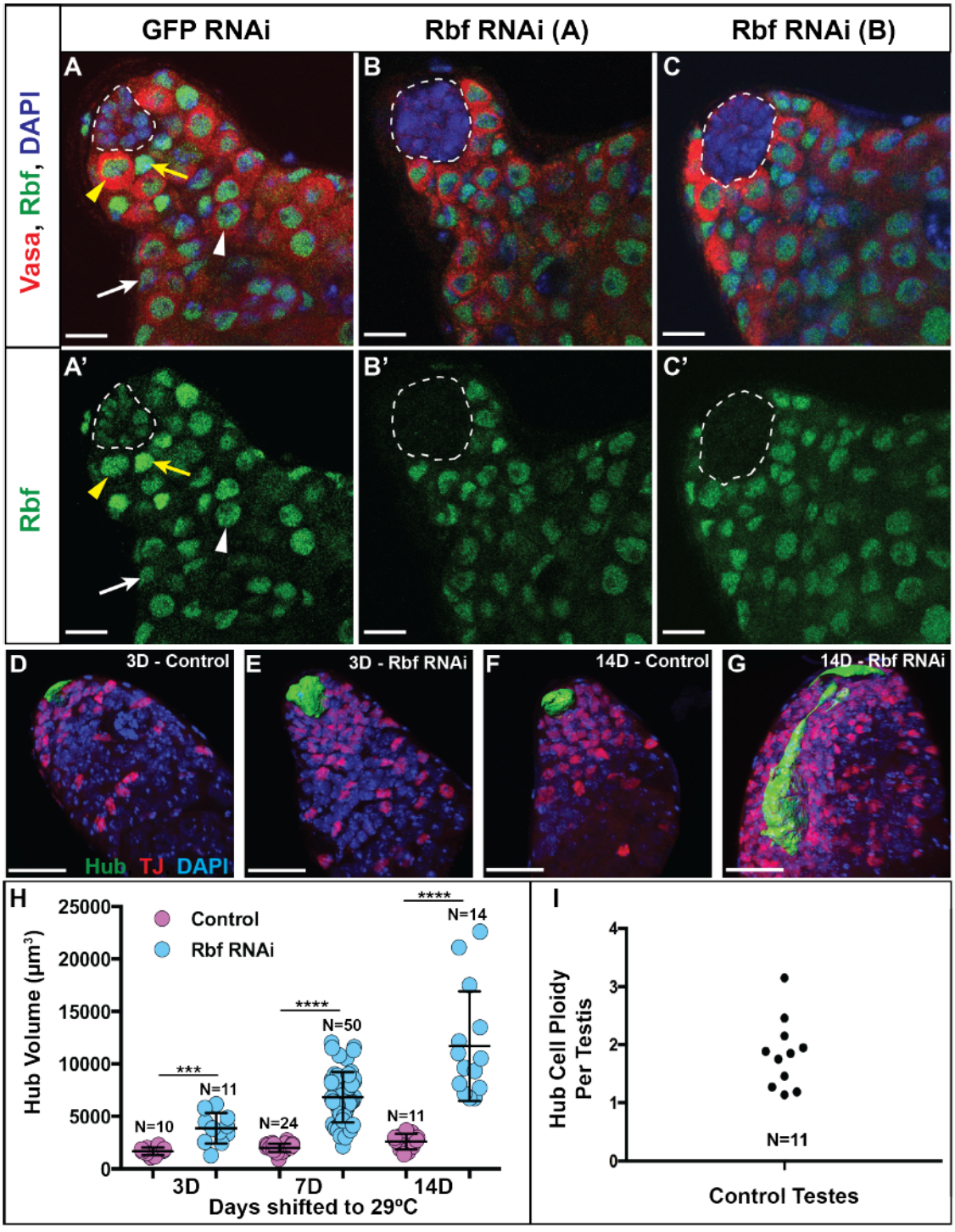
GFP RNAi
Rbf RNAi (A)
Rbf RNAi (B)
Vasa, Rbf, DAPI
Rbf
A
B
C
A'
B'
C'
D
3D - Control
E
3D - Rbf RNAi
F
14D - Control
G
14D - Rbf RNAi
Hub TJ DAPI
H
Hub Volume (µm³)
25000
20000
15000
10000
5000
0
Control
Rbf RNAi
N=10
N=11
N=24
N=50
N=11
N=14
***
****
****
3D
7D
14D
Days shifted to 29ºC
I
Hub Cell Ploidy Per Testis
4
3
2
1
0
N=11
Control Testes

Figure S2.2: Converting hub cells express cyst lineage markers. (A-D’’’) Single confocal sections through the testis apex expressing *Tub>CD2>Gal4,UAS-GFP; UAS-Flp/UAS-Rbf RNAi* using the drug inducible hub driver GS2295-Gal4. Flies were fed the drug RU-486 for 3 days to induce gene switch (GS) Gal4 expression leading to a flip out event that would continuously mark these cells with GFP while driving Rbf knockdown for a total of 21 days at 25°C. Testes were immunostained for GFP (hub cells and cells derived from hub cells, green), Fas III (hub, membranous white), DAPI (nuclei, blue) and either ZFH1 (CySCs, red, A-B) or TJ (cyst cells, red, C-D). Merged and single channels are shown. Hubs are outlined with a dotted white line. (A-A’’’ and C-C’’’) Control testes expressing the marking system only. Only a couple GFP positive hub cells (white arrowheads) can be seen within the hub cluster (white outline) with no GFP positive cells outside. (B-B’’’ and D-D’’’) Upon Rbf knockdown, multiple hub cells are marked within the hub cluster (white arrowheads) and GFP positive cells can be seen outside the main cluster (yellow arrowheads). These cells do not express the hub marker Fas III (white) but do highly express either the CySC marker ZFH1 (red, B-B’) or the cyst lineage marker TJ (red, D-D’) indicating they have converted. Scale bars represent 20μm.

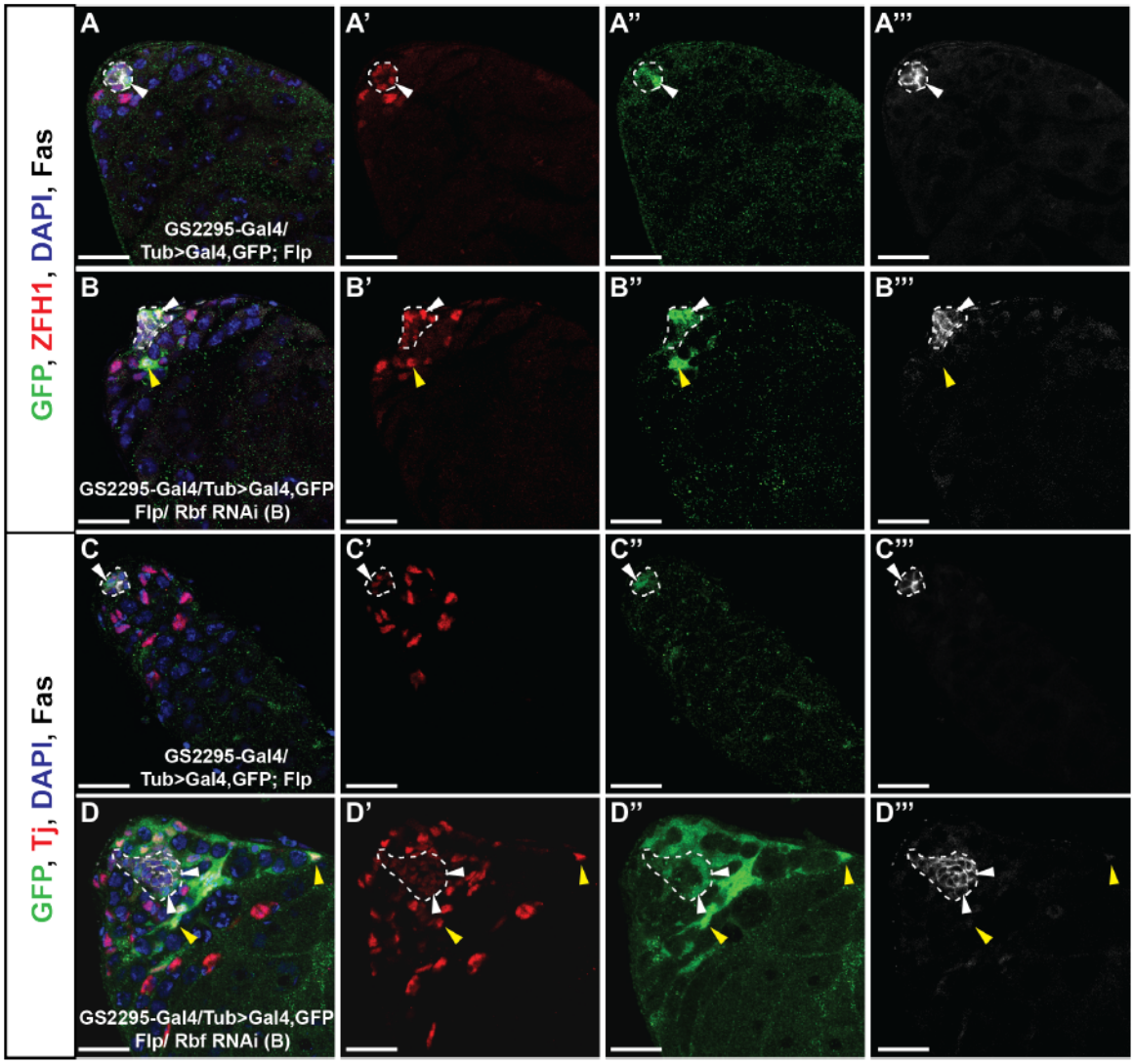
GFP, ZFH1, DAPI, Fas
GFP, Tj, DAPI, Fas
A
A'
A''
A'''
GS2295-Gal4/
Tub>Gal4,GFP; Flp
B
B'
B''
B'''
GS2295-Gal4/Tub>Gal4,GFP
Flp/ Rbf RNAi (B)
C
C'
C''
C'''
GS2295-Gal4/
Tub>Gal4,GFP; Flp
D
D'
D''
D'''
GS2295-Gal4/Tub>Gal4,GFP
Flp/ Rbf RNAi (B)

Figure S2.3: Converting hub cells make aberrant cyst cells. (A-D’’’) Single confocal sections through the testis apex marked with the G-TRACE lineage tracing system using the E132Gal4;;TubGal80^{ts} driver. G-TRACE only control testes are shown in A and C, while G-TRACE testes with Rbf knocked down in the hub are shown in B and D. Marking and RNAi induction occurred for 7 days at 29°C. Testes are immunostained for dsRed (Gal4 expressing hub cells, red), GFP (hub cells and cells derived from hub cells, green), DAPI (nuclei, blue), and either Vasa (germ cells, white, A-B) or Arm and PH3 (hub membrane and mitotic cells respectively, white, C-D). Merged and single channels are shown. Hubs are outlined with a dotted white line. (A-A’’) Hub cells are marked with RFP and GFP and stay within a tight cluster at the apical end of the testis. These cells are surrounded by germ cells (white). (B-B’’) Hub derived traced cells are seen outside the main hub cluster ($RFP^{-}GFP^{+}FasIII^{-}$) and do not express the germ cell marker Vasa (yellow arrowheads) indicating that converting cells do not become germ cells. (C-C’’) No marked cells are seen outside of the hub cluster in control testes. (D-D’’) Hub derived traced cells ($RFP^{-}GFP^{+}$) can be seen proliferating just outside the main hub cluster (yellow arrow). In addition, traced somatic cells can also be seen proliferating more than two cell diameters away from the hub (yellow arrowhead), in contrast to control testes that never show somatic cells proliferating that far down the tissue (yellow arrowheads in C and D). Scale bars represent 20μm.

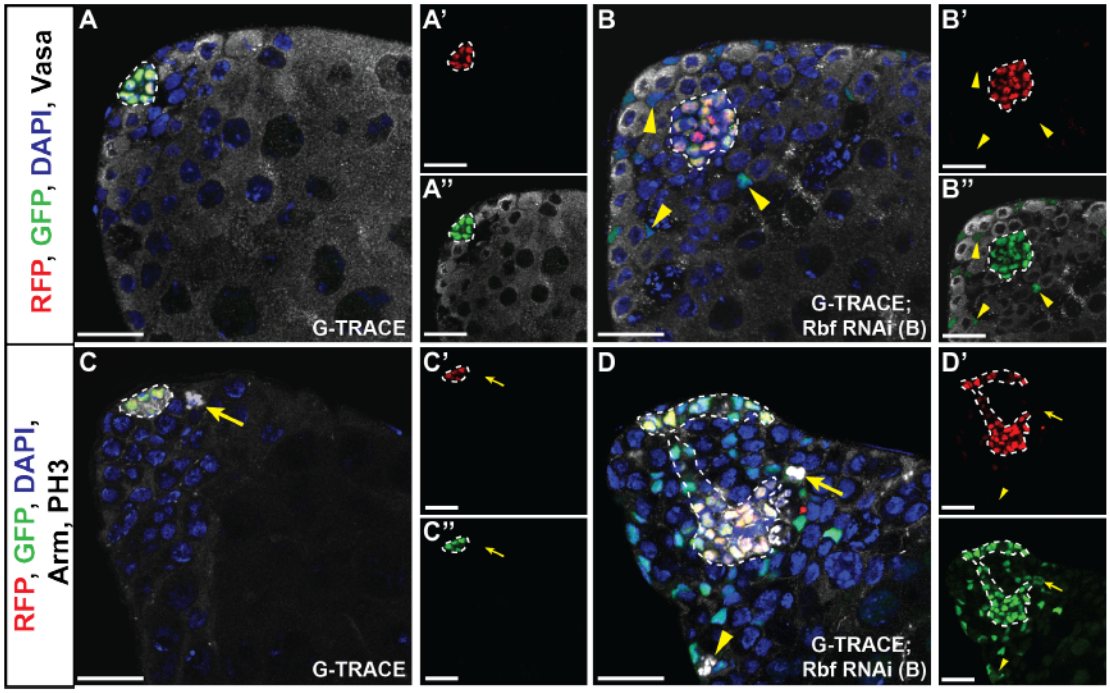
RFP, GFP, DAPI, Vasa
A
A'
A''
G-TRACE
B
B'
B''
G-TRACE;
Rbf RNAi (B)
RFP, GFP, DAPI,
Arm, PH3
C
C'
C''
G-TRACE
D
D'
G-TRACE;
Rbf RNAi (B)

Figure S2.4: Rbf is required for cyst cell quiescence. (A-D) Single confocal sections through the testis apex immunostained for TJ (cyst lineage, red, A-B), and Arm and PH3 (hub membrane and mitotic cells respectively, green, A-B), or Fas III (hub, membranous red, C-D) and ZFH1 (CySCs, green, C-D). All testes were counterstained with DAPI (nuclei, blue). Hubs are outlined by a dotted white line. Merged and single channels are shown (A-B''). Magnified testes apexes are shown (C'-D'). GFP RNAi (control) or Rbf RNAi was driven by the cyst cell driver EyaGal4 with a temperature sensitive TubGal80. Flies were shifted to 25°C for 10 days to induce RNAi knockdown only in cyst cells. (A) Control testis showing the extent of TJ-positive cells along the testis tubule (yellow dotted line). Only the TJ-positive cells within two cell diameters of the hub proliferate as indicated by PH3 (yellow arrow). Note that TJ is not expressed in late cyst cells that encapsulate spermatocytes, and the spermatocytes express low levels of DAPI (white arrowheads). (B) Loss of Rbf in cyst cells causes an expansion of TJ-positive cells along the testis tubule (yellow dotted line) in all testes. In addition, most testes have proliferating cyst cells away from the hub as indicated by PH3 (yellow arrow). Furthermore there is a non-autonomous increase in undifferentiated germ cells (TJ-negative, DAPI-bright nuclei) and a lack of spermatocytes (DAPI-dim nuclei) where they normally reside. (C-D) Extent of ZFH1-positive CySCs and their early daughters (yellow dotted lines) in either control testes (C) or testes with Rbf knocked down in cyst cells (D). Note that the zone of ZFH1-positive cells in control and mutant testes is similar, with ZFH1-positive cells spanning only a few cell diameters from the hub indicating that loss of Rbf does not regulate cyst cell identity. Scale bars represent 20μm.

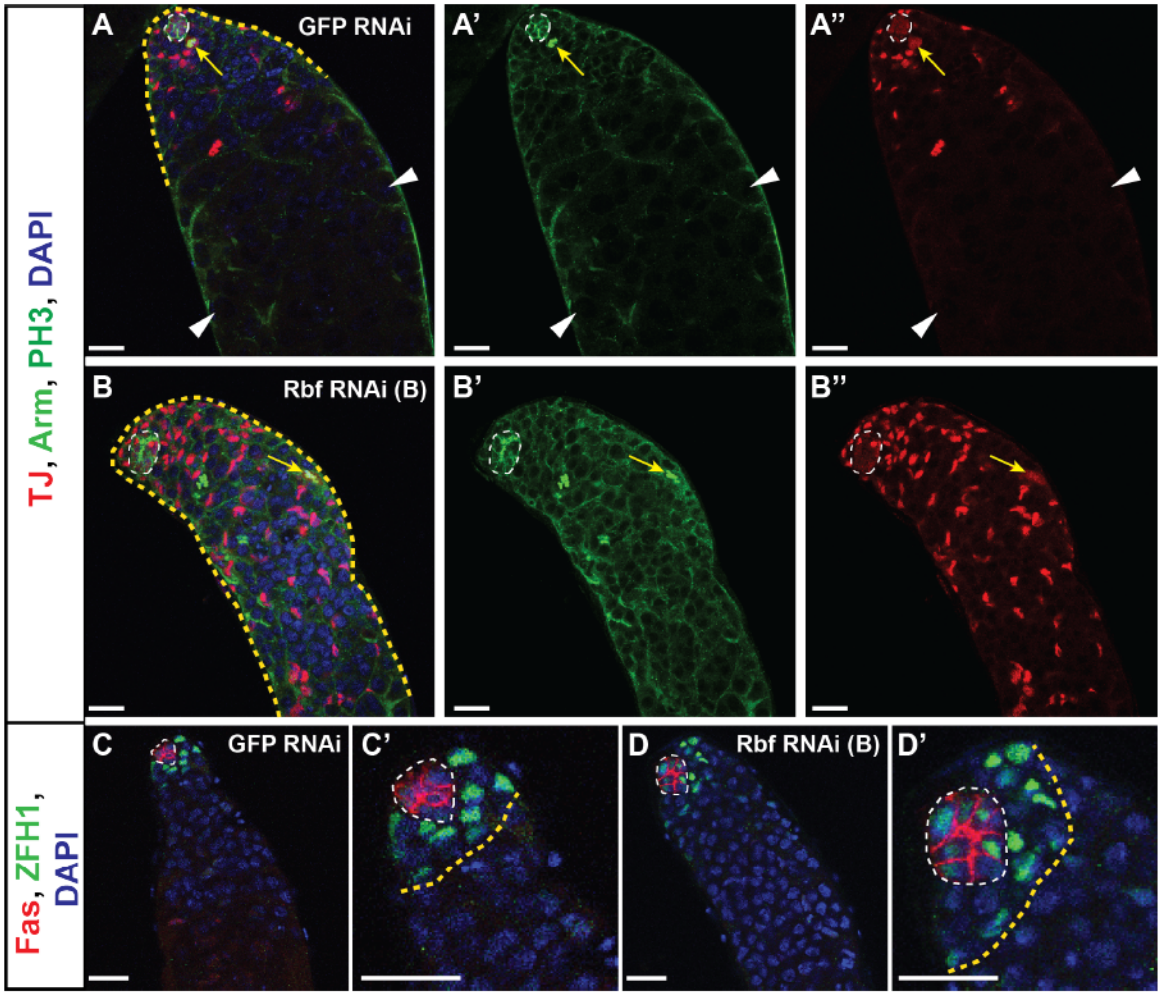
TJ, Arm, PH3, DAPI
A
GFP RNAi
A'
A''
B
Rbf RNAi (B)
B'
B''
Fas, ZFH1, DAPI
C
GFP RNAi
C'
D
Rbf RNAi (B)
D'

Figure S2.5: Ectopic hubs form functional niches.

Single confocal sections through the testis apex of the hub specific driver E132Gal4 with the temperature sensitive TubGal80 driving Rbf RNAi in the experimental flies (B, D, F, G). Flies were shifted to 29°C for 14 days. Nuclei are counterstained with DAPI (blue). (A-B) Testes immunostained for Vasa (germ cells, red) and β-gal (LacZ expression, green). β-gal expression is driven by Hh-LacZ. (A'-B') Green channel only. (A) Sibling control testis expressing only the hub specific driver and Hh-LacZ. LacZ expression can be seen within the single hub (white outline) at the apical end of the testis. (B) When Rbf is knocked down in hub cells, LacZ expression is detected in the most apical hub as well as ectopic hubs throughout the testis apex (white outlines). (C-D) Testes immunostained for dsRed (Gal4 expressing hub cells, red) and Fas III (hub, membranous white). (C) Control testis expressing only the hub driver and RFP shows Gal4 expression specifically within the hub (white outline). (D) Upon Rbf knockdown, Gal4 expression can be detected in multiple Fas III positive cell clusters (white outlines), indicating these clusters express the hub specific ligand Unpaired. (E-G) Testes immunostained for Stat92E (stem cells, red) and Fas III (hub, membranous green). (E'-G') Stat92E channel only. (E) Control testis expressing GFP RNAi shows single hub cluster (white outline) surrounded by Stat92E positive stem cells (yellow outlines). (F-G) Loss of Rbf in hub cells generates multiple hubs (white outlines) each surrounded by stem cells (yellow outlines). Scale bars for A-B and E-G represent 10μm. Scale bars for C-D represent 20μm.

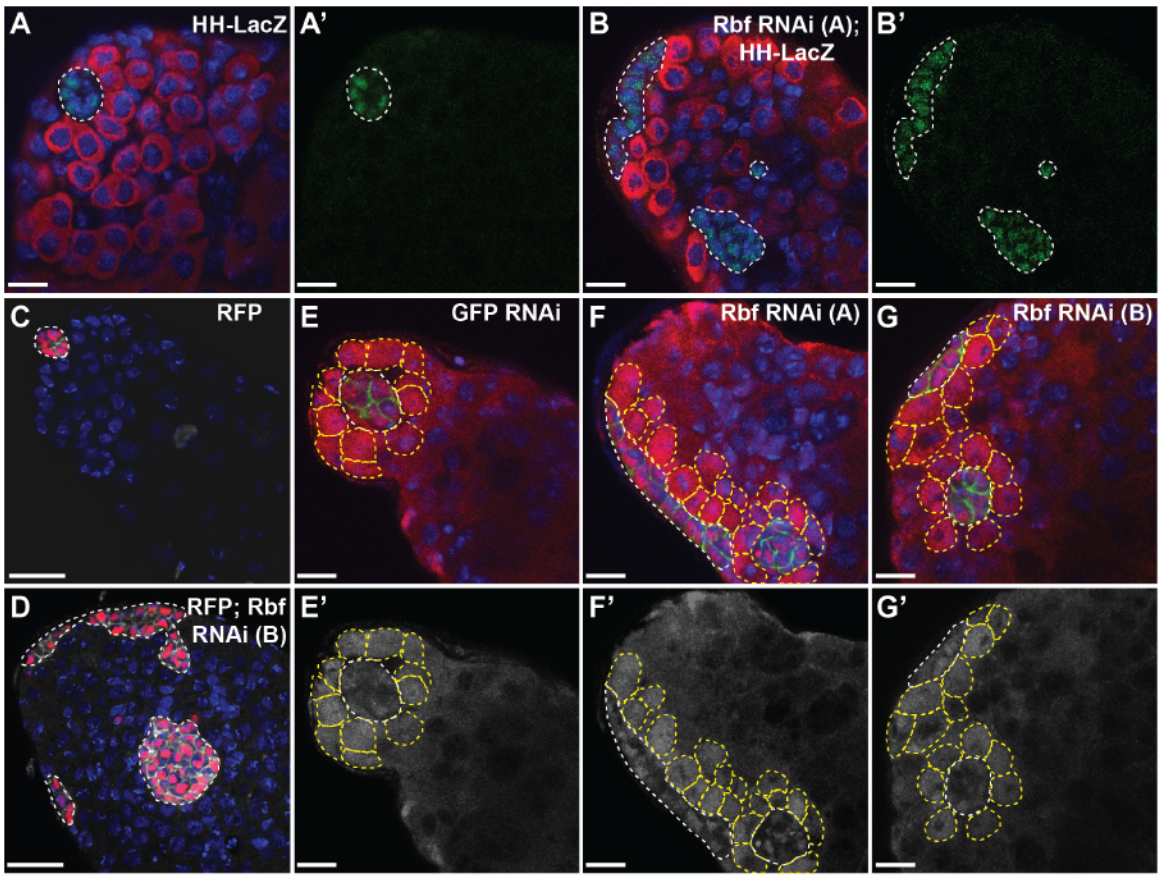
A
HH-LacZ
A'
B
Rbf RNAi (A);
HH-LacZ
B'
C
RFP
E
GFP RNAi
F
Rbf RNAi (A)
G
Rbf RNAi (B)
D
RFP; Rbf
RNAi (B)
E'
F'
G'

Figure S2.6: E-cadherin expression is reduced upon Rbf knockdown in hub cells.

(A-B) Single confocal sections through the testis apex immunostained for E-cadherin (green), and DAPI (nuclei, blue). Hubs are indicated with an asterisk. Flies were shifted to 29°C for 7 days to induce RNAi knockdown using the E132Gal4;;TubGal80^{ts} driver. (A) E-cadherin protein is expressed strongly on hub cell membranes in GFP RNAi control testes. (B) Rbf knockdown in hub cells leads to loss of E-cadherin protein expression within the hub suggesting an overall loss of adhesion. (C) Bar graph depicting the mean fluorescence intensity of E-cadherin protein expression normalized to DAPI. There is a significant reduction in E-cadherin expression levels when Rbf is knocked down in hub cells. Scale bars represent 20μm. Error bars indicate mean fluorescence with standard deviation. Unpaired t test with Welch's correction, ****p<0.0001.

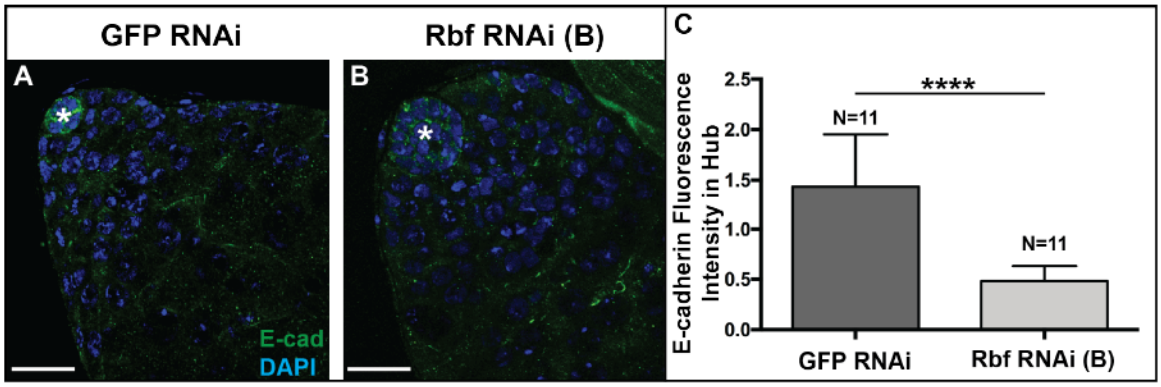

Movie S2.1, Related to Figure 2.2: Lineage-traced hub cells lacking Rbf are very dynamic. Time-lapse movie of live testis with Rbf knocked down in the hub expressing the G-TRACE lineage tracing system specifically in hub cells ($E132^{ts}$>G-TRACE; Rbf RNAi). Flies were shifted to 29°C for 10 days prior to imaging. Testis was imaged live for approximately 15 hours with images acquired every ten minutes. Merged RFP and GFP channels shown. One hub cell marked by a blue circle divides over the course of imaging with both daughter cells staying in the hub cluster. Another hub cell marked by a grey circle is seen leaving the hub cluster from the basement membrane.

Movie S2.2, Related to Figure 2.3: Lineage-traced hub cells from control testis stay confined to apical tip. Time-lapse movie of live control testis expressing the G-TRACE lineage tracing system specifically in the hub ($E132^{ts}$>G-TRACE). Flies were shifted to 29°C for 10 days prior to imaging. Testis was imaged live for approximately 15 hours with images acquired every ten minutes. Merged RFP and GFP channels shown. All hub cells continue to express RFP indicating they maintain their hub identity. These cells show slight movement but ultimately all cells stay confined within the cluster. Two hub cells marked by grey circles can be tracked over the course of imaging and were used for fluorescence quantification (See Figure 2.3C).

Movie S2.3, Related to Figure 2.3: Lineage-traced hubs cells lacking Rbf lose hub expression as they migrate away from hub cluster. Time-lapse movie of live testis with Rbf knocked down in the hub expressing the G-TRACE lineage tracing system specifically in hub cells ($E132^{ts}$>G-TRACE; Rbf RNAi). Flies were shifted to 29°C for 10 days prior to imaging. Testis was imaged live for approximately 15 hours with images acquired every ten minutes. Merged RFP and GFP channels shown. Three hub cells marked by circles have already left the hub cluster at the start of imaging and appear yellow. The grey marked hub cell shrinks and condenses its DNA indicating it is dying. The pink and blue marked hub cells move farther away

from the hub cluster and lose RFP expression appearing green, indicating they have lost their hub identity. See Figure 2.3A-B for red channel only and Figure 2.3C for fluorescence quantification.

Movie S2.4, Related to Figure 2.5: Ectopic hubs form through fission of enlarged hub cluster. Time-lapse movie of live testis with Rbf knocked down in the hub expressing a bright cytoplasmic GFP transgene specifically in hub cells ($E132^{ts}$>GFP; Rbf RNAi). Flies were shifted to 29°C for 13 days prior to imaging. Testis was imaged live for approximately 15.5 hours with images acquired every twenty-five minutes. A 3D surface rendering of the hub is depicted for better visualization. At the beginning of imaging a dumbbell shaped hub is seen connected by a thin cytoplasmic neck. By the end of imaging the neck has been broken causing two hub clusters to form.

Table S2.1: Lineage Tracing Hub Cells Upon Rbf Loss Shows Hub Cell Fate Conversion

Condition	Genotype	% Testes with GFP+ Cells Outside the Hub
7 Days at 29°C	[a]E132Gal4/Y; UAS-GTRACE/+; TubGal80^{ts}/+	25% (n = 21/85)
	[a]E132Gal4/Y; UAS-GTRACE/+; TubGal80^{ts}/UAS-Rbf RNAi	78% (n = 70/90)[b]
21 Days at 25°C	GS2295-Gal4/Tub>CD2>Gal4,UAS-GFP; UAS-Flp/+	0% (n = 0/64)
	GS2295-Gal4/Tub>CD2>Gal4,UAS-GFP; UAS-Flp/UAS-Rbf RNAi	21% (n = 8/38)[c]

[a] UAS-GTRACE: UAS-Redstinger, UAS-Flp, Ubi>stop>Stinger
[b] Fisher's Exact Test, $p<0.0001$, compared to controls without Rbf RNAi
[c] Fisher's Exact Test, $p<0.001$, compared to controls without Rbf RNAi

CHAPTER 3

The EGF/MAPK pathway drives niche cell conversion after tissue damage in the *Drosophila* testis stem cell niche

This chapter is a modified version of the manuscript Greenspan LJ, de Cuevas M, and Matunis EL. (2018). The EGF/MAPK pathway drives niche cell conversion after tissue damage in the *Drosophila* testis stem cell niche. In preparation.

Summary

Adult stem cells are maintained in niches, specialized microenvironments that regulate their self-renewal and differentiation. In the *Drosophila* testis stem cell niche, somatic hub cells produce signals that maintain and regulate adjacent germline stem cells (GSCs) and somatic cyst stem cells (CySCs). Hub cells normally divide only during embryogenesis and are quiescent in adult flies. We previously showed that complete genetic ablation of CySCs causes hub cells to exit quiescence, delaminate from the hub, and transdifferentiate into functional CySCs. Forced expression of cell cycle activators, or knockdown of the cell cycle inhibitor Retinoblastoma-family protein (Rbf), directly in hub cells also causes hub cells to proliferate and transdifferentiate into CySCs. These findings suggest that CySC ablation alters signaling pathways within the niche, triggering hub cells to re-enter the cell cycle and change fate to replace the missing stem cells. To identify these signaling pathways, we knocked down or overexpressed candidate pathway genes in hub cells and screened for loss of hub cell quiescence. We found that the EGFR-MAPK pathway plays a key role in this process. In an otherwise normal testis, activation of EGFR signaling causes hub cells to proliferate and transdifferentiate to CySCs. Moreover, after genetic ablation of CySCs, reduction of EGFR causes fewer testes to successfully regain CySCs. These results suggest that EGFR signaling is necessary and sufficient for promoting hub cell proliferation and transdifferentiation to CySCs. Taken together, our studies reveal that existing signals in the testis are repurposed after injury to drive tissue recovery and that precise modulation of signals is required to ensure regeneration without disease.

Introduction

Stem cells are unique in their ability to both self renew and produce daughter cells that differentiate producing the mature cells of a tissue (Greenspan et al., 2015). These cells reside in specialized microenvironments, called niches, which contain signals vital for prolonged stem cell maintenance (de Cuevas and Matunis, 2011; Greenspan et al., 2015; Ohlstein et al., 2004). Loss of a stem cell population due to injury or aging can be detrimental to tissue function, but recent studies have shown that new stem cells can be formed even when an entire population is lost. Germline progenitor cells in both *Drosophila* and mammals can dedifferentiate into stem cells (Brawley and Matunis, 2004; Cheng et al., 2008; Hara et al., 2014; Kai and Spradling, 2004; Sheng and Matunis, 2011). New stem cells can also be created through the direct conversion of niche cells to stem cells (Hétié et al., 2014; Voog et al., 2014; Greenspan and Matunis, 2018). However, the mechanisms that trigger these events remain unknown. Uncovering the molecular signals that drive *de novo* stem cell formation will be beneficial for both regenerative and anti-aging therapies.

The *Drosophila* testis stem cell niche provides a well-characterized model system to study stem cell dynamics *in vivo*. This niche contains a cluster of somatic quiescent hub cells that signal to two types of stem cells: germline stem cells (GSCs), which differentiate into sperm, and cyst stem cells (CySCs), which give rise to the somatic cyst cells that enclose differentiating germ cells (**Figure 3.1A**) (Hardy et al., 1979; Kiger et al., 2001; Tulina and Matunis, 2001). Upon damage to the niche via genetic ablation of all the CySCs and their early daughters, the hub cells exit quiescence, leave the hub, and

transdifferentiate into CySCs, thereby replenishing the lost population of stem cells (Hétié et al., 2014). This degree of niche cell plasticity was unexpected, since hub cells were considered terminally differentiated. Further studies have shown that the same cell fate conversion occurs when either the Snail family transcription factor Escargot or the tumor suppressor Retinoblastoma is knocked down in hub cells (Voog et al., 2014; Greenspan and Matunis, 2018), but the extrinsic signals that trigger hub cells to proliferate and transdifferentiate upon damage to the niche remain unknown.

The EGF/MAPK signaling pathway is a conserved receptor tyrosine kinase pathway that regulates many aspects of development including cell survival, growth, proliferation, and differentiation (Wee and Wang, 2017). This pathway is also aberrantly activated in many cancers (Wee and Wang, 2017), underscoring how precise regulation of signaling is essential for proper tissue maintenance. In the *Drosophila* testis, EGF signaling is essential for the differentiation and function of cyst lineage cells. During embryogenesis, these cells derive from the same pool of somatic gonadal precursor cells as hub cells (Le Bras and Van Doren, 2006), and EGF signaling is required for cyst lineage specification by repressing hub cell fate (Kitadate and Kobayashi, 2010). Thus precursor cells destined to become hub cells do not activate EGF signaling. In the adult testis, EGF signaling is required in cyst cells for their enclosure of the germ cells, which is vital for germ cell differentiation and maturation into sperm (Sarkar et al., 2007; Schulz et al., 2002).

Here we show that EGF signaling is triggered during CySC ablation conditions to initiate tissue recovery after testis damage. We show that activation of different EGF pathway members in hub cells is sufficient to drive hub cell proliferation and transdifferentiation. In addition, EGF signaling is activated in hub cells upon CySC ablation, and loss of EGF signaling leads to a reduction in tissue recovery. Together our results suggest a mechanism in which an existing signal is repurposed for recovery after tissue injury recapitulating embryonic development.

Results

EGF/MAPK pathway activation in the hub drives hub cell proliferation

Hub cells begin traversing S-phase in the first few hours of recovery from CySC ablation (Hétié et al., 2014), suggesting that a change in signaling occurs in the niche upon damage that triggers hub cells to re-enter the cell cycle. We hypothesized that this change could be gain of a new signal, loss of an existing signal, or a combination of the two. To identify changes in signaling that are sufficient to drive hub cell proliferation, we conducted a genetic screen in which we knocked down or over-expressed components of major signaling pathways, including transcription factors, downstream effectors, and receptors, in the hub and assayed testes for dividing hub cells (**Fig. 3.1B**). We used the GAL4-UAS system to conditionally over-express or knock down candidate genes specifically in adult hub cells by crossing flies carrying the hub-specific driver E132-Gal4 and temperature sensitive Gal4 inhibitor tub-Gal80^{ts} to flies carrying either a gene over-expression construct (UAS-X) or RNAi-inducing construct (UAS-RNAi). Adult male flies were shifted to the restrictive temperature 31°C for 7 days to induce Gal4

expression. Testes were fixed and immunostained for the mitotic marker Phospho-histone H3 (PH3) and the hub membrane marker Fasciclin III (Fas) to assess hub cell division. Out of the 15 signaling pathways tested only the EGF/MAPK signaling pathway had multiple pathway members cause hub cell divisions. This well conserved pathway is known for its role in cell proliferation among many others (Wee and Wang, 2017). PH3 positive hub cells were seen in 7.3% (n=4/55) and 6.6% (n=5/76) of testes with the Mitogen-activated protein kinase (MAPK) transcription factor Pointed overexpressed in the hub ($p<0.001$, Pnt.P1 and Pnt.P2 isoforms respectively) compared to GFP RNAi controls, in which mitotic cells were never seen (n=0/210) (**Fig. 3.1C, E, F, and Table 3.1**). This rate of proliferation was similar to the 10% maximum percent of testes with hub cell proliferation seen upon CySC ablation but lower than the proliferation rate seen when the cell cycle inhibitor Rbf is knocked down in hub cells (26.7% n=39/146) (**Fig. 3.1D and Table 3.1**).

Many different receptor tyrosine kinases feed into the MAPK pathway leading to Pointed activation. To determine which receptors were sufficient to drive hub cell proliferation we expressed activated forms of the EGF receptor, the FGF receptors Heartless (Htl) and Breathless (Btl), the PvR receptor, and the Insulin receptor. Only activation of the EGF receptor Type II showed a significant difference in testes with proliferating hub cells compared to GFP RNAi controls (4.4% n=5/113 compared to 0% n=0/210 respectively) (**Figure 3.1G, H, I and Table 3.1**). Occasionally a proliferating hub cell was seen when Htl or PvR was activated in the hub (**Table 3.1**), but this was not significant compared to controls suggesting that hub cell proliferation was specific to EGFR. In addition to the

activation of the EGF receptor, loss of the inhibitors Sprouty, which inhibits the MAPK effector RAS (Shilo, 2014), and the phosphatase PTEN, which dephosphorylates PIP3, led to hub cell proliferation (2.4% n=3/126 and 3.2% n=4/125) (**Figure 3.1J and Table 3.1**). However only knockdown of PTEN showed a significant difference compared to control testes ($p<0.05$). Altogether our candidate screen found multiple hits in the EGF/MAPK pathway that when activated in hub cells were sufficient to induce hub cell proliferation.

EGF/MAPK pathway activation in the hub drives hub cell transdifferentiation

In order for testes to recover after all CySCs and their early daughters are ablated, hub cells must convert to CySCs. To test if activating EGF signaling is sufficient to drive hub cell to CysC conversion we wanted to lineage trace hub cells upon EGF activation. We used the Gal4 Technique for Real-time and Clonal Expression (G-TRACE) system (Evans et al., 2009), which labels cells currently expressing Gal4 with a red fluorescent protein (RFP) and permanently marks cells that originated from the Gal4 expressing cells with a green fluorescent protein (GFP). We expected that hub cells would express both RFP and GFP appearing yellow while those cells that transdifferentiated would lose their RFP expression and appear only green. Flies expressing the E132-Gal4 hub driver with the G-TRACE lineage tracing system were crossed with flies that activated the EGF signaling pathway and grown at 16°C to reduce Gal4 expression since no Gal80 was present. Upon eclosion, flies were shifted to the restrictive temperature 29°C for 14 or 15 days to simultaneously induce marking and EGF pathway activation. Multiple lines with an activated EGF receptor showed a significant number of testes with green cells outside

of the main hub cluster indicated by the hub membrane marker Fascilin III, suggesting they had lost their hub cell identity (70.3% n=19/27 for EGFR type I, 100% n=12/12 for EGFR Type II, and 53.8% n=21/39 for EGFR Lambda) (**Figure 3.2A-B and Table 3.2**). By contrast, control testes occasionally had green cells outside of the main hub cluster (21.3% n=27/127), most likely due to marking during development since hub cells and cyst cells derive from the same precursor pool (Le Bras and Van Doren, 2006), but this was significantly less than when EGF signaling was activated (**Table 3.2**).

In addition to over-expression of the EGF receptor, loss of the inhibitor Sprouty in hub cells caused 93.6% of testes (n=44/47) to have green cells outside of the hub cluster (**Figure 3.2D and Table 3.2**), while knockdown of PTEN in hub cells also caused a modest conversion rate (59.1% n=13/22) (**Figure 3.2E and Table 3.2**). These data suggest that EGF signaling must be actively inhibited in hub cells in order to maintain their cell identity and that activation of this pathway is sufficient to drive hub cell conversion. Furthermore, activation of the receptor tyrosine kinases Htl and PvR did not show significant hub cell transdifferentiation rates compared to controls (**Figure 3.2C and Table 3.2**), suggesting that hub cell conversion is specific to EGF signaling. Because EGF signaling is necessary to specify cyst cells from the shared hub cell/cyst cell precursor pool in the male embryonic gonad (Kitadate and Kobayashi, 2010), these results could imply that activation of this pathway in the hub cells of adult flies is recapitulating development.

<u>The EGF/MAPK pathway is important for testis recovery after CySC ablation</u>

Since the EGF/MAPK pathway is sufficient to drive hub cell proliferation and transdifferentiation, we next wanted to test if this pathway was activated in hub cells after CySC ablation to drive recovery. We wanted to first confirm where the EGF/MAPK pathway is normally active since its been shown to be required for germ cell encystment by cyst cells (Sarkar et al., 2007; Schulz et al., 2002). Consistent with previous findings, we saw that under normal conditions the EGF ligand Spitz (Spi) was expressed in germ cells and late cyst cells while the EGF ligand Vein (Vn) was expressed in the CySCs and cyst cells (**Figure 3.3A-B**) (Sarkar et al., 2007; Singh et al., 2016). Furthermore, immunostaining for di-phosphorylated Erk (dpErk), which is an indication of pathway activity, showed activation of the pathway in CySCs and their differentiating daughters (**Figure 3C**) (Chen et al., 2013b; Fairchild et al., 2016; Singh et al., 2016), and only occasional EGF pathway activity in hub cells (**Figure 3.3E**). To assay for dpERK activity in testes recovering from CySC ablation, flies with the early cyst lineage driver c587-Gal4 and the temperature sensitive TubGal80 were crossed with flies expressing the pro-apoptotic gene Grim. Adult males were shifted to the restrictive temperature of 31°C for 2 days to induce Gal4 expression, thereby ablating cyst lineage cells. Flies were then allowed to recover for one day at the permissive temperature 18°C, and their testes were immunostained for dpERK activity. After 1 day of recovery there was a significant increase in the percent of testes that had dpERK activity in the hub compared to driver controls (38% n=21/55 compared to 16.7% n=6/36, $p<0.05$) (**Figure 3.3C-E**). This result suggests that the EGF pathway is activated in hub cells upon CySC ablation.

To test if the EGF/MAPK pathway is required for testes to recover CySCs after damage, we ablated cyst lineage cells in flies that had only one wild type copy of the EGF receptor gene, and thus had a reduction in EGF receptor gene dosage throughout the entire fly, and compared their rate of recovery after 7 days to ablated control flies with two wild type copies of the EGFR gene. Before ablation, testes contain hub cells, germ cells, and cyst lineage cells (**Figure 3.4A**). After CySCs and their early daughters have been ablated, testes still contain hub cells and some germ cells that push up against the hub as well as very late germ cells (**Figure 3.4B**), as has been previously described (Hétié et al., 2014; Lim and Fuller, 2012). Upon a 7-day recovery after ablation, three major phenotypes and a few minor phenotypes are observed, although the distribution varied depending on whether there were one or two copies of the EGFR gene (**Figure 3.4G**). These phenotypes include testes where germ cells remain and the cyst lineage has recovered as indicated by TJ-positive cells (**Figure 3.4C**), testes where germ cells remain but no cyst lineage cells have recovered (**Figure 3.4D**), and testes where germ cells and cyst lineage cells are lost and only the hub remains (**Figure 3.4E**). Flies with only one wild type copy of the EGFR gene showed a significant difference ($p<0.0001$) in the phenotype distribution of testes 7 days after CySC ablation compared to ablated controls (**Figure 3.4G**). A significantly lower percentage of these EGFR ablated testes recovered their cyst lineage (53% n=53/100 compared to 81.3% n=122/150) (**Figure 3.4G and Table 3.3**), and instead a higher percentage of testes had a hub and germ cells or a hub only (21% n=21/100 compared to 4.7% n=7/150 for Hub/GC and 24% n=24/100 compared to 10.7% n=16/150 for Hub only) (**Figure 3.4G and Table 3.3**). By 14 days after CySC ablation, the difference in testis phenotype distribution decreased but was still significant

($p<0.05$, **Figure 3.4G and Table 3.3**). Altogether these results suggest that the EGF/MAPK pathway is activated in hub cells after CySC ablation and is important for cyst lineage recovery.

Reduced EGF signaling does not affect ectopic hub formation after CySC ablation

Another phenotype that develops upon extended (14 days) recovery after CySC ablation is ectopic hub formation (**Figure 3.4F**) (Hétié et al., 2014). Ectopic hubs are capable of maintaining stem cells and form through fission of the original hub upon Rbf knockdown (Greenspan and Matunis, 2018). To test if EGF signaling is needed for ectopic hub formation, testes with either wild type or reduced levels of EGFR had their CySCs ablated and were allowed to recover for 14 days. Since only testes that retain their germ cells and recover their cyst lineage cells are able to form ectopic hubs, we chose to assay ectopic hub formation from only those testes that had hub cells, germ cells, and TJ-positive cells and thus were considered recovered. Testes with only one wild type copy of EGFR showed no significant difference in ectopic hub formation compared to testes with two wild type copies of EGFR, with 18% (n=9/50) of testes forming ectopic hubs after extended recovery compared to 30.6% (n=33/108) in controls (**Table 3.4**). This suggests that EGF signaling may not be necessary for ectopic hub formation. In support of this conclusion, constitutive activation of EGF signaling in the hub for 14 days without CySC ablation did not lead to ectopic hub formation (0% n=0/91 for EGFR lambda, data not shown). These findings indicate that EGF/MAPK signaling is not sufficient to induce ectopic hub formation, and is not necessary for ectopic hubs to form after CySC ablation, suggesting that additional signals may be activated after injury that drive this phenotype.

Discussion

Here we show that activation of the EGF signaling pathway in the hub is sufficient to drive hub cell proliferation and transdifferentiation (**Figure 3.1 and 3.2**). This pathway must be actively inhibited in the hub to maintain hub cell quiescence and fate since loss of the inhibitors Sprouty and PTEN specifically in hub cells can also drive both phenotypes. Furthermore, we show that the EGF pathway is activated in hub cells upon CySC ablation (**Figure 3.3**) and that reduced EGF signaling causes a significant impairment to cyst lineage recovery (**Figure 3.4**).

The hub cells and cyst lineage cells are derived from the same pool of somatic gonadal precursor cells in the male embryonic gonad (Le Bras and Van Doren, 2006). During development, EGF ligand is secreted from the primordial germ cells and received by the posterior somatic cells to drive cyst lineage specification by repressing hub cell differentiation (Kitadate and Kobayashi, 2010). In the adult testes, EGF ligand is also secreted from the germ cells and received by the cyst cells to ensure proper encystment (Sarkar et al., 2007; Schulz et al., 2002). Thus it is likely that upon CySC ablation, EGF ligand is still secreted from the germ cells but is now received by the hub cells since no CySCs remain, suggesting that germ cells must be present for testes to recover. In support of this model, testes that contain no germ cells after ablation are rarely seen recovering their cyst cells (**Figure 3.4G and Table 3.3**) (Hétié et al., 2014), and those that do most likely had germ cells early in recovery after ablation but lost them. Furthermore, hub cells will only divide when all the CySCs are ablated, indicating all cells must be gone for a signal to be triggered (Hétié et al., 2014). In addition

proliferation of hub cells ceases around 7 days recovery after ablation (Hétié et al., 2014), suggesting a waning of signal. We hypothesize that this waning of signal could be due to an inhibitory signal normally secreted by CySCs and received by hub cells, which is lost when the cells are ablated and returns once they recover. In support of this idea, loss of the secreted EGF inhibitor Argos in CySCs is sufficient to non-autonomously drive hub cell divisions (4.7% n=2/43, data not shown). Therefore altogether we propose a model where upon CySC ablation, the germ cells secrete the EGF ligand that can no longer be received by the cyst cells. Since the secreted inhibitor Argos is no longer present to sequester the ligand, the hub cells receive the signal and activate the MAPK pathway. This is turn causes Pointed to transcribe genes that drive hub cell proliferation and cell fate conversion (**Figure 3.5**).

Hub cells are capable of dividing and transdifferentiating upon EGF pathway activation, but ectopic hubs do not form in these testes. This finding is in contrast to testes recovering for 14 days after CySC ablation, where ectopic hub formation is common. Therefore, additional signals triggered after ablation may be needed to drive this phenotype. Because EGF signaling can drive hub cell fate conversion, perhaps a different signal is needed to ensure maintenance of hub cells so all hub cells do not convert to a CySC fate. One possibility is Notch signaling. Notch is expressed in almost all the somatic gonadal precursor cells during development and is required for hub cell specification (Kitadate and Kobayashi, 2010; Okegbe and DiNardo, 2011). In adult testes, the Notch ligand Delta is expressed in the hub but the role of Notch signaling is not well understood (Fairchild et al., 2016). However, adult cyst cells with septate

junction loss have activated Notch signaling and a reduction in EGF signaling causing them to join the endogenous hub and turn on hub fate markers (Fairchild et al., 2016). Therefore even in adulthood these two cell types are closely linked. Thus it is likely that Notch signaling could be necessary in adult hub cells for their maintenance, and required for ectopic hubs to form. It would be interesting to see what happens to hub cells upon simultaneous activation of EGF and Notch signaling.

The ability for tissues/organs to regenerate after injury, whether physical, genetic, radiation, or chemical, is conserved throughout evolution but the breadth, the mode, and the signals needed for repair vary depending on the organism and even the tissue (Lai and Aboobaker, 2018). While invertebrates such as the Planarian and Hydra can regenerate their entire body, others such as *Drosophila* and *Parhyale* can only regenerate certain tissues or cell types. Vertebrates such as zebrafish, salamanders, and frogs can regrow both internal organs and appendages (Tanaka and Reddien, 2011), but mammals are more limited in their regenerative ability. Mammals are capable of regenerating certain tissues such as bone, skeletal muscle, digit tip, and peripheral nerve but these are only individual body components, not entire appendages (Carlson, 2005; Johnston et al., 2016). Therefore better understanding how other organisms are able to rebuild a tissue after injury provides valuable insight for regenerative therapies, including both the mode used to repair the tissue and the signals needed to trigger repair. Planarians contain adult pluripotent stem cells called neoblasts that once triggered by wound-induced signals can divide and differentiate to replace damaged tissue (Lai and Aboobaker, 2018; Tanaka and Reddien, 2011). Other organisms such as the zebrafish have cells near the wound site

dedifferentiate and proliferate to form a blastema, which can then pattern and reform the injured tissue (Gemberling et al., 2013; Tanaka and Reddien, 2011). A third mode of regeneration is the direct conversion of one cell type to another cell type termed transdifferentiation, which we show here occurs in the *Drosophila* testis upon CySC ablation. This mode has also been shown to occur upon beta cell ablation in the mammalian pancreas, where alpha or delta cells can convert to become the insulin producing beta cells (Chera et al., 2014; Thorel et al., 2010). How cells know whether to proliferate, dedifferentiate, or transdifferentiate is a long standing question in the regenerative biology field.

Signals triggered upon injury are vital for proper tissue repair. One example that has been well characterized is injury to the *Drosophila* wing imaginal disc where the formation of reactive oxygen species (Ros) triggers JNK signaling activation during damage. In turn ligands for many other signaling pathways are produced in the surviving cells around the injury including Dpp, Wnt, and JAK-STAT (Ahmed-de-Prado and Baonza, 2018). In addition, apoptotic cells within the injury site are also able to secrete ligands to trigger signaling pathways in surviving cells, leading to tissue repair (Ahmed-de-Prado and Baonza, 2018). However, during the course of regeneration, structures meant for a different type of disc occasionally develop (Hariharan and Serras, 2017), thus underscoring the need for precise signal modulation during recovery. Here we present a genetic induced injury model where the niche cells of the *Drosophila* testis transdifferentiate into somatic cyst stem cells upon their ablation. We show that existing signals within the testis are repurposed during recovery after tissue injury, which may

recapitulate embryonic development. In addition, loss of an inhibitory signal helps trigger the conversion event and once CySCs recover, the inhibitory signal returns ensuring a waning of signal. Thus the coordination of signals between different cells types within a tissue is vital for proper repair after injury. Future studies into how different cell types coordinate recovery will provide better insights toward regenerative therapies.

Materials and Methods

Drosophila husbandry and strains

Flies were raised on a standard yeast/molasses medium (1212.5mL water, 14.7mL agar, 20.4g yeast, 81.8g cornmeal, 109.1ml molasses, 10.9mL Tegosept, 3.4mL propionic acid, 0.4mL phosphoric acid/ per tray of 100 vials) supplemented with dry yeast at 18°C unless otherwise indicated. Male flies between 0-5 days of age were used for all experiments and subject to different conditions as noted within the text, figures, legends, and methods. The following stocks were used c587-Gal4/ c587-Gal4 (from A. Spradling laboratory), UAS-Grim/UAS-Grim (from J. Nambu laboratory). Other stocks were from the Bloomington Drosophila Stock Center (BDSC). For a complete list of strains see the key resource table.

Transgene Induction

Heat induction: Flies containing a TubGal80^{ts} were grown at the permissive temperature 18°C and shifted to the non-permissive temperature 29°C or 31°C for either 7 or 14-15 days as indicated to induce transgene expression of RNAi lines or over-expression lines.

CySC Ablation (Hétié et al., 2014)

The c587Gal4 driver was used to express the pro-apoptotic gene Grim in CySCs along with a temperature sensitive TubGal80. Flies were grown at the permissive temperature 18°C and shifted to the restrictive temperature 31°C for 2 days to induce cell death in all CySCs and their early daughters. Flies were then allowed to recover back at the permissive temperature for varying lengths of time at indicated.

Dissection and Immunohistochemistry (Matunis et al., 1997)

Dissection: Flies were anesthetized using CO_2 then dissected with the cuticle still surrounding the testes in 1X Becker Ringer's solution (111 mM NaCl, 1.88 mM KCl, 64 μM NaH_2PO_4, 816 μM $CaCl_2$, 2.38 mM $NaHCO_3$) (Ashburner, 1989) and transferred immediately to fixation solution (4% paraformaldehyde in 1X PBS with 0.1% Trition X-100) for 22 minutes at room temperature on a nutator. With the exception of testes being stained with dpErk in which they were dissected in Shields and Sang M3 media with 1:100 dilution of phosphatase inhibitor cocktail 2 (Fairchild et al., 2016).

Immunohistochemistry: All washes were conducted using 1X PBX (1X PBS with 0.1% Trition X-100) except the final wash before adding mounting media in which 1X PBS was used. Testes were blocked overnight at 4°C in 1X PBX with 3% BSA, 0.02% NaN_3, and 2% goat or donkey serum. Antisera was diluted in 1X PBX with 3% BSA and 0.02% NaN_3. Testes were immunostained in primary antisera overnight at 4°C with the exception of mouse anti-Eyes Absent which was incubated at 4°C for three days and rabbit anti-STAT92E which was incubated at 4°C for one day and room temperature for one day. Secondary antibodies were diluted in 1X PBX containing 3% BSA and 0.02% NaN_3 and testes incubated overnight at 4°C. The nuclear counterstain 4,6-diamidino-2-phenylindole (DAPI) (Millapore/Sigma) was added to most secondary antibody dilutions at a final concentration of 1μg/mL. All testes were mounted in Vectashield antifade mounting medium (Vector Laboratories). Only testes being immunostained for dpErk were washed in 1X Testis Buffer with phosphatase inhibitor instead of PBX as described in (Fairchild et al., 2016).

All polyclonal antibodies were stored in a 1:2 dilution at -20°C, and all monoclonal antibodies were stored at 4°C except for mouse anti-Phospho-Histone H3 and mouse anti- β-Galactosidase which were stored at -20°C in a 1:2 glycerol dilution. Antisera was used at the following final concentrations: mouse anti-Fasciclin III (1:50), mouse anti-Phospho-Histone H3 (1:400), guinea pig anti-Traffic Jam (1:20,000), rabbit anti-Vasa (1:200), chick anti-GFP (1:10000), rabbit anti-dsRed (1:10000), mouse anti- β-Galactosidase (1:1000), rabbit anti-dpErk (1:100).

All Fluor 488 secondary antibodies were used at a final concentration of 1:400. All other secondary antibodies were used at a final concentration of 1:200.

Lineage Tracing

In the following genotypes, expression of the Gal4 driver caused permanent expression of GFP in hub cells and their descendants. Marked cells were detected by immunostaining. Testes with GFP cells outside the confines of the hub cluster that no longer expressed hub markers were considered positive for converting cells. The hub cluster was defined as hub-Gal4 expressing cells marked by RFP and Fasciclin III. To trace hub cells upon EGF or other pathway activation, *E132Gal4/Y; UAS-GTRACE /SM6B* stock virgins were crossed to males of the indicated genotype (see Table 3.2) and raised at 16°C to reduce Gal4 expression since no Gal80 was present. Upon eclosion 0-5 day old males were shifted to 29°C for 14 or 15 days to induce Gal4 expression. *E132Gal4/Y; UAS-GTRACE/SM6B* control males and *E132Gal4/Y; UAS-GTRACE/+; UAS-X/+* experimental males were processed in parallel to control for age, temperature, and to determine the extent of hub cell conversion.

Microscopy and Image Analysis

Image acquisition: Fixed images were obtained using either a Zeiss LSM 5 Pascal equipped with a 63x oil immersion objective, 405nm diode, 488nm ArKr, and 543nm HeNe lasers with digital zoom or a Zeiss LSM 700 (JHU SOM microscope facility) equipped with a 63x oil immersion objective, 405nm diode, 488nm solid-state, 561nm solid-state, and 639nm diode lasers with digital zoom. Images were acquired using either Zeiss LSM or Zen software. All Z stacks through the testis tissue had a step size of 1.25μm.

Image processing: Images acquired using Zeiss LSM or Zen software were processed using Fiji. Brightness for individual channels from single confocal slices was enhanced using Fiji, then each channel overlaid to form a merged image.

Quantification and Statistical Analysis

Hub cell proliferation quantification

To quantify hub cell divisions, testes were immunostained with the mitotic marker Phospho-Histone H3. Testes with PH3 marked cells within the confines of the hub cluster were considered positive for dividing hub cells. The hub cluster was defined as those cells marked by the hub membrane marker Fasciclin III.

Ectopic hub quantification

To quantify ectopic hubs, testes were immunostained with the hub membrane marker Fasciclin III. Z stacks were acquired to include the entire hub range. Hub clusters whose

membranes were no longer connected in any Z planes were considered separate hubs. Testes with more than one hub cluster were considered positive for ectopic hubs.

Statistical Analysis

For all quantifications, *n* represents the number of testes analyzed. Statistical significance was expressed as P values and determined using a Fisher's exact test for most measurements except ablation distribution phenotypes in which Chi-square test with was used. All statistical tests were run using PRISM 6 software. (*) denotes $p<0.05$, (**) denotes $p<0.01$, (***) denotes $p<0.001$, and (****) denotes $p<0.0001$ and (*ns*) denotes values that were not significant.

Bar graphs and tables indicate the percent of testes with a certain phenotype out of all the testes analyzed with that genotype.

Figures

Figure 3.1: Activation of the EGF/MAPK pathway in the hub drives hub cell proliferation. (A) Schematic of *Drosophila* testis stem cell niche. Somatic hub cells (green) secrete signals to the attached germline stem cells (GSCs, dark red) and somatic cyst stem cells (CySCs, dark blue). Both types of stem cells divide asymmetrically to produce differentiating daughter cells. Somatic cyst cells (blue) envelop dividing spermatogonia (red) and together they move away from the testis apex as they differentiate. (B) Hub quiescence screen schematic. Different signaling pathways were either activated (green) or knocked down (red) in the hub using the hub specific driver E132Gal4 with a temperature sensitive TubGal80. Flies were shifted to the restrictive temperature 31°C for 7 days to induce over-expression or knockdown. Testes were then dissected and hub cells assayed for proliferation using the mitotic marker phospho-histone H3 (PH3). (C-J) Single confocal sections through the testis apex immunostained for Fas III (hub, membranous green), PH3 (mitotic cells, nuclear green), DAPI (nuclei, blue), and either Vasa (germ cells, red, C-F) or TJ (cyst lineage, red, G-J). Hubs are outlined in white. Insets in G-J show green channel only. (C, G) Testes expressing GFP RNAi in the hub were used as a negative control and never had mitotic hub cells. (D) In contrast, testes expressing Rbf RNAi were used as a positive control since loss of this cell cycle inhibitor has been shown to induce hub cell proliferation (white arrowhead). Multiple members of the EGF/MAPK pathway caused hub cells to proliferate (white arrowheads) when either overexpressed (E, F, H, I) or knocked down (J). These include over-expression of the transcription factors Pointed P1 and Pointed P2 (E-F), activation of the EGF receptor (H-I), and loss of the inhibitor Sprouty (J). Scale bars represent 20μm. Inset scale bars represent 5μm.

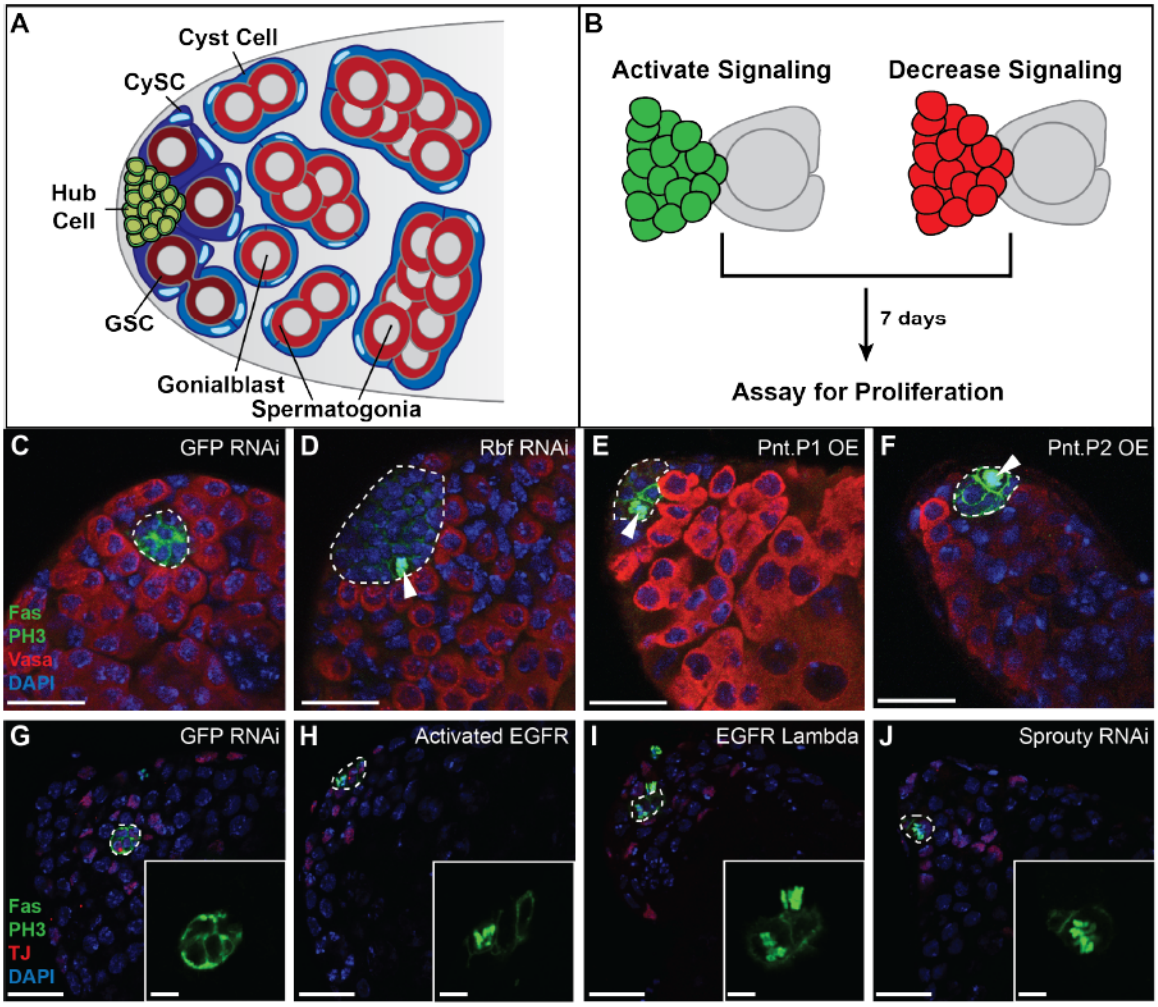
A
Cyst Cell
CySC
Hub Cell
GSC
Gonialblast
Spermatogonia
B
Activate Signaling
Decrease Signaling
7 days
Assay for Proliferation
C
GFP RNAi
Fas
PH3
Vasa
DAPI
D
Rbf RNAi
E
Pnt.P1 OE
F
Pnt.P2 OE
G
GFP RNAi
Fas
PH3
TJ
DAPI
H
Activated EGFR
I
EGFR Lambda
J
Sprouty RNAi

Figure 3.2: Activation of the EGF/MAPK pathway is sufficient to drive hub cell conversion. (A-E) Single confocal sections through the testis apex marked with the G-TRACE lineage tracing system using the hub specific driver E132Gal4. Flies were grown at the permissive temperature of 16°C to reduce Gal4 expression during development since these flies had no Gal80. Marking and over-expression or RNAi induction occurred for 14 days at 29°C. G-TRACE only control testes are shown in A-A''' while G-TRACE testes with EGF or PvR pathway activation in the hub are shown in B-E'''. Testes are immunostained for dsRed (Gal4 expressing hub cells, red), GFP (hub cells and cells derived from hub cells, green), and FasIII (hub membrane, blue). Merged and single channels are shown. (A) Control testis showing hub cells confined to the apical tip of the testis expressing both red and green fluorescence ($RFP^{+}GFP^{+}$) and thus appearing yellow. All cells remain in the confines of the hub membrane (blue). In contrast, hub cells with activated EGFR (B) but not a different receptor tyrosine kinase PvR (C) lose their hub identity and leave the hub cluster (white arrowheads). This is indicated by the green only cells ($RFP^{-}GFP^{+}$), which have turned off their Gal4 expression and lost their red fluorescence. These cells no longer reside within the hub cluster (blue). Loss of the inhibitors Sprouty (D) and PTEN (E) in hub cells is also sufficient to drive hub cell conversion as shown by the green only cells ($RFP^{-}GFP^{+}$) outside of the hub cluster (arrowheads). Scale bars represent 20μm.

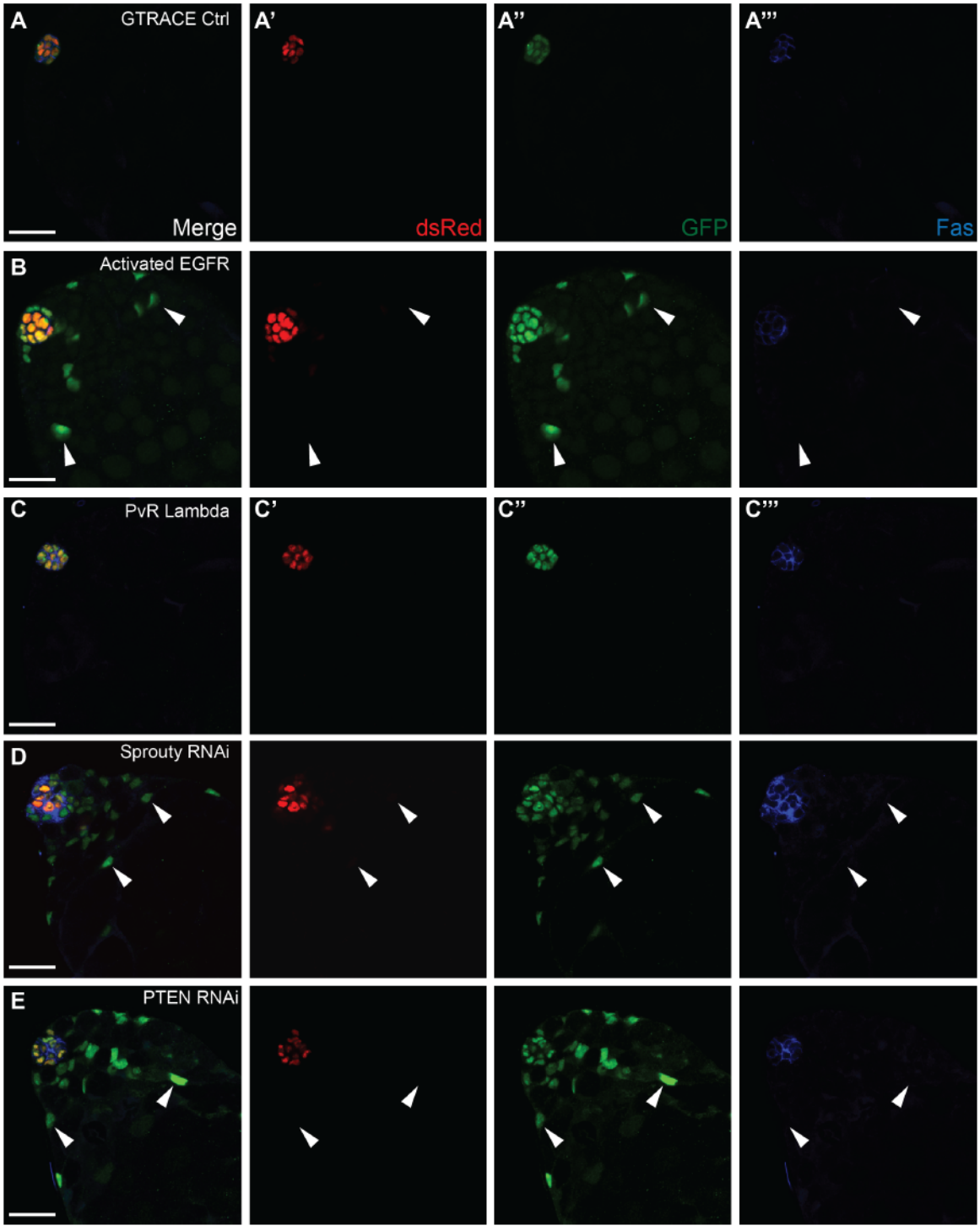
A
GTRACE Ctrl
Merge
A'
dsRed
A''
GFP
A'''
Fas
B
Activated EGFR
C
PvR Lambda
C'
C''
C'''
D
Sprouty RNAi
E
PTEN RNAi

Figure 3.3: EGF/MAPK pathway is activated in hub cells upon CySC ablation. (A-D) Single confocal sections through the testis apex immunostained for βGal (LacZ expression, green), Vasa (germ cells, red) and DAPI (nuclei, blue) (A-B) or Fas III (hub, membranous green), dpErk (EGF pathway activation, red) and DAPI (nuclei, blue) (C-D). A' and B' show green channels only. C' and D' show enlarged merged red and green channels. (A-A') The EGF ligand Spitz is normally expressed in the germline stem cells and their differentiating daughters (yellow arrowhead and arrow respectively). It is also expressed in late cyst cells (white arrow). (B-B') The EGF ligand Vein is expressed in both the CySCs (white arrowhead) and the cyst cells (white arrow). (C-D') Flies expressing the early cyst lineage driver c587Gal4 with the temperature sensitive TubGal80 were shifted to the restrictive temperature of 31°C for 2 days then allowed to recover back at the permissive temperature 18°C for one day. Those flies expressing the pro-apoptotic gene Grim had their CySCs ablated compared to driver only controls. (C) In control testes, the EGF pathway is normally active in the cyst lineage including the CySCs (white arrowhead) and their differentiating daughters (white arrow) but not in the hub as indicated by the lack of red staining within the hub membrane (green) (C'). In ablated testes (D) all CySCs and their early daughters are gone and only the hub (green) and some germ cells (yellow arrowheads) remain. (D') dpErk expression is seen in one hub cell, suggesting that it is activating the EGF pathway (red staining, blue arrowhead). (E) Bar graph showing the percent of testes with dpErk expression in the hub of ablated testes compared to control testes. There is a significant increase in testes with hub cells expressing dpErk after CySCs have been ablated. Fisher's exact test, *$p<0.05$. Scale bars represent 20μm.

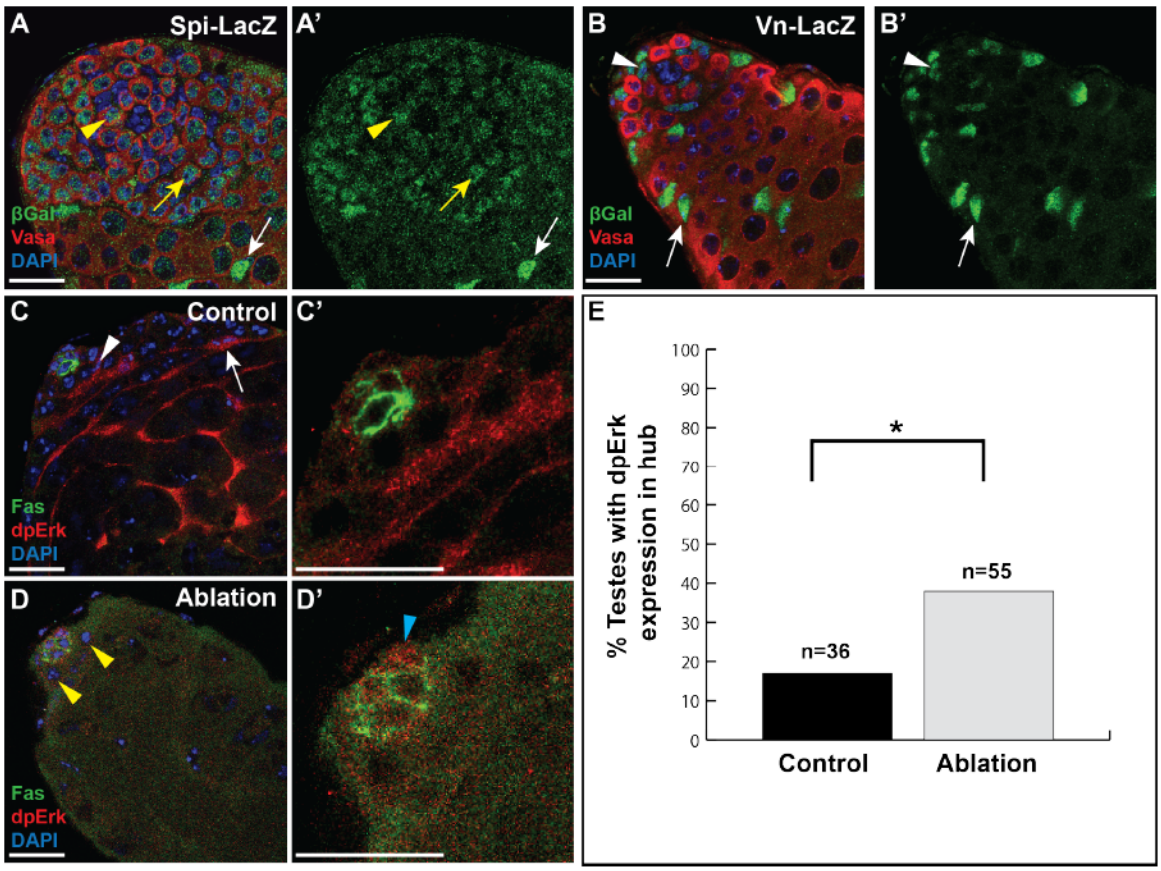
A
Spi-LacZ
βGal
Vasa
DAPI
A'
B
Vn-LacZ
βGal
Vasa
DAPI
B'
C
Control
Fas
dpErk
DAPI
C'
D
Ablation
Fas
dpErk
DAPI
D'
E
% Testes with dpErk expression in hub
100
90
80
70
60
50
40
30
20
10
0
*
n=36
n=55
Control
Ablation

Figure 3.4: Decreased EGF signaling prevents testes from recovering after CySC ablation. Single confocal sections through the testis apex immunostained for Fas III (hub, membranous green), DAPI (nuclei, blue), and either Vasa (germ cells, red, C-F) and TJ (cyst lineage, white, A-E) or just TJ (cyst lineage, red, F). Hubs are outlined in white. The pro-apoptotic gene Grim was expressed using the early cyst lineage driver c587Gal4 with the temperature sensitive TubGal80. Flies were shifted to the restrictive temperature of 31°C for 2 days so CySCs could be ablated. Flies were then allowed to recover back at the permissive temperature 18°C for 0 days, 7 days, or 14 days. Without ablation (A), testes retain all their cells types including hub cells (white outline), GSCs (yellow arrowhead), differentiating germ cells (yellow arrow), CySCs (white arrowhead), and cyst cells (white arrow). Upon ablation (B), all CySCs and their early daughters are gone and only the hub (white outline) and some germ cells remain (yellow arrowhead). Note that the late differentiating spermatocytes (yellow arrow) are found near the hub. (C-E) Testes show various phenotypes 7 days after recovery from ablation. (C) The majority of testes show recovery of CySCs and cyst cells (white arrowhead and white arrow respectively) while retaining germ cells (GSCs, yellow arrowhead, and differentiating germ cells, yellow arrow). Other testes (D) retain germ cells (yellow arrowhead) around the hub but do not recover CySCs and cyst cells. Testes in a third category (E) do not regain CySCs and cyst cells and lose all of their germ cells so only hub cells remain (white outline). (F) 14 days after recovery from ablation a portion of testes develop ectopic hubs (white outlines). (G) Bar graph depicting phenotypes observed 0, 7, and 14 days after ablation. These phenotypes consist of testes with hub cells, germ cells, and TJ-positive cells (black bar), testes with only hub cells and germ cells (blue bar), testes with only hub cells and TJ-positive cells (gray bar), testes containing only hub cells and thus lacking both germ cells and TJ-positive cells (green bar), and testes that have no hub cells (red bar). Significantly fewer testes with reduced EGFR recover CySCs and cyst cells (black bar) 7 and 14 days after ablation. Hub: Hub cells, GC: germ cells, TJ: CySCs and cyst cells. Chi Square Test, *$p<0.05$, ****$p<0.0001$. Scale bars represent 20μm.

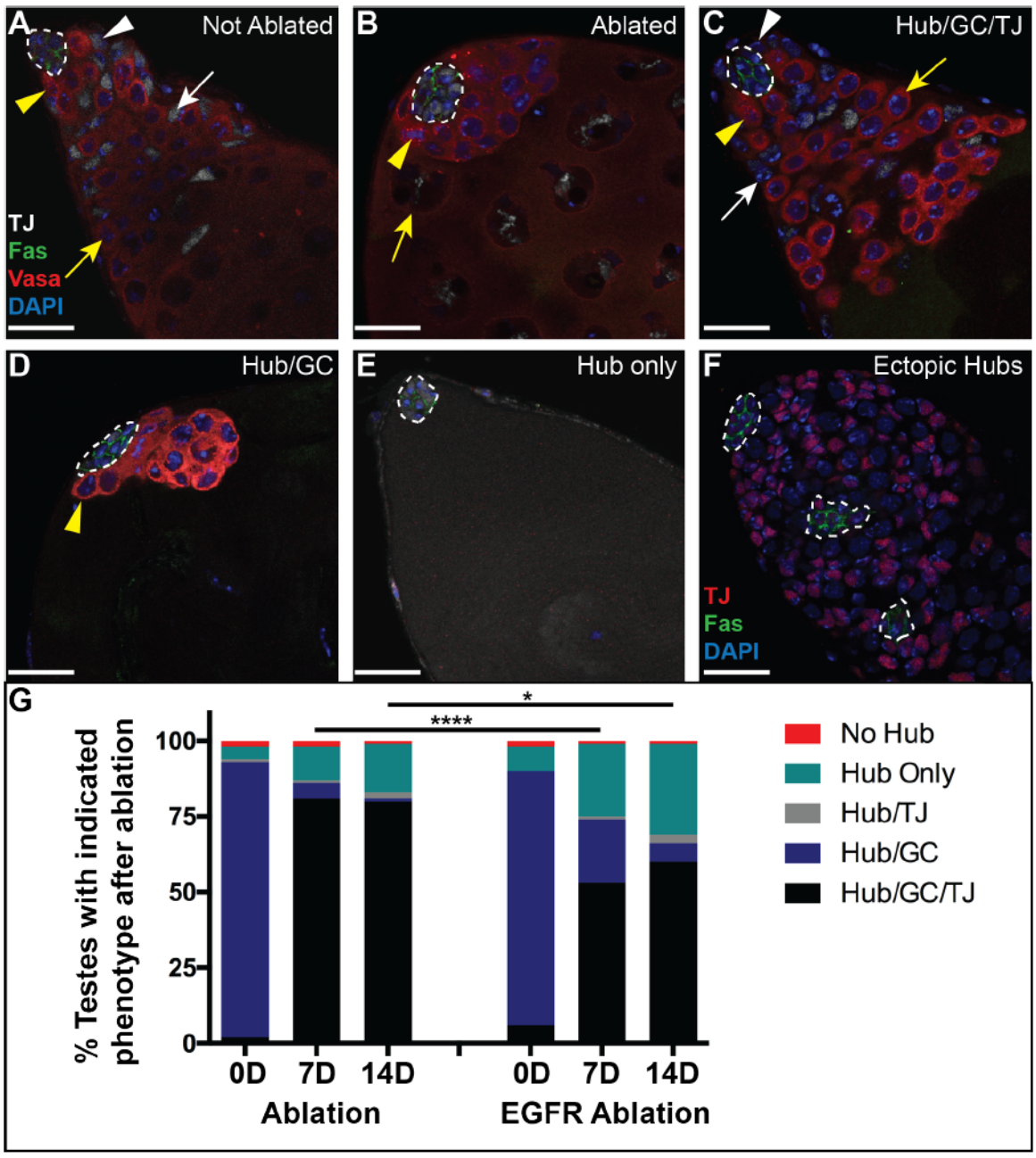
A
Not Ablated
TJ
Fas
Vasa
DAPI
B
Ablated
C
Hub/GC/TJ
D
Hub/GC
E
Hub only
F
Ectopic Hubs
TJ
Fas
DAPI
G
% Testes with indicated phenotype after ablation
100
75
50
25
0
*
****
0D
7D
14D
Ablation
0D
7D
14D
EGFR Ablation
No Hub
Hub Only
Hub/TJ
Hub/GC
Hub/GC/TJ

Figure 3.5: Model for cyst lineage recovery after ablation. After CySC ablation, the EGF ligand secreted by germ cells is no longer sequestered by the inhibitor Argos, and is now received by the hub. This in turn activates MAPK signaling in the hub cells driving the downstream transcription factor Pointed to express genes needed for proliferation and transdifferentiation of hub cells to CySCs. Once new CySCs are made, Argos becomes re-expressed leading to a waning of MAPK signaling in the hub.

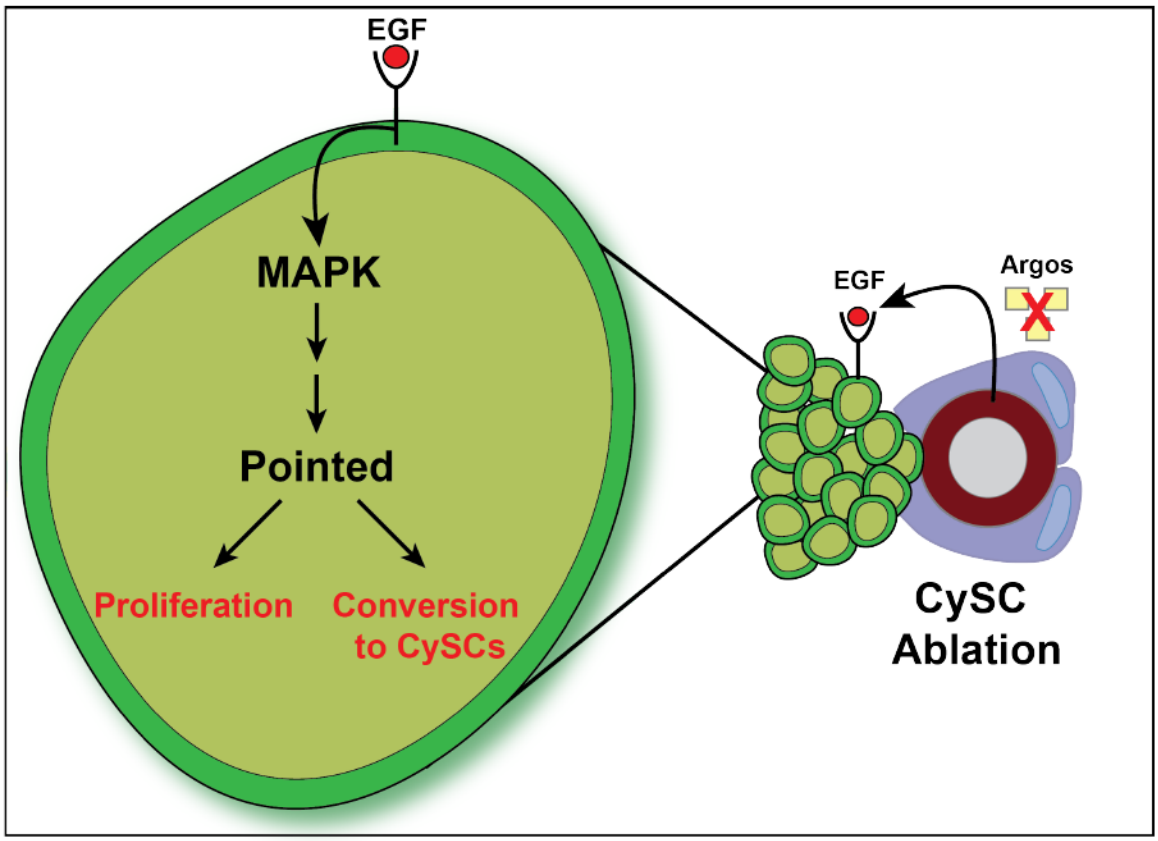

Tables

Table 3.1: EGF pathway activation in hub cells causes proliferation

Genotype: E132Gal4;; TubGal80^{ts}	% Testes with PH3+ Hub Cells
UAS-GFP RNAi	0% (n=0/210)
UAS-Rbf RNAi	26.7% (n=39/146)****
UAS-pnt.P1	7.3% (n=4/55)**
UAS-pnt.P2	6.6% (n=5/76)**
UAS-Ras85D	1.7% (n=1/58)^{ns}
UAS-rl	0% (n=0/92)^{ns}
UAS-EGFR Type I	0.7% (n=1/143)^{ns}
UAS-EGFR Type II	4.4% (n=5/113)**
UAS-EGFR Lambda	0.6% (n=1/163)^{ns}
UAS-PvR Lambda A	0.9% (n=1/106)^{ns}
UAS-PvR Lambda B	0% (n=0/156)^{ns}
UAS-InR A (8250)	0% (n=0/48)^{ns}
UAS InR B (8263)	0% (n=0/41)^{ns}
UAS-Htl Lambda	1.7% (n=3/181)^{ns}
UAS-Btl Lambda	0% (n=0/90)^{ns}
UAS-Sprouty RNAi	2.4% (n=3/126)^{ns}
UAS-PTEN RNAi	3.2% (n=4/125)*

Compared to GFP RNAi: Fisher's Exact Test, *p<0.05, **p<0.01, ***p<0.001, ****p<0.0001, ns=not significant

Table 3.2: EGF pathway activation in hub cells causes cell fate conversion

Genotype: E132Gal4; UAS-GTRACE	% Testes with GFP+ Cells Outside the Hub
Stock Control	21.3% (n=27/127)
UAS-EGFR Type I	70.3% (n=19/27)****
UAS-EGFR Type II	100% (n=12/12)**
UAS-EGFR Lambda	53.8% (n=21/39)***
UAS-PvR Lambda A	15.4% (n=2/13)^{ns}
UAS-PvR Lambda B	28% (n=7/25)^{ns}
UAS-Htl Lambda	24.2% (n=8/33)^{ns}
UAS-Sprouty RNAi	93.6% (n=44/47)****
UAS-PTEN RNAi	59.1% (n=13/22)***

Compared to stock control: Fisher's Exact Test, *p<0.05, **p<0.01, ***p<0.001, ****p<0.0001, ns=not significant

Table 3.3: Ablation phenotypes with and without reduced EGFR

Genotype	Days Recovered	Not Ablated	Hub/GC/TJ+	Hub/GC	Hub/TJ+	Hub only	No Hub
c587Gal4; UAS-Grim; TubGal80ts	0	4.9% (n=7/142)	1.5% (n=2/135)	91.1% (n=123/135)	0.7% (n=1/135)	4.4% (n=6/135)	2.2% (n=3/135)
c587Gal4;UAS-Grim/ $EGFR^{F24}$; TubGal80ts	$0^{a,d,ns}$	7.3% (n=4/55)	5.9% (n=3/51)	84.3% (n=43/51)	0% (n=0/51)	7.8% (n=4/51)	2% (n=1/51)
c587Gal4; UAS-Grim; TubGal80ts	7	4.5% (n=7/157)	81.3% (n=122/150)	4.7% (n=7/150)	1.3% (n=2/150)	10.7% (n=16/150)	2% (n=3/150)
c587Gal4;UAS-Grim/ $EGFR^{F24}$; TubGal80ts	$7^{b,d,****}$	4.8% (n=5/105)	53% (n=53/100)	21% (n=21/100)	1% (n=1/100)	24% (n=24/100)	1% (n=1/100)
c587Gal4; UAS-Grim; TubGal80ts	14	ND	80% (n=108/135)	1.5% (n=2/135)	2.2% (n=3/135)	15.6% (n=21/135)	0.7% (n=1/135)
c587Gal4;UAS-Grim/ $EGFR^{F24}$; TubGal80ts	$14^{c,d,*}$	ND	59.5% (n=50/84)	6% (n=5/84)	3.4% (n=3/84)	29.8% (n=25/84)	1.2% (n=1/84)

[a] Compared with c587Gal4; UAS-Grim; TubGal80ts at 0 days recovered
[b] Compared with c587Gal4; UAS-Grim; TubGal80ts at 7 days recovered
[c] Compared with c587Gal4; UAS-Grim; TubGal80ts at 14 days recovered
[d] Chi Square Test, *p<0.05, **p<0.01, ***p<0.001, ****p<0.0001, ns=not significant

Table 3.4: Ectopic hubs form in testes after 14 day recovery from CySC ablation

Genotype	Recovered with Ectopic Hubs	Recovered without Ectopic Hubs
c587Gal4; UAS-Grim; TubGal80ts	30.6% (n=33/108)	69.4% (n=75/108)
c587Gal4;UAS-Grim/ $EGFR^{F24}$; TubGal80ts	18% (n=9/50)	82% (n=41/50)

CHAPTER 4

Live imaging of the *Drosophila* testis stem cell niche

This chapter is a modified version of the manuscript Greenspan LJ, and Matunis EL. (2017). Live imaging of the *Drosophila* testis stem cell niche. *Methods Mol Biol*. 1463:63-74

SUMMARY

Live imaging of adult tissue stem cell niches provides key insights into the dynamic behavior of stem cells, their differentiating progeny and their neighboring support cells, but few niches are amenable to this approach. Here we discuss a technique for long term live imaging of the *Drosophila* testis stem cell niche. Culturing whole testes *ex vivo* for up to 12.5 hours allows for tracking of cell-type specific behaviors under normal and various chemically or genetically modified conditions. Fixing and staining tissues after live imaging allows for the molecular confirmation of cell identity and behavior. Utilization of live imaging in intact niches will facilitate further understanding of the cellular and molecular mechanisms that regulate stem cell function *in vivo*.

INTRODUCTION

Adult stem cells both self-renew and differentiate in order to regulate proper tissue maintenance. While the analysis of fixed tissues provides important information regarding adult stem cell biology, live imaging of stem cells within an intact local microenvironment, or niche, reveals unique insights into stem cell behavior that cannot always be extrapolated from fixed images. For example, live imaging of the *Drosophila* testis niche has shown that although stem cells primarily undergo asymmetric divisions where one daughter cell remains a stem cell while the other daughter goes on to differentiate, germline stem cells can self-renew via symmetric renewal (in which two stem cells are made) or dedifferentiation (in which differentiated daughters migrate back to the niche and revert to stem cells) (Sheng and Matunis, 2011). Spermatogonial fragmentation has since been shown to occur in mammalian testes using live imaging and lineage tracing (Hara et al., 2014).

The well-characterized *Drosophila* testis stem cell niche provides an ideal model system to study stem cell behavior and function (de Cuevas and Matunis, 2011) (**Figure 4.1**). It supports two types of stem cells, germline stem cells (GSCs) and somatic cyst stem cells (CySCs), which attach to a group of terminally differentiated hub cells that secrete ligands promoting stem cell fate. GSCs divide asymmetrically to produce a differentiating daughter (or gonialblast) that undergoes transit-amplifying divisions to form a cluster of interconnected spermatogonia. Spermatogonia subsequently enter meiosis and spermiogenesis, eventually forming sperm. CySCs also divide asymmetrically and produce daughters called cyst cells that encapsulate the germline and

elongate with the growing spermatogonial clusters. The CySCs and their progeny are essential for the survival and proper differentiation of the germline (de Cuevas and Matunis, 2011).

Previous work in the *Drosophila* ovary provided the groundwork for live imaging in *Drosophila* gonadal tissues (Prasad and Montell, 2007; Prasad et al., 2007) including extended live imaging (14 hours) of the ovarian stem cell niche (Morris and Spradling, 2011). In addition, protocols for imaging testis tips (Cheng and Hunt, 2009) or whole mounted testes on slides (Sheng and Matunis, 2011) have been established. Here we describe a method for imaging the stem cell niche of whole *Drosophila* testes using glass bottom imaging dishes. Using this type of dish, allows for the manipulation of imaging media and also the capacity to fix and stain testes after long-term imaging. This protocol is updated from that published by Sheng and Matunis (2011) with new adaptations developed by our lab and the DiNardo lab (Lenhart and DiNardo, 2015).

MATERIALS

Prepare all solutions using ultrapure water (sensitivity 16-18 MΩ-cm dH_2O) and molecular grade reagents unless specified otherwise.

Dissection of testes from adult male *Drosophila*

1. Flies expressing fluorescent reporters or proteins in cells of interest (*see* **Note 1**).
2. Dumont #5 forceps, blunt and fine tipped pairs.
3. Dissecting dish: Beveled edge watch glass lined with silicone to protect forceps from damage (*see* **Note 2**).

4. 9 ” glass Pasteur pipettes.

5. Stereomicroscope (e.g. Zeiss Stemi SV 6 with a Schott-Fostec external light source)

6. CO_2 pad for anesthetizing flies.

7. Round #2 camel hair paintbrush with most of the hair removed.

8. 1 X Becker Ringer’s solution (Ashburner, 1989): 111 mM NaCl, 1.88 mM KCl, 64 μM NaH_2PO_4, 816 μM $CaCl_2$, 2.38 mM $NaHCO_3$. To make a 10 X stock solution combine 220 mL of 5 M NaCl, 18.8 mL of 1 M KCl, 3.2 mL of 0.2 M $NaH_2PO_4 \bullet 2H_2O$, 8.16 mL of 1 M $CaCl_2 \bullet 2H_2O$, and 500 mL of ultrapure water in a 1 L graduated cylinder. Add 2 g of $NaHCO_3$ last to prevent precipitation. Add ultrapure water to a final volume of 1 L. Cover graduated cylinder with parafilm and invert 5 times to mix. Filter-sterilize through a 0.1 μm PES bottle-tip filter into an autoclaved 1 L glass bottle. Solution keeps many months at room temperature if the bottle is tightly sealed (wrap cap with parafilm). Dilute 1:10 with ultrapure water for 1X Becker Ringer’s solution, store at room temperature.

Live imaging of *Drosophila* testes

1. Insulin stock solution: Dissolve powdered bovine pancreas insulin in acidified water (1 μL concentrated HCl + 1 mL ultrapure water) at a final concentration of 10 mg/mL. Store 50 μL aliquots in 1.5 mL microcentrifuge tubes at -20°C.

2. *Drosophila* tissue culture media: 15% fetal bovine serum (v/v), 0.5 X penicillin/streptomycin in Schneider’s media, pH 7. Adjust Schneider’s media to pH 7, sterilize using a 0.1 μm PES syringe filter (this can be stored for many months at 4°C).

Combine 2111.25 µL of pH 7 Schneider's media, 375 µL of fetal bovine serum and 13.75 µL of 100 X penicillin/streptomycin (10,000 U/mL of penicillin and 10,000 µg/mL streptomycin in 10 mM citrate buffer) in 15 mL sterile conical tube. Vortex briefly, store at 4°C. Make fresh every week.

3. Live imaging solution: 0.2 mg/mL insulin in *Drosophila* tissue culture media. Add 10 µL of the 10 mg/mL insulin stock solution to 500 µL of *Drosophila* tissue culture media. Make fresh on the day of imaging (*see* **Note 3**).

4. Poly-$_L$-lysine: 1 mg/mL in 0.1 M Trizma buffer pH 8.5. Dissolve 10 mg of Poly-$_L$-lysine in 10 mL 0.1 M filter-sterilized Trizma buffer pH 8.5. Store 200 µL aliquots in 1.5 mL microcentrifuge tubes at -20°C.

5. Imaging dish: 35-mm glass-bottom Petri dish with 10-mm microwell.

6. Laser scanning or spinning disc confocal microscope (e.g. Zeiss LSM 780 confocal microscope with Zen software or a similar microscope).

Immunostaining testes after live imaging

1. 9 " and 5.75 " glass Pasteur pipettes.
2. 1 X Phosphate Buffered Saline (PBS): 137 mM NaCl, 2.7 mM KCl, 1.5 mM KPO_4 monobasic, 8.1 mM $NaPO_4$ dibasic anhydrous. To make 10 X PBS combine 80 g NaCl, 2 g KCl, 2 g KPO_4 monobasic, 11.44 g $NaPO_4$ dibasic anhydrous, and 700 mL of ultrapure water in a 2 L beaker and stir with a magnetic stir bar. When dissolved, transfer solution to a 1 L graduated cylinder and add ultrapure water to a final volume of 1 L. Filter sterilize (PES bottle-tip filter, 0.1 µm pore size) into a 1 L autoclaved glass container and store at room temperature or at 4°C. Dilute 1:10 with ultrapure water to make 1 X PBS.

3. 1 X Phosphate Buffered Saline with 0.1% Triton X-100 (v/v) (PBX): Add 1 mL of Triton X-100 to a 2L beaker containing 1 L 1 X PBS. Stir with a magnetic stir bar for 20 minutes. Store in 1 L glass bottle at room temperature or 4°C.
4. Fixative solution: 4% paraformaldehyde (v/v) in PBX. Dilute 16% paraformaldehyde (open a fresh ampule each week) in PBX to a final concentration of 4%. Make fresh each time.
5. Block solution: 3% BSA (w/v), 0.02% NaN_3 (w/v) in PBX. Add 15 g bovine serum albumin (BSA) to a 1 L beaker containing 500 mL PBX. Mix with a magnetic stir bar until dissolved. Add 500 µL 20% sodium azide, filter sterilize (PES filter, 0.1µm pore size), and store at 4°C. This solution can be used for several months.
6. Normal goat serum. Store 300 µL aliquots in 1.5 mL microcentrifuge tubes at -20°C. Working aliquot can be stored at 4°C.
7. Primary antibodies.
8. Secondary antibodies with conjugated fluorophores.
9. Vectashield mounting medium.

METHODS

All methods are performed at room temperature unless stated otherwise.

Preparing Imaging Dish

1. Thaw 200 µL aliquot of 1 mg/mL Poly-$_L$-Lysine and pipette onto the coverslip portion of the imaging dish.
2. Cover dish and incubate at room temperature on the bench for at least one hour.

3. Remove Poly-$_L$-Lysine from coverslip with a micropipettor and return to the original tube. Poly-$_L$-Lysine can be stored at 4°C and re-used for 1-2 weeks.
4. Wash coverslip: Add 200 µL of sterile distilled water to coverslip, pipette up and down 3 times, and discard. Repeat 3 times.
5. Pipette 200 µL of sterile distilled water onto coverslip, replace the cover on the dish and keep at room temperature while dissecting testes. Leave water on the coverslip until ready to directly transfer testes.

Dissecting and Mounting Whole Testes

1. Clean all forceps, dissecting dishes, CO_2 pad, and dissecting area with ethanol before dissecting.
2. Anesthetize adult flies using CO_2. Using the stereomicroscope, collect 20-50 males with the paintbrush to be dissected.
3. Pour approximately 20 mL 1 X Becker Ringer's solution into dissecting dish.
4. Hold the blunter pair of forceps in your non-dominant hand, and use them to grasp a fly by the thorax. Anchor fly to the bottom of the dissecting dish so that it is completely submerged in Becker Ringer's solution. Without releasing the fly, use the finer pair of forceps in your dominant hand to gently puncture the cuticle near the middle of the fly's abdomen to partially release the testes into the media. Grasp the posterior cuticle that contains the testes and associated structures, and gently pull until it separates from the rest of the fly (**Figure 4.2A**). Anchor the posterior cuticle to the bottom of the dish using the blunter pair of forceps and gently use one prong of the finer pair of forceps to dissociate the testes from the cuticle. Separate the testes from the accessory glands and

ejaculatory duct but not the seminal vesicle, by severing the connection between the seminal vesicle and the accessory gland (*see* **Note 4**) (**Figure 4.2A', B, B'**). Testes can be left in the Becker Ringer's solution in the dissecting dish until all testes are dissected.

5. Once finished dissecting, discard any ruptured testes (**Figure 4.2A**).
6. Coat 9 " Pasteur pipette with 1 X Becker Ringer's solution by pipetting up and down.
7. Remove all the water from imaging dish using a micropipettor. Immediately transfer testes from the dissecting dish to the coverslip portion of the imaging dish using the coated Pasteur pipette (*see* **Note 5**).
8. Using the tip of the blunter pair of forceps, carefully press testes onto the coverslip so their apical ends adhere and lie flat against the coverslip. There should be no overlap between samples (*see* **Note 6**) (**Figure 4.2A").**
9. Remove all of the Becker Ringer's solution with a Pasteur pipette. Immediately add back enough fresh Becker Ringer's solution to coat testes, preventing samples from drying out. This will cause testes to strongly adhere to the coverslip allowing them to withstand several media changes if applicable.
10. When ready to image, remove Becker Ringer's solution and immediately add live imaging solution using a micropipettor (*see* **Note 7**).

Overnight Time-Lapse Imaging of the Testis Niche

Imaging instructions are based on using a Zeiss LSM 780 confocal microscope with Zen software.

1. Mount covered imaging dish onto movable stage of the microscope (*see* **Note 8**).

2. Use a 60 x objective oil lens that will be in contact with the coverslip. For a wider field of view, a 40 x objective oil lens can be used.
3. Locate testes using bright field or fluorescent channels (*see* **Note 9**). Adjust the laser power, exposure time, and gain for each wavelength used in order to obtain an optimal signal without photobleaching. This will differ depending on the microscope and fluorophore used. The more fluorophores imaged, the greater the chance for photobleaching.
4. Evaluate the fluorescent signal for each testis and select about 7 that are favorable for imaging (*see* **Note 10**). Save the position of those selected to image at the center plane of the Z range.
5. Once each testis position is selected, set the Z stack to range around the center of the field of interest. Typically a 30 μm range with 1.25 μm steps will suffice.
6. Set the total time for imaging testes and the time between each scan. Typically 25-minute intervals over 12.5 hours will be enough to follow cellular behaviors (*see* **Note 11**).
7. Germline divisions should be seen throughout the entire movie indicating viability of the tissue during the imaging period (**Figure 4.3A**). Nuclear markers can be used to detect cell death since DNA will condense causing bright dense signals. While some spermatogonial death is expected to occur in wild-type testes (**Figure 4.3A**) (Yacobi-Sharon et al., 2013), massive amounts of cell death, especially stem cell and hub cell death which normally does not occur in wild type testes (Brawley and Matunis, 2004; Hasan et al., 2015), is indicative of a non-viable tissue (**Figure 4.3B**).

Immunolocalization after time-lapse imaging

Once live imaging is complete, testes can be fixed and stained directly in the dish for additional markers.

1. Remove all imaging media from the imaging dish using a Pasteur pipette (*see* **Note 12**).
2. Quickly add 600 µL of fixative solution onto the coverslip portion of the imaging dish. Incubate at room temperature for 22 minutes.
3. Remove formaldehyde with Pasteur pipette and discard. Rinse testes twice briefly with ~1 mL PBX.
4. Wash testes 3 times for 10 minutes each with ~1 mL PBX and allow the dish to remain stationary at room temperature. Keep the dish covered to minimize evaporation.
5. Remove PBX and add 500 µL of 2% Normal goat serum in block solution to the imaging dish. Testes should remain covered and stationary for at least 1 hour at room temperature or overnight at 4°C to reduce any non-specific antibody binding (*see* **Note 13**).
6. Remove Normal goat serum in block solution and add 500 µL of primary antibody diluted in block solution to an empirically determined working concentration. Incubate dish for 1-2 hours at room temperature or overnight at 4°C. Keep dish covered and stationary during incubation.
7. Remove primary antibody with a Pasteur pipette and quickly add ~1 mL PBX (*see* **Note 14**).
8. Rinse twice with ~1 mL PBX then wash 3 times for 10 minutes with ~1 mL PBX as in steps 3 and 4.

9. Remove PBX, and add 500 µL of secondary antibody diluted in block solution to an empirically determined working concentration. Keep imaging dish covered and stationary and incubate dish for 1-4 hours at room temperature or overnight at 4°C (*see* **Note 15**). Place dish inside a foil-covered box to protect samples from light during the secondary antibody incubation and **ALL** subsequent steps.
10. Remove secondary antibody solution and rinse twice briefly, then twice for 10 minutes with ~1 mL PBX.
11. Remove PBX then rinse once briefly and once for 10 minutes with ~1 mL PBS.
12. Remove PBS and immediately cover testes with a drop of Vectashield.
13. Store covered imaging dish with fixed and stained testes on a horizontal surface in a foil-covered box at -20 °C until ready to image.
14. Image fixed and stained testes with the same microscope used for live imaging, if possible, to eliminate variation between instruments.
15. Using the map of testes' locations (or tile scan), locate testes that were previously imaged live. It is helpful to compare the last frame of the movie to fixed testes to ensure they correspond (**Figure 4.4**).

NOTES

1. Not all fluorescent reporters or fluorescently tagged proteins are strong enough for live imaging. Those that work well in adult testes include but are not limited to: nos::Moe-GFP to visualize the germline (from R. Lehmann) (Sano et al., 2005), His2Av-RFP to visualize nuclei of all cells (Bloomington Stock Center), G-TRACE reporter for lineage tracing (Bloomington Stock Center) (Evans et al., 2009), and FUCCI reporter for cell

cycle analysis (Bloomington Stock Center) (Zielke et al., 2014). Flies should be raised in incubators at constant temperature (18°C or 25°C) and humidity (65%), and shifted to the appropriate temperatures (29°C or 31°C) prior to dissection if applicable to the experiment.

2. To make lined dissecting dishes, add 9 mL of elastomer base and 1 mL curing agent from a Sylgard 184 Silicone Elastomer Kit (Dow Corning) to a disposable 15 mL conical tube. Add a pinch of 100-400 mesh activated charcoal powder (Sigma Aldrich) and invert gently to mix. Continue to add charcoal until the elastomer is opaque, and then pour solution into a clean beveled edge watch glass. Remove bubbles from elastomer surface with a Pasteur pipette. Place dish in a covered container and cure overnight at room temperature.
3. Dyes such as MitoTracker Red CMXRos (1μM) (Molecular Probes) can be added to the imaging media as well as various drugs. Test toxicity of new dyes or drugs to the tissue over a 12.5-hour period prior to use in live imaging.
4. To separate the testis from the cuticle use both prongs of the forceps to pull the testis off the accessory gland or place one prong of the forceps between the spiral of the testis (careful to not puncture the testis) and pull with the anchor hand. Testes should also be separated from each other.
5. If there is excess debris in the media following dissection, testes can be gently transferred to a separate dissecting dish containing fresh Becker Ringer's solution, rinsed a few times with fresh Becker Ringer's solution, and then transferred to the imaging dish. Try to minimize handling of testes and number of transfers as this could damage the tissue.

6. Testes will loosely adhere to the coverslip portion of the imaging dish due to the Poly-$_{L}$-Lysine. If repositioning of testes is necessary, be extremely gentle since too much force can damage the tissue.
7. Media will spill over the coverslip portion of the dish. Try to keep as much media over the testes as possible. Too little media will lead to evaporation causing the testes to dry out during imaging. If desired, incubate testes in media containing dye or drug prior to imaging.
8. Using a microscope fitted with an environmental chamber is desirable to further stabilize the dish on the stage. Utilizing the heat or humidity controls is optional.
9. Using paper, map the location of each testis on the imaging dish prior to mounting the dish on the microscope. Alternatively, create a tiled image using the 10 x objective to get an overview of where each testis is located. This helps to ensure that each testis is evaluated before choosing which to image.
10. Select testes in which the fluorescent signal is strong, indicating the field of interest is closest to the coverslip, and there is little movement due to muscle contractions in order to prevent blurred images. If using multiple fluorophores, ensure all have a strong signal.
11. The interval between scans should allow for enough time for each testis to be imaged before the next cycle begins. On a LSM 780 microscope, 7-8 testes imaged with GFP and RFP with 30 μm stacks takes approximately 15 minutes to image. This allows for 10 minutes between time points that the testes are not being exposed to the laser thus helping to maintain tissue viability and minimize photobleaching.

12. It is easiest to remove solutions from the dish using a long 9 ” Pasteur pipette and to add in fresh solutions when washing testes using a shorter 5.75 ” Pasteur pipette. Position pipette so that it isn’t directly over any testes since too much suction can cause testes to dissociate from the coverslip.
13. If evaporation of the solution during overnight incubations is a concern, covered dishes can be kept in a sealed container containing a wet Kimwipe.
14. Many primary antibodies can be saved, stored at 4°C and reused.
15. A nuclear counterstain such as 4’-6-diamidino-2-phenylindole (DAPI) can be added to the secondary antibody solution at a final concentration of 1 μg/mL.

Figures

Figure 4.1: The *Drosophila* testis stem cell niche consists of terminally differentiated quiescent hub cells (red) that signal to the surrounding germline (GSCs, green) and somatic cyst stem cells (CySCs, white). GSCs divide asymmetrically to produce daughter cells that transit amplify to form spermatogonial clusters (green). These clusters undergo meiosis and differentiate into sperm. CySCs also divide asymmetrically to produce daughter cyst cells (white). Two cyst cells encase each spermatogonial cluster and are required for the differentiation process.

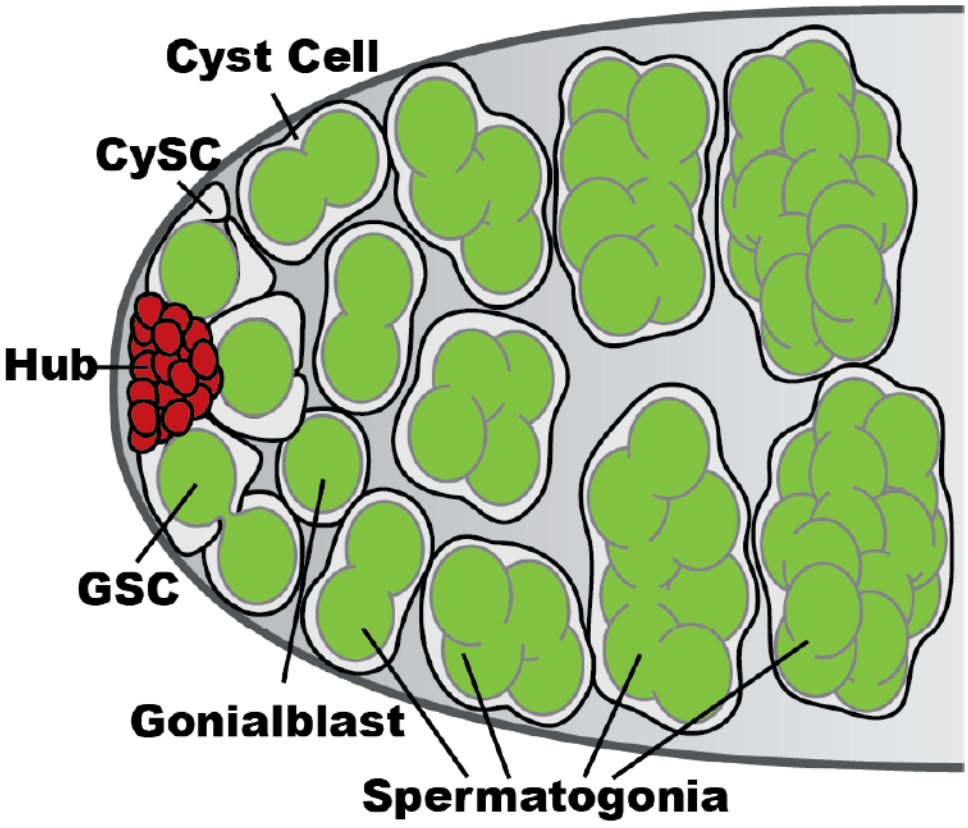

Figure 4.2: Testes dissected from an adult male *Drosophila* are shown attached to the cuticle (**a**) completely detached from the cuticle, accessory glands, and ejaculatory duct (**a'**) and mounted on the circular coverslip portion of an imaging dish (**a"**). Yellow arrow (**a**) indicates a rupture in one of the testes, making it unfit for imaging. Mounted testes (**a"**) are flat on the coverslip and do not overlap. Diagram (**b**) and image (**b'**) of *Drosophila* testes, accessory glands, and ejaculatory duct. Testes with seminal vesicles attached should be separated from the accessory glands and ejaculatory duct (red arrow) prior to imaging.

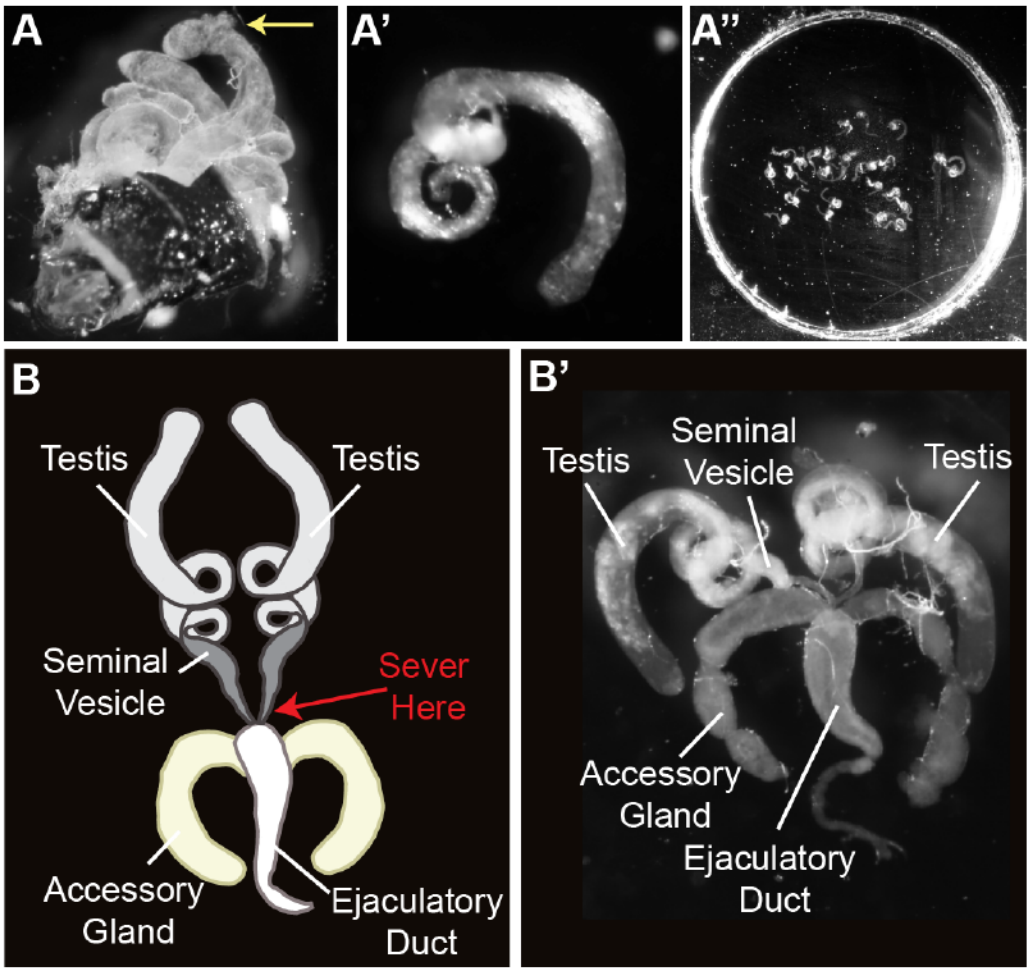

Figure 4.3: Single time point images from overnight movies of a viable (**a**) and non-viable (**b**) testis expressing histone-RFP (red) and germline-GFP (green). (**a**) Viable testes show germline divisions throughout the imaging period (yellow arrow) with some cell death seen in spermatogonia (white arrow). (**b**) In non-viable testes, cell death is seen in most cells including germline stem cells (yellow arrow) and hub cells (white arrowhead). Dying cells can be detected through the condensation of nuclei as indicated by the dense red signal from the histone-RFP marker.

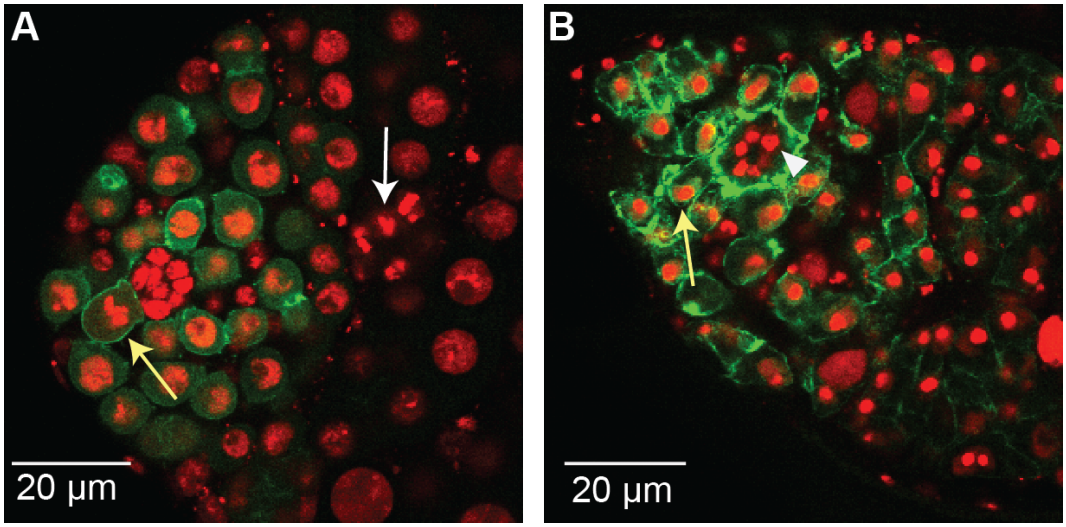

Figure 4.4: Comparison of a live (**a**) and fixed (**b**) testis after 12.5 hours of imaging. Staining after imaging allows for the use of cell specific markers. Cells tracked live that are histone-RFP positive (red), germline-GFP negative (non-green), and close to the hub can be accurately identified as CySCs through ZFH1 staining (white) (compare **a** and **b** yellow arrow). Hub cells (white asterisk) are encircled by the germline stem cells, but can also be identified by Fasciclin 3 staining (**b**, blue).

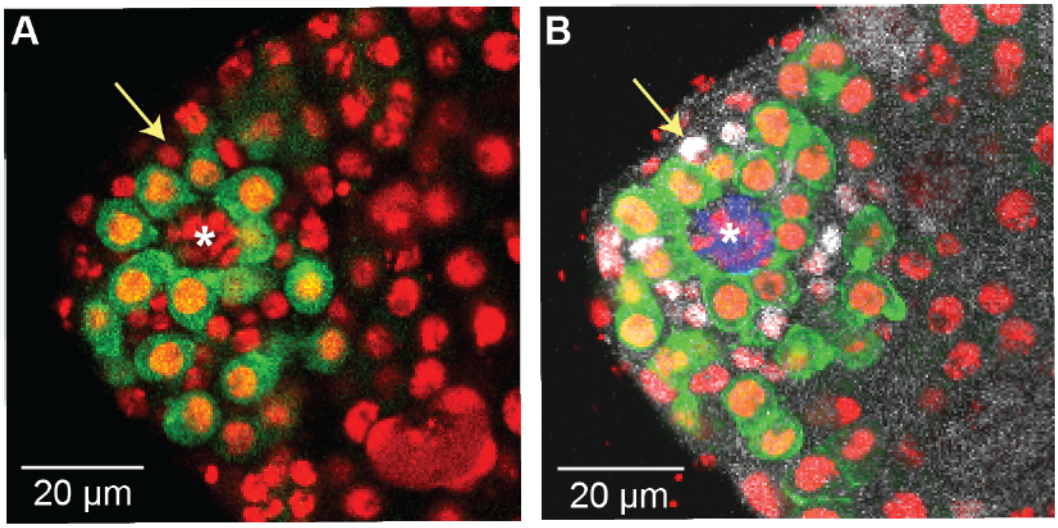

CHAPTER 5

Concluding Remarks

Adult stem cells are required in many organisms for the proper maintenance of their tissues. The microenvironment or niche, where the stem cells reside, provides signals to ensure stem cells are constantly maintained. However, disruptions in niche signaling during homeostatic conditions can lead to over-proliferation or depletion of the stem cell pool. Furthermore, damage to a tissue can cause changes in signaling needed to initiate repair. Therefore understanding the niche signals required for the maintenance of stem cells during both normal and injury conditions will provide great insight into *in vivo* stem cell biology and regenerative medicine.

In this dissertation I use the well-characterized *Drosophila* testis stem cell niche to understand the signals needed for proper niche cell maintenance under normal and injury conditions. Little is known about the mechanisms needed to regulate niche cell quiescence, niche cell fate, or niche number *in vivo*. Here I have shown that the tumor suppressor gene and Retinoblastoma homolog Rbf is required in the terminally differentiated niche cells of the *Drosophila* testis, known as the hub, to regulate these properties. Loss of Rbf causes hub cells to proliferate and convert into somatic stem cells. Extended loss of Rbf eventually leads to the formation of ectopic hubs driving aberrant tissue function. Furthermore, I have shown that upon injury to the testis by genetic ablation of somatic cyst stem cells (CySCs), the EGF/MAPK pathway is activated in the hub cells. This in turn causes hub cells to divide and transdifferentiate in order to replace the lost CySC population. Together these results uncover a mechanism for hub cell maintenance under both normal and injury conditions.

In this body of work, I show that loss of Rbf in the hub cells of the *Drosophila* testis can lead to an excess of many different cell types within the tissue through non-autonomous and autonomous means. Increasing niche cell number allows for more germline and somatic stem cells to be maintained due to the increase in niche signals. In addition, Rbf knockdown and EGFR activation in the hub leads to an increase of cyst lineage cells due to the conversion of hub cells to somatic cyst stem cells. Together these initial effects cause an increase in stem cell number, which consequently lead to an increase in early-differentiated daughters, thus driving an expansion of different cell populations within the tissue. Furthermore, the formation of ectopic niches within the testis leads to stem cells residing in aberrant locations. These results demonstrate how mutations in a particular cell type can drive the formation of several aberrant phenotypes. Future studies understanding the signals that precisely modulate niche cells, not just the stem cells they support, will further illuminate the role they can play in tissue regeneration and disease progression.

APPENDIX - I

Data not included in other chapters

FIGURES

Figure A1: The FUCCI system can be used in the hub to indicate cell cycle status. (A-C) The fluorescent ubiquitination based cell cycle indicator (FUCCI) (Zielke et al., 2014) can be driven specifically in hub cells to evaluate their cell cycle status. Those cells expressing GFP only are in G1 phase, those that express RFP are in S phase, and those cells that are yellow (GFP and RFP positive) are in G2/M phase. Single confocal sections through the testis apex immunostained for GFP and dsRed to indicate cell cycle status, and DAPI (nuclei, blue). Flies were shifted to 29°C for 7 days to induce FUCCI and RNAi knockdown using the E132Gal4;;TubGal80^{ts} driver. Zoomed images show green and red channels only. (A) Control testis expressing FUCCI system shows that most hub cells are normally quiescent in G1. In 5% of testes, an occasional hub cell will enter the cell cycle as has been previously shown to occur with EDU incorporation but these cells never undergo mitosis (see Figure 2.1). (B) Testes with Rbf knocked down in the hub show cycling hub cells (S or G2/M) in 86% of testes as demonstrated by the red cell (arrowhead and B'') suggesting this cell is in S phase. This is a significant increase compared to controls. Furthermore, 63% (22/35) of these testes show at least one cell in S phase which matches the 60% seen with EDU staining (Figure 2.1). (C) Testes with Esg knocked down in the hub occasionally have cycling hub cells in 12% of testes but this is not significantly more than controls. This could suggest that either Esg loss does not greatly affect hub cell proliferation, or that most cells are converting (Voog et al., 2014) so there are too few to monitor. Fisher's exact test, $p<0.0001$. Scale bars represent 20μm. Inset scale bars represent 10μm.

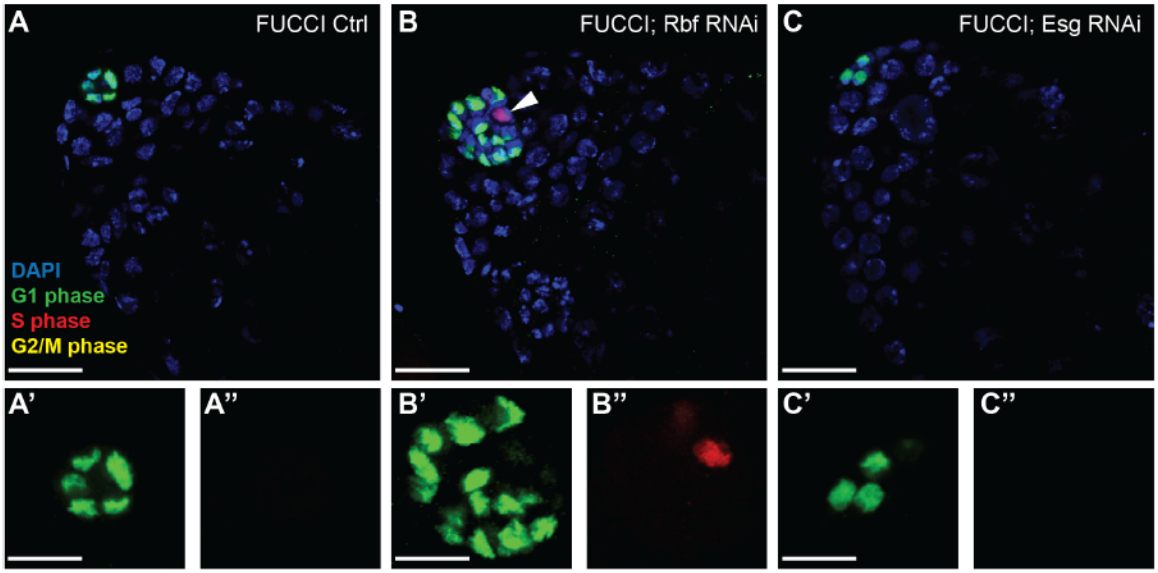

Percent testes with hub cells in the cell cycle

FUCCI Ctrl	FUCCI; Rbf RNAi	FUCCI; Esg RNAi
5% (n=3/56)	86% (n=30/35)****	12% (n=3/25)

Figure A2: Hub cells do not proliferate upon germline ablation in adult testes. (A-D) Single confocal sections through the testis apex for Arm and PH3 (hub membrane and mitotic cells respectively, green), Vasa (germ cells, red), and DAPI (DNA, blue). Insets show ZFH1 staining (CySCs and early daughters, white, B-D). Flies expressing the pro-apoptotic gene Hid using the germ cell driver Nanos-Gal4 were shifted to 31°C for the 4, 6, or 8 days to induce germ cell ablation. (A) Unablated testes contain hub cells, germ cells, and cyst lineage cells. (B) After 4 days of ablation, some testes have their GSCs ablated with only somatic cells near the hub (inset) but later germ cells (yellow arrowhead) still remain. (C) After 6 days of ablation, all germ cells are gone and somatic cells over-proliferate (white arrowheads). (D) After 8 days of ablation, somatic cells have filled the empty space where germ cells used to reside (inset). Hub cells are never seen proliferating during germ cell ablation. (E) Table indicating percent of testes in which germ cells were ablated during development (agametic testes) and percent in which germ cells were ablated during adulthood out of those that were not agametic. About 30-40% of testes developed as agametic since Hid was not repressed during development. Out of those testes that were not agametic, 6 days of Hid expression was sufficient to drive full germline ablation. Scale bars represent 40µm. Inset scale bars represent 20µm.

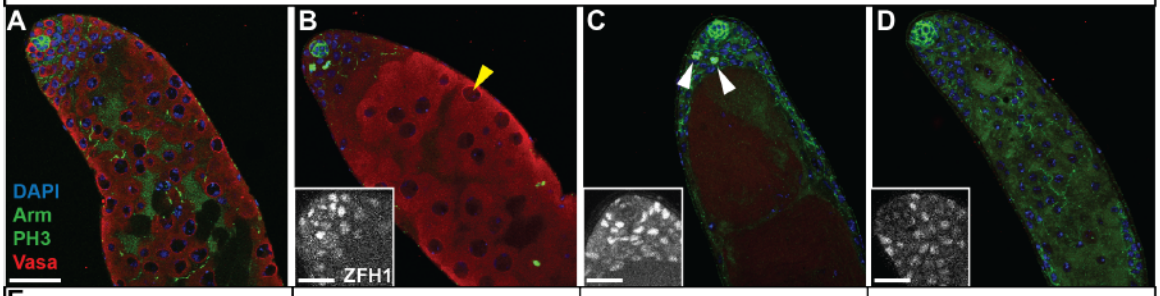

E

% Agametic Testes	36.8% (n=7/19)	40% (n=10/25)	32.4% (n=11/34)
% GSC Ablated Testes	16.6% (n=2/12)	100% (n=15/15)	100% (n=23/23)

Figure A3: The Raeppli marking system can be used in the *Drosophila* testis for multi-color labeling of hub cells. (A) The Raeppli marking system construct as described in (Kanca et al., 2014). When combined with a cell specific Gal4 driver and a flippase, recombination will occur and mark a cell with E2-orange (orange), mKate (red), TFP1(green), or TagBFP (blue). (B-D) Single confocal sections through the testis apex show Raeppli marking system and are immunostained with Fas (hub membrane, white). Flies expressing Raeppli and Rbf RNAi were grown at 16°C and shifted to 29°C for 14 days to induce marking and RNAi knockdown using the E132Gal4 driver. Various examples of marking system are shown. Hub cells can be seen marked with green, blue, or orange, but the mKate red color was never observed. Hubs can be seen becoming misshapen (C) or elongating (D) as is known to occur when Rbf is knocked down. Scale bars represent 20μm.

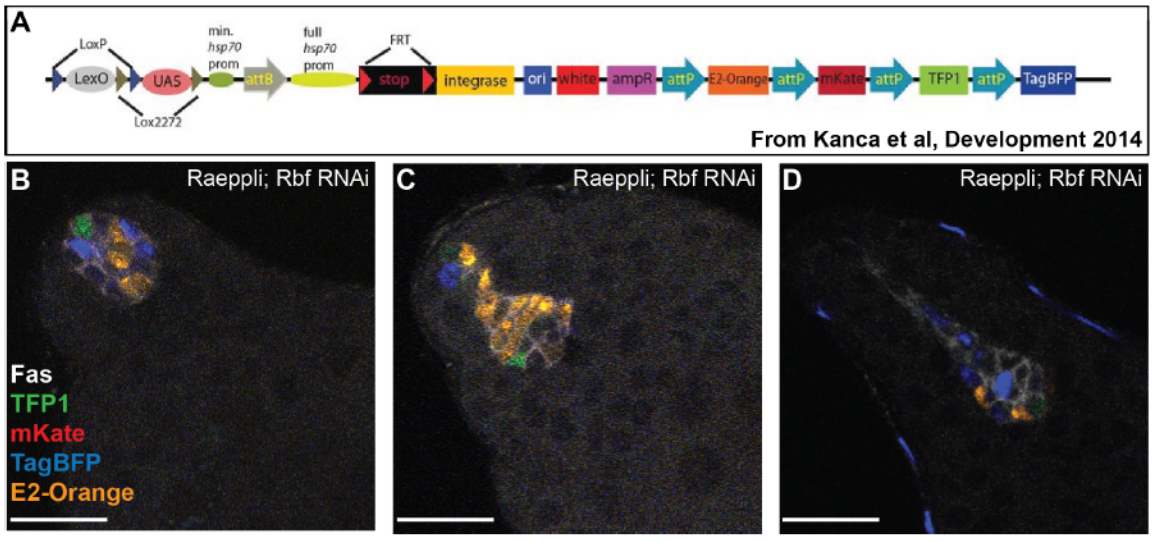

Figure A4: Hub cells migrate farther distances and turn on cyst lineage markers after CySC ablation. (A-B and D-E) Still frame images of testes imaged live expressing the germ cell marker NosGMA and the DNA marker HisRFP. Testes were imaged for 12.5 hours then fixed and immunostained immediately after imaging for Fas (hub membrane, blue), and ZFH1 (CySCs, white). Cells were tracked over time (white arrowheads) to determine distance traveled and marker expression. (A-B) Control testes show slight hub cell movement throughout imaging but hub cells remain in a confined area at the apex of the testis between the first (A) and last (B) frames of the movie. (C) These hub cells are within the confines of the hub cluster as indicated by Fasciclin III staining and do not express the CySC marker ZFH1. (D-F) Testes that have recovered for 5 days after CySC ablation show dispersed hub cells throughout the testis apex. These cells are capable of dividing as indicated by the single arrowhead in the first still frame (D) and the two arrowheads in the last still frame (E). While one daughter cell stayed near its starting position, the other daughter cell migrated farther away. Immunostaing after imaging (F) indicates that both daughter cells are still within the confines of the hub cluster (blue membrane) but have turned on the CySC marker ZFH1 (white) suggesting they are starting to change cell fate. (G) Scatterplot depicting the distance hub cells travel in control testes and testes that have recovered for 5 days after CySC ablation. Hub cells from control testes consistently travel a total of 27.6μm throughout the course of the movie, while hub cells from ablated and recovered testes travel significantly farther at 37.5μm. However, these cell dynamics are much more variable as indicated by the spread. Error bars indicate mean distance with standard deviation. Unpaired t test with Welch's correction, *$p<0.05$. Scale bars represent 15μm for A-C, and10μm for D-F.

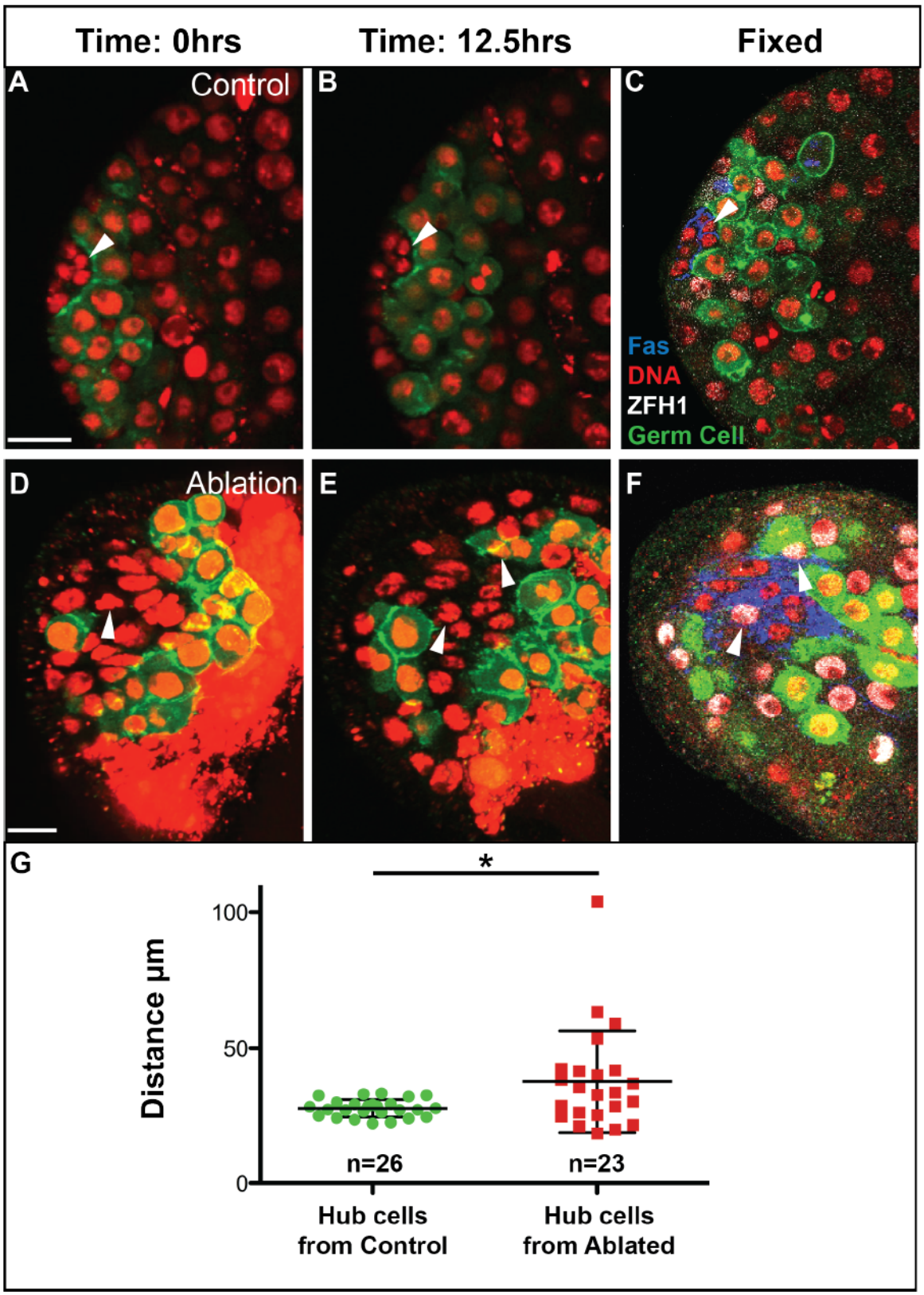
Time: 0hrs
Time: 12.5hrs
Fixed
A
Control
B
C
Fas
DNA
ZFH1
Germ Cell
D
Ablation
E
F
G
*
Distance µm
100
50
0
n=26
n=23
Hub cells from Control
Hub cells from Ablated

APPENDIX – II

Key Resource Table

REAGENT or RESOURCE	SOURCE	IDENTIFIER
Antibodies		
Mouse monoclonal anti–Fasciclin III (*Drosophila*)	DSHB	Cat#: 7G10; RRID: AB_528238
Mouse monoclonal anti-phospho-Histone H3 (Ser10) (6G3)	Cell Signaling Technology	Cat#: 9706S; RRID: AB_331748
Guinea Pig polyclonal anti-Traffic Jam	Laboratory of D. Godt (Li et al., 2003)	N/A
Rabbit polyclonal anti-Vasa (d-260)	Santa Cruz Biotechnology	Cat#: SC-30210; RRID: AB_793874
Mouse monoclonal anti-Rbf	Laboratory of N. Dyson (Frolov et al., 2003)	N/A
Chick polyclonal anti-GFP	Abcam	Cat#: ab13970; RRID: AB_300798
Rabbit polyclonal anti-DsRed	Clontech	Cat#: 632496; RRID: AB_10013483
Goat polyclonal anti-DsRed (C-20)	Santa Cruz Biotechnology	Cat#: SC-33354; RRID: AB_639922
Mouse monoclonal anti-Discs large (*Drosophila*)	DSHB	Cat#: 4F3; RRID: AB_528203
Mouse monoclonal anti-Eyes Absent	DSHB	Cat#: eya10H6; RRID: AB_528232
Mouse monoclonal anti-Armadillo	DSHB	Cat#: N27A1; RRID: AB_528089
Guinea Pig polyclonal anti-Zfh1	Laboratory of E. Matunis	N/A
Rabbit polyclonal anti-cleaved *Drosophila* Dcp1 (Asp216)	Cell Signaling Technology	Cat#: 9578; RRID: AB_2721060
Mouse monoclonal anti-hu-li tai shao	DSHB	Cat#: 1B1; RRID: AB_528070
Mouse monoclonal anti-β-Galactosidase	Promega	Cat#: Z378A; RRID: AB_2313752
Rabbit polyclonal anti-Stat92E	Laboratory of Erika Bach (Flaherty et al., 2010)	N/A
Rat monoclonal anti-DE-cadherin	DSHB	Cat#:DCAD2; RRID: AB_528120
Rabbit polyclonal anti-Castor	Laboratory of Denise Montell	N/A
Mouse monoclonal anti-Cut	DSHB	Cat#: 2B10; RRID: AB_528186
Rabbit polyclonal anti-dpErk	Cell Signaling Technology	Cat#: 4370; RRID: AB_2315112
Goat anti-chicken IgY (H+L) secondary antibody, Alexa Fluor 488 conjugate	ThermoFisher Scientific	Cat#: A11039; RRID: AB_2534096
Donkey anti-chicken IgY (H+L), highly cross absorbed, CF 488A	Millipore/Sigma (formerly Sigma-Aldrich)	Cat#: SAB4600031; RRID: AB_2721061
Goat anti-Mouse IgG (H+L) secondary antibody, Alexa Fluor 405 conjugate	ThermoFisher Scientific	Cat#: A31553; RRID: AB_221604

Goat anti-Mouse IgG (H+L) secondary antibody, Alexa Fluor 488 conjugate	ThermoFisher Scientific	Cat#: A11029; RRID: AB_2534088
Goat anti-Mouse IgG (H+L) secondary antibody, Alexa Fluor 568 conjugate	ThermoFisher Scientific	Cat#: A11004; RRID: AB_2534072
Goat anti-Mouse IgG (H+L) secondary antibody, Alexa Fluor 633 conjugate	ThermoFisher Scientific	Cat#: A21050; RRID: AB_2535718
Goat anti-Guinea Pig IgG (H+L) secondary antibody, Alexa Fluor 488 conjugate	ThermoFisher Scientific	Cat#: A11073; RRID: AB_2534117
Goat anti-Guinea Pig IgG (H+L) secondary antibody, Alexa Fluor 568 conjugate	ThermoFisher Scientific	Cat#: A11075; RRID: AB_2534119
Goat anti-Guinea Pig IgG (H+L) secondary antibody, Alexa Fluor 633 conjugate	ThermoFisher Scientific	Cat#: A21105; RRID: AB_2535757
Goat anti-Rabbit IgG (H+L) secondary antibody, Alexa Fluor 568 conjugate	ThermoFisher Scientific	Cat#: A11011; RRID: AB_143157
Donkey anti-Rabbit IgG Antibody Cy5 CON	Millipore/Sigma (formerly Sigma-Aldrich)	Cat#: AP182SA6; RRID: AB_2721062
Donkey anti-Goat IgG (H+L) secondary antibody, Alexa Fluor 568 conjugate	ThermoFisher Scientific	Cat#: A11057; RRID: AB_2534104
Chemicals, Peptides, and Recombinant Proteins		
4,6-diamidino-2-phenylindole (DAPI)	Millapore/Sigma (formerly Sigma-Aldrich)	Cat#: 10236276001; CAS: 28718-90-3
MIFEPRISTONE-11beta-(4-Dimethy amino) phenyl-17beta-hydroxy-17-(1-propynyl) estra-4,9-dien-3-one; RU-38486; RU-486	Millapore/Sigma (formerly Sigma-Aldrich)	Cat#: M8046; CAS: 84371-65-3
Insulin from Bovine Pancreas powder	Millapore/Sigma (formerly Sigma-Aldrich)	Cat#: I6634; CAS: 11070-73-8
Fetal Bovine Serum heat inactivated US-FBS	Millapore/Sigma (formerly Sigma-Aldrich)	Cat#: F4135
Penicillin-Streptomycin (10,000 U/mL)	ThermoFisher Scientific	Cat#: 15140122; CAS: 69-57-8 (Penicillin) and 3810-74-0 (Sreptomycin)
16% Paraformaldehyde (formaldehyde) aqueous solution	Electron Microscopy Sciences	Cat#: 15710; CAS: 50-00-0
Goat Serum	Millapore/Sigma (formerly Sigma-Aldrich)	Cat#: G9023
Donkey Serum	Millapore/Sigma (formerly Sigma-Aldrich)	Cat#: D9663;
Green food color	McCormick	N/A
Schneider's *Drosophila* Medium	ThermoFisher Scientific	Cat#: 21720024
Shields and Sang M3 Insect Medium	Millapore/Sigma (formerly Sigma-Aldrich)	Cat#: S3652
Vectashield antifade mounting medium	Vector Laboratories	Cat#: H-1000

Poly-L-lysine Hydrobromide Mol Wt 30000 - 70000	Millapore/Sigma (formerly Sigma-Aldrich)	Cat#: P2636; CAS: 25988-63-0
Phosphatase Inhibitor Cocktail 2	Millapore/Sigma (formerly Sigma-Aldrich)	Cat#: P5726
DMSO (Dimethyl Sulfoxide), Sterile	Cell Signaling Technology	Cat#: 12611P
Erlotinib	Cell Signaling Technology	Cat#: 5083S
Gefitinib >=98% (HPLC)	Millapore/Sigma	Cat#: SML1657
Critical Commercial Assays		
Click-iT EdU Alexa Fluor 555 Imaging Kit	ThermoFisher Scientific	Cat#: C10338
Experimental Models: Organisms/Strains		
D. melanogaster: P{w[+mW.hs]=GawB}E132, w[*] (also called upd-Gal4)	Bloomington *Drosophila* Stock Center	BDSC: 26796; FlyBase: FBti0002638
D. melanogaster: w[*]; P{w[+mW.hs]=Switch2}GSG2295	Laboratory of H. Keshishian (Nicholson et al., 2008)	BDSC: 40266 Flybase: FBti0115018
D. melanogaster: HH-LacZ/TM3,Sb	Laboratory of K. Vani (Mohler et al., 1995)	N/A
D. melanogaster: EyaA3-Gal4	Laboratory of S. DiNardo (Leatherman and DiNardo, 2008)	N/A
D. melanogaster: c587Gal4	Laboratory of A. Spradling (Kai and Spradling, 2003)	N/A
D. melanogaster: w[*]; P{w[+mC]=tubP-GAL80[ts]}2/TM2	Bloomington *Drosophila* Stock Center	BDSC: 7017; FlyBase: FBst0007017
D. melanogaster: w[*]; P{w[+mC]=UAS-FLP.D}JD2	Bloomington *Drosophila* Stock Center	BDSC: 4540; FlyBase: FBst0004540
D. melanogaster: RNAi of GFP: w[1118]; P{w[+mC]=UAS-GFP.dsRNA.R}142	Bloomington *Drosophila* Stock Center	BDSC: 9330; FlyBase: FBst0009330
D. melanogaster: RNAi of Rbf: y[1] sc[*] v[1]; P{y[+t7.7] v[+t1.8]=TRiP.HMS03004}attP2/TM3, Sb[1]	Bloomington *Drosophila* Stock Center	BDSC: 36744; FlyBase: FBst0036744
D. melanogaster: RNAi of Rbf: y[1] sc[*] v[1]; P{y[+t7.7] v[+t1.8]=TRiP.GL01293}attP40/CyO	Bloomington *Drosophila* Stock Center	BDSC: 41863; FlyBase: FBst0041863
D. melanogaster: GTRACE: w[*]; P{w[+mC]=UAS-RedStinger}4, P{w[+mC]=UAS-FLP.D}JD1, P{w[+mC]=Ubi-p63E(FRT.STOP)Stinger}9F6/CyO	Bloomington *Drosophila* Stock Center	BDSC: 28280; FlyBase: FBst0028280

D. melanogaster: RNAi of E2F: y[1] v[1]; P{y[+t7.7] v[+t1.8]=TRiP.JF02718}attP2	Bloomington *Drosophila* Stock Center	BDSC: 27564; FlyBase: FBst0027564
D. melanogaster: y[1] w[*]; PBac{y[+mDint2] w[+mC]=20XUAS-6XGFP}VK00018/CyO, P{Wee-P.ph0}Bacc[Wee-P20]	Bloomington *Drosophila* Stock Center	BDSC: 52261; FlyBase: FBst0052261
D. melanogaster: ywhsFlp; UAS-esg/CyO; UAS-LacZ/TM2	Laboratory of A. Tomlinson (Kumar et al., 2015)	N/A
D. melanogaster: hs-FLP; tub>CD2>Gal4, UAS-GFP/CyO	Laboratory of B. Ohlstein	N/A
D. melanogaster: E132Gal4;;TubGal80^{ts}	Laboratory of E. Matunis	N/A
D. melanogaster: EyaA3Gal4;TubGal80^{ts}	Laboratory of E. Matunis	N/A
D. melanogaster: c587Gal4;;TubGal80^{ts}	Laboratory of E. Matunis	N/A
D. melanogaster: UAS-GTRACE/SM6B; UAS-Rbf RNAi/TM6B: P{w[+mC]=UAS-RedStinger}4, P{w[+mC]=UAS-FLP.D}JD1, P{w[+mC]=Ubi-p63E(FRT.STOP)Stinger}9F6/SM6B; P{y[+t7.7] v[+t1.8]=TRiP.HMS03004}attP2/TM6B	This Paper	N/A
D. melanogaster: GS2295-Gal4/Sm6B; UAS-Rbf RNAi/TM6B: w[*]; P{w[+mW.hs]=Switch2}GSG2295/SM6B; P{y[+t7.7] v[+t1.8]=TRiP.HMS03004}attP2/TM6B	This Paper	N/A
D. melanogaster: tub>CD2>Gal4, UAS-GFP/SM6B; UAS-Flp/TM6B: tub>CD2>Gal4, UAS-GFP/SM6B; P{w[+mC]=UAS-FLP.D}JD2/TM6B	This Paper	N/A
D. melanogaster: UAS-Rbf RNAi/SM6B; UAS-E2F RNAi/TM6B: P{y[+t7.7] v[+t1.8]=TRiP.GL01293}attP40/SM6B; P{y[+t7.7] v[+t1.8]=TRiP.JF02718}attP2/TM6B	This Paper	N/A
D. melanogaster: UAS-Esg/SM6B; UAS-Rbf RNAi/TM6B: UAS-Esg/SM6B;]; P{y[+t7.7] v[+t1.8]=TRiP.HMS03004}attP2/TM6B	This Paper	N/A
D. melanogaster: UAS-GFP RNAi/SM6B; UAS-Rbf RNAi/TM6B: P{w[+mC]=UAS-GFP.dsRNA.R}142/SM6B; P{y[+t7.7] v[+t1.8]=TRiP.HMS03004}attP2/TM6B	This Paper	N/A
D. melanogaster: UAS-Rbf RNAi/SM6B; HH-LacZ/TM6B: P{y[+t7.7] v[+t1.8]=TRiP.GL01293}attP40/SM6B; HH-LacZ/TM6B	This Paper	N/A

D. melanogaster: 20XUAS-6XGFP/SM6B; UAS-Rbf RNAi/TM6B: PBac{y[+mDint2] w[+mC]=20XUAS-6XGFP}VK00018/CyO, P{Wee-P.ph0}Bacc[Wee-P20]/SM6B; P{y[+t7.7] v[+t1.8]=TRiP.HMS03004}attP2/TM6B	This Paper	N/A
D. melanogaster: w; Frt40A; UAS-Shg	Laboratory of J.P. Vincent (Sanson et al., 1996)	N/A
D. melanogaster: UAS-Rbf RNAi/SM6B; UAS-Shg/TM6B: P{y[+t7.7] v[+t1.8]=TRiP.GL01293}attP40/SM6B; UAS-Shg/TM6B	This Paper	N/A
D. melanogaster: w[1118]; P{w[+mC] pnt[P1.UAS]=UAS-pnt.P1}3	Bloomington *Drosophila* Stock Center	BDSC: 869; FlyBase: FBti0002115
D. melanogaster: w[1118]; P{w[+mC] pnt[P2.UAS]=UAS-pnt.P2}2/TM3, Sb[1]	Bloomington *Drosophila* Stock Center	BDSC: 399; FlyBase: FBti0002117
D. melanogaster: w[1118]; P{w[+mC]=UAS-Ras85D.V12}TL1	Bloomington *Drosophila* Stock Center	BDSC: 4847; FlyBase: FBti0012505
D. melanogaster: y[1] w[*]; P{w[+mC]=UAS-rl[Sem].S}2	Bloomington *Drosophila* Stock Center	BDSC: 59006; FlyBase: FBti0164913
D. melanogaster: w[*]; P{w[+mC]=Egfr.1.A887T.UAS}12-4/CyO, P{ry[+t7.2]=sevRas1.V12}FK1	Bloomington *Drosophila* Stock Center	BDSC: 9534; FlyBase: FBti0074608
D. melanogaster: w[*]; P{w[+mC]=Egfr.2.A887T.UAS}8-2	Bloomington *Drosophila* Stock Center	BDSC: 9533; FlyBase: FBti0074611
D. melanogaster: w[*]; P{w[+mC]=UAS-Egfr.lambdatop}3/TM6C, Sb[1]	Bloomington *Drosophila* Stock Center	BDSC: 59843; FlyBase: FBti0166942
D. melanogaster: w[1118]; P{w[+mC]=UAS-Pvr.lambda}mP10	Bloomington *Drosophila* Stock Center	BDSC: 58496; FlyBase: FBti0164798
D. melanogaster: w[1118]; P{w[+mC]=UAS-Pvr.lambda}mP1	Bloomington *Drosophila* Stock Center	BDSC: 58428; FlyBase: FBti0164797
D. melanogaster: y[1] w[1118]; P{w[+mC]=UAS-InR.R418P}2	Bloomington *Drosophila* Stock Center	BDSC: 8250; FlyBase: FBti0040685
D. melanogaster: y[1] w[1118]; P{w[+mC]=UAS-InR.A1325D}2	Bloomington *Drosophila* Stock Center	BDSC: 8263; FlyBase: FBti0040693
D. melanogaster: w[*]; P{w[+mC]=UAS-htl.lambda\cI.M}40-22-2	Bloomington *Drosophila* Stock Center	BDSC: 5367; FlyBase: FBti0013301
D. melanogaster: w[*]; P{w[+mC]=UAS-btl.lambda}2	Bloomington *Drosophila* Stock Center	BDSC: 29045; FlyBase: FBti0127909

D. melanogaster: RNAi of Sprouty: y[1] sc[*] v[1]; P{y[+t7.7] v[+t1.8]=TRiP.HMS01599}attP2	Bloomington *Drosophila* Stock Center	BDSC: 36709; FlyBase: FBti0146721
D. melanogaster: RNAi of PTEN: y[1] v[1]; P{y[+t7.7] v[+t1.8]=TRiP.HMS00044}attP2	Bloomington *Drosophila* Stock Center	BDSC: 33643; FlyBase: FBti0140116
D. melanogaster: RNAi of Argos: y[1] v[1]; P{y[+t7.7] v[+t1.8]=TRiP.JF03020}attP2	Bloomington *Drosophila* Stock Center	BDSC: 28383; FlyBase: FBti0127158
D. melanogaster: cn[1]; P{ry[+t7.2]=PZ}vn[10567] ry[506]/TM3, ry[RK] Sb[1] Ser[1]	Bloomington *Drosophila* Stock Center	BDSC: 11749; FlyBase: FBti0005605
D. melanogaster: w[1118]; P{w[+mC]=lacW}spi[s3547]/CyO	Bloomington *Drosophila* Stock Center	BDSC: 10462; FlyBase: FBti0005380
D. melanogaster: w; UAS-Grim	Laboratory of J. Nambu (Wing et al., 1998)	N/A
D. melanogaster: E132Gal4; UAS-GTRACE/SM6B: P{w[+mW.hs]=GawB}E132, w[*];P{w[+mC]=UAS-RedStinger}4, P{w[+mC]=UAS-FLP.D}JD1, P{w[+mC]=Ubi-p63E(FRT.STOP)Stinger}9F6/SM6B	This Paper	N/A
D. melanogaster: Egfr[f24]/T(2;3)TSTL, CyO: TM6B, Tb[1]	Bloomington *Drosophila* Stock Center	BDSC: 6500; FlyBase: FBal0003552
D. melanogaster: c587Gal4; Egfr[f24]/SM6B:	This Paper	N/A
D. melanogaster: UAS-Grim/SM6B;TubGal80^{ts}/TM6B	This Paper	N/A
Software and Algorithms		
Fiji	(Schindelin et al., 2012)	https://www.fiji.sc/
Zeiss LSM	Carl Zeiss Microscopy	https://www.zeiss.com/microscopy/us/downloads/lsm-5-series.html
Zen	Carl Zeiss Microscopy	https://www.zeiss.com/microscopy/int/products/microscope-software/zen.html
Imaris version 7.6.5	Bitplane	http://www.bitplane.com/imaris/imaris
Prism 6	GraphPad	http://www.graphpad.com/scientific-software/prism/
Other		
35mm glass-bottom petri dish with 10mm microwell	MatTek Corporation	Cat#: P35G-1.5-10-C
25 mm Diameter Syringe Filters, 0.2 µm Pore NY Membrane, Sterile	Corning®	Cat#: 431224
10mL Syringe Luer-Lok Tip with BD PrecisionGlide Needle (20 G x 1in)	BD	Cat#: 309644

APPENDIX – III

Protocols

dpErk staining protocol for the *Drosophila* testis

This protocol is adapted from Fairchild et al., 2016 and can be used for immunostaining whole testes with any phospho-specific antisera.

1. Make 1X Testis Buffer with 0.2% Bovine Serum Albumin (BSA), and 0.3% Triton X called TB Buffer. To make 150mL of TB buffer add 15mL of 10X Testis buffer (47 mM NaCl, 183 mM KCl, 10 mM Tris-HCL (pH 6.8) in ultrapure water) (Ashburner, 1989), 0.3g BSA, and 450µL of Triton-X. Add ultrapure water up to 150mL.
2. Dissect flies in Shields and Sang M3 media (Sigma S3652) with phosphatase inhibitor (Sigma P5726) at a 1:100 dilution. Keep testes in cuticle. To make media add 30µL of phosphatase inhibitor to 3mL of Shields and Sang M3 media. Once dissected, make sure testes remain on ice until fixed.
3. Fix testes in 3.7% paraformaldehyde diluted in TB buffer with phosphatase inhibitor. To make enough fixative for 3 tubes add 450µL of 16% paraformaldehyde and 18µL of phosphatase inhibitor to 1332µL of TB buffer. Fix testes for 15-22min on a nutator.
4. For rinses and washes use TB buffer with phosphatase inhibitor (add 140µL of phosphatase inhibitor to 14mL of TB buffer). After fixing, rinse testes quickly 3X then wash 1X for 15min on nutator. Rinse testes again 1X then wash 3X for 15min on nutator. Wash for a minimum of 1 hour.

5. Add primary antibody to TB buffer with phosphatase inhibitor. Use the rabbit anti – dpErk antibody (Cell Signaling Technology 4370) at a final concentration of 1:100. Stain overnight on a nutator at 4°C.
6. For rinses and washes use TB buffer without phosphastase inhibitor. Remove primary antibody then rinse testes quickly 3X then wash 1X for 15min on nutator. Rinse testes again 1X then wash 3X for 15min on nutator. Wash for a minimum of 1 hour.
7. Add secondary antibody and DAPI to TB buffer. Stain overnight on a nutator at 4°C.
8. For rinses and washes use TB buffer without phosphastase inhibitor. Remove secondary antibody then rinse testes quickly 3X then wash 1X for 15min on nutator. Rinse testes again 1X then wash 3X for 15min on nutator. Wash for a minimum of 1 hour.
9. Mount testes in Vectashield.

EGF Inhibitor Feeding Protocol

This protocol is used to administer EGF inhibitors to adult flies via feeding over longer periods of time (7-8 days).

1. Create a 10mg/mL stock solution of each EGF inhibitor by adding 1mL of DMSO (Cell Signaling Technology 12611P) to 10mg of inhibitor. Aliquot the solution into 50µL tubes and store at -20°C. Note: the EGF inhibitors Erlotinib (Cell Signaling Technology 5083S) and Gefitinib (Sigma SML1657) can be purchased in the core store. These drugs start to lose potency after 3 months in solution. For more product details see the key resource table.
2. To create a 0.1mg/mL working solution of each inhibitor combine 5µL of the 10mg/mL stock solution for the desired inhibitor with 10µL of green food dye (McCormick) and 485µL of dH_20. The food dye helps to identify flies that have eaten the inhibitor.
3. Add 500µL of drug inhibitor working solution to one well of a glass multi-well dish. Add dry yeast and continually mix until yeast is dissolved. Add enough yeast to create a smooth peanut butter consistency. This should create enough yeast for about 2-3 vials.
4. Add yeast/inhibitor mixture to empty vials that have no additional food.
5. Add about 15-20 flies to each vial. Make sure to not overcrowd.
6. Change vial with yeast inhibitor mixture daily to ensure yeast does not dry out.

7. After flies have been fed yeast/inhibitor mixture for the desired length of time, select flies with green guts for dissection. This ensures you are only selecting those flies that you know have eaten the drug.
8. Dissect, fix, and immunostain testes according to normal protocol.

Live Imaging Protocol for the *Drosophila* Testis

This protocol is adapted from Sheng and Matunis, 2011, Lenhart and DiNardo, 2015, and Greenspan and Matunis, 2017. See key resource table for details on reagents used.

Lysine Coated Coverslip

1. Weigh out 10mg of Poly-L-Lysine (Sigma P2636) powder into a 50mL conical tube.
2. Dissolve in 0.1M filter-sterilized Trizma buffer pH8.5 (Sigma T1194) to a concentration of 1mg/mL.
3. Aliquot into 1mL eppendorfs and store at -20 degrees.
4. Thaw one tube of lysine at a time and pipette onto coverslip portion of imaging dish (200uL). Use a 35mm glass bottom dish with a 10mm microwell (MatTek Corporation).
5. Let sit at room temp with cover on for at least 1hr.
6. Remove lysine, return to original tube and store at 4 degrees. Can re-use 1-2 weeks.
7. Pipette 200µL water over coverslip vigorously 3 times to rinse.
8. Pipette 200µL water onto coverslip and let sit until ready to mount samples.

Insulin stock solution

1. Dissolve powdered bovine pancreas insulin (Sigma I6634) in acidified water (1µL concentrated HCl + 1mL ultrapure water) at a final concentration of 10 mg/mL. Store 50µL aliquots in 1.5mL microcentrifuge tubes at -20°C.

Imaging Solution

1. Make imaging media in a tissue culture hood to ensure sterility.
2. In a 50mL conical tube, add 750µL FBS (Sigma F4135), 25µL Pen/Strep (0.5X final) (Fisher 15140122), and 100µL of 10mg/mL insulin solution (~0.2mg/mL final).
3. Bring up to 5mL with Schneider's Media (Fisher 21720024) or Shield and Sang's M3 media (Sigma S3652).
4. Filter sterilize the solution using a 10mL syringe (BD 309644) and a 0.2µm filter (Corning 431224) into a 15mL conical tube.
5. Store at 4°C and make fresh every week.

Preparing and Mounting Testes

1. Dissect testes in Ringers solution.
2. Remove testes from all other tissue and separate pairs from each other.
3. I usually dissect between 20-50 males for each imaging, if possible.
4. Pipette testes in Ringers onto coverslip portion of imaging dish (after having removed remaining water from final wash). If there is excess debris in the media following dissection, testes can be gently transferred to a separate dissecting dish containing fresh Ringers solution, rinsed a few times with fresh Ringers solution, and then transferred to the imaging dish. Try to minimize handling of testes and number of transfers as this could damage the tissue.
5. If necessary, carefully move testes around dish to ensure as little overlap as possible between samples. You might also need to push down on testes gently to ensure the apex is flush with the coverslip.

6. Remove all Ringers to cause testes to fully adhere to coverslip. As quickly as possible, add back solution to testes to prevent drying out (add either Ringers or imaging media; the testes will be very adherent at this point and will remain attached to coverslip even after multiple solution changes).
7. Use 1000uL of imaging media to cover the base of dish to ensure testes do not dry out overnight. Make sure to cover the dish with a lid before imaging.
8. After imaging, media can be removed and testes fixed and immunostained directly in the dish using standard protocols.

BIBLIOGRAPHY

Ahmed-de-Prado, S. and Baonza, A. (2018). Drosophila as a Model System to Study Cell Signaling in Organ Regeneration. *Biomed Res. Int.* **2018**, 7359267.

Aloisio, G. M., Nakada, Y., Saatcioglu, H. D., Peña, C. G., Baker, M. D., Tarnawa, E. D., Mukherjee, J., Manjunath, H., Bugde, A., Sengupta, A. L., et al. (2014). PAX7 expression defines germline stem cells in the adult testis. *J. Clin. Invest.* **124**, 3929–3944.

Amoyel, M., Sanny, J., Burel, M. and Bach, E. A. (2013). Hedgehog is required for CySC self-renewal but does not contribute to the GSC niche in the Drosophila testis. *Development* **140**, 56–65.

Amoyel, M., Simons, B. D. and Bach, E. A. (2014). Neutral competition of stem cells is skewed by proliferative changes downstream of Hh and Hpo. *EMBO J.* **33**, 2295 LP-2313.

Ashburner M. (1989) *Drosophila*: A laboratory manual. Cold Spring Harbor Laboratory Press, New York, p. 376 and 381.

Baker, A. M., Cereser, B., Melton, S., Fletcher, A. G., Rodriguez-Justo, M., Tadrous, P. J., Humphries, A., Elia, G., McDonald, S. A. C., Wright, N. A., et al. (2014). Quantification of crypt and stem cell evolution in the normal and neoplastic human colon. *Cell Rep.* **8**, 940–947.

Barroca, V., Lassalle, B., Coureuil, M., Louis, J. P., Le Page, F., Testart, J., Allemand, I., Riou, L. and Fouchet, P. (2009). Mouse differentiating spermatogonia can generate germinal stem cells in vivo. *Nat. Cell Biol.* **11**, 190–196.

Beumer, J. and Clevers, H. (2016). Regulation and plasticity of intestinal stem cells during homeostasis and regeneration. *Development* **143**, 3639–3649.

Bondar, T. and Medzhitov, R. (2010). p53-Mediated Hematopoietic Stem and Progenitor Cell Competition. *Cell Stem Cell* **6**, 309–322.

Brawley, C. and Matunis, E. (2004). Regeneration of male germline stem cells by spermatogonial dedifferentiation in vivo. *Science (80-.).* **304**, 1331–1334.

Buaas, F. W., Kirsh, A. L., Sharma, M., McLean, D. J., Morris, J. L., Griswold, M. D., De Rooij, D. G. and Braun, R. E. (2004). Plzf is required in adult male germ cells for stem cell self-renewal. *Nat. Genet.* **36**, 647–652.

Burkhart, D. L. and Sage, J. (2008). Cellular mechanisms of tumour suppression by the retinoblastoma gene. *Nat. Rev. Cancer* **8**, 671–682.

Cairnie, A. B. and Millen, B. H. (1975). FISSION OF CRYPTS IN THE SMALL INTESTINE OF THE IRRADIATED MOUSE. *Cell Prolif.* **8**, 189–196.

Calo, E., Quintero-Estades, J. A., Danielian, P. S., Nedelcu, S., Berman, S. D. and Lees, J. A. (2010). Rb regulates fate choice and lineage commitment in vivo. *Nature* **466**, 1110–1114.

Carlson, B. M. (2005). Some principles of regeneration in mammalian systems. *Anat. Rec. - Part B New Anat.* **287**, 4–13.

Carter, S. L., Eklund, A. C., Kohane, I. S., Harris, L. N. and Szallasi, Z. (2006). A signature of chromosomal instability inferred from gene expression profiles predicts clinical outcome in multiple human cancers. *Nat. Genet.* **38**, 1043–1048.

Castanieto, A., Johnston, M. J. and Nystul, T. G. (2014). EGFR signaling promotes self-renewal through the establishment of cell polarity in Drosophila follicle stem

cells. *Elife* **3**,.

Cayirlioglu, P., Ward, W. O., Silver Key, S. C. and Duronio, R. J. (2003). Transcriptional repressor functions of Drosophila E2F1 and E2F2 cooperate to inhibit genomic DNA synthesis in ovarian follicle cells. *Mol. Cell. Biol.* **23**, 2123–2134.

Chan S.T. 1970. Natural sex reversal in vertebrates. *Philosophical transactions of the Royal Society of London. Series B, Biological sciences* 259: 59-71.

Chen, D. and McKearin, D. (2003). Dpp Signaling Silences bam Transcription Directly to Establish Asymmetric Divisions of Germline Stem Cells. *Curr. Biol.* **13**, 1786–1791.

Chen, S., Lewallen, M. and Xie, T. (2013a). Adhesion in the stem cell niche: biological roles and regulation. *Development* **140**, 255–265.

Chen, H., Chen, X. and Zheng, Y. (2013b). The nuclear lamina regulates germline stem cell niche organization via modulation of EGFR signaling. *Cell Stem Cell* **13**, 73–86.

Cheng, J. and Hunt, A. J. (2009). Time-lapse live imaging of stem cells in drosophila testis. *Curr. Protoc. Stem Cell Biol.*

Cheng, J., Türkel, N., Hemati, N., Fuller, M. T., Hunt, A. J. and Yamashita, Y. M. (2008). Centrosome misorientation reduces stem cell division during ageing. *Nature* **456**, 599–604.

Chera, S., Baronnier, D., Ghila, L., Cigliola, V., Jensen, J. N., Gu, G., Furuyama, K., Thorel, F., Gribble, F. M., Reimann, F., et al. (2014). Diabetes recovery by age-dependent conversion of pancreatic δ-cells into insulin producers. *Nature* **514**, 503–507.

Cheung, T. H. and Rando, T. A. (2013). Molecular regulation of stem cell quiescence. *Nat. Rev. Mol. Cell Biol.* **14**, 329–340.

Clayton, E., Doupé, D. P., Klein, A. M., Winton, D. J., Simons, B. D. and Jones, P. H. (2007). A single type of progenitor cell maintains normal epidermis. *Nature* **446**, 185–189.

Coschi, C. H., Ishak, C. A., Gallo, D., Marshall, A., Talluri, S., Wang, J., Cecchini, M. J., Martens, A. L., Percy, V., Welch, I., et al. (2014). Haploinsufficiency of an RB-E2F1-Condensin II Complex Leads to Aberrant Replication and Aneuploidy. *Cancer Discov.* **4**, 840–853.

Costoya, J. A., Hobbs, R. M., Barna, M., Cattoretti, G., Manova, K., Sukhwani, M., Orwig, K. E., Wolgemuth, D. J. and Pandolfi, P. P. (2004). Essential role of Plzf in maintenance of spermatogonial stem cells. *Nat. Genet.* **36**, 653–659.

Dagogo-Jack, I. and Shaw, A. T. (2018). Tumour heterogeneity and resistance to cancer therapies. *Nat. Rev. Clin. Oncol.* **15**, 81–94.

de Cuevas, M. and Matunis, E. L. (2011). The stem cell niche: lessons from the Drosophila testis. *Development* **138**, 2861–9.

De La Cova, C., Abril, M., Bellosta, P., Gallant, P. and Johnston, L. A. (2004). Drosophila myc regulates organ size by inducing cell competition. *Cell* **117**, 107–116.

De Navascués, J., Perdigoto, C. N., Bian, Y., Schneider, M. H., Bardin, A. J., Martínez-Arias, A. and Simons, B. D. (2012). Drosophila midgut homeostasis involves neutral competition between symmetrically dividing intestinal stem cells. *EMBO J.* **31**, 2473–2485.

DeGregori, J., Leone, G., Miron, A., Jakoi, L. and Nevins, J. R. (1997). Distinct roles for E2F proteins in cell growth control and apoptosis. *Proc. Natl. Acad. Sci.* **94**, 7245–7250.

DiNardo, S., Okegbe, T., Wingert, L., Freilich, S. and Terry, N. (2011). lines and bowl affect the specification of cyst stem cells and niche cells in the Drosophila testis. *Development* **138**, 1687–1696.

Dominado, N., La Marca, J. E., Siddall, N. A., Heaney, J., Tran, M., Cai, Y., Yu, F., Wang, H., Somers, W. G., Quinn, L. M., et al. (2016). Rbf Regulates Drosophila Spermatogenesis via Control of Somatic Stem and Progenitor Cell Fate in the Larval Testis. *Stem Cell Reports* **7**, 1152–1163.

Doupé, D. P., Klein, A. M., Simons, B. D. and Jones, P. H. (2010). The Ordered Architecture of Murine Ear Epidermis Is Maintained by Progenitor Cells with Random Fate. *Dev. Cell* **18**, 317–323.

Doupé, D. P., Alcolea, M. P., Roshan, A., Zhang, G., Klein, A. M., Simons, B. D. and Jones, P. H. (2012). A single progenitor population switches behavior to maintain and repair esophageal epithelium. *Science (80-.).* **337**, 1091–1093.

Dyson, N. J. (2016). RB1: A prototype tumor suppressor and an enigma. *Genes Dev.* **30**, 1492–1502.

Eliazer, S. and Buszczak, M. (2011). Finding a niche: Studies from the Drosophila ovary. *Stem Cell Res. Ther.* **2**, 45.

Eun, S. H., Shi, Z., Cui, K., Zhao, K. and Chen, X. (2014). A non-cell autonomous role of E(z) to prevent germ cells from turning on a somatic cell marker. *Science (80-.).* **343**, 1513–1516.

Evans, C. J., Olson, J. M., Ngo, K. T., Kim, E., Lee, N. E., Kuoy, E., Patananan, A. N., Sitz, D., Tran, P. T., Do, M. T., et al. (2009). G-TRACE: Rapid Gal4-based cell lineage analysis in Drosophila. *Nat. Methods* **6**, 603–605.

Fairchild, M. J., Yang, L., Goodwin, K. and Tanentzapf, G. (2016). Occluding Junctions Maintain Stem Cell Niche Homeostasis in the Fly Testes. *Curr. Biol.* **26**, 2492–2499.

Fichelson, P., Moch, C., Ivanovitch, K., Martin, C., Sidor, C. M., Lepesant, J. A., Bellaiche, Y. and Huynh, J. R. (2009). Live-imaging of single stem cells within their niche reveals that a U3snoRNP component segregates asymmetrically and is required for self-renewal in Drosophila. *Nat. Cell Biol.* **11**, 685–693.

Flaherty, M. S., Salis, P., Evans, C. J., Ekas, L. A., Marouf, A., Zavadil, J., Banerjee, U. and Bach, E. A. (2010). Chinmo Is a Functional Effector of the JAK/STAT Pathway that Regulates Eye Development, Tumor Formation, and Stem Cell Self-Renewal in Drosophila. *Dev. Cell* **18**, 556–568.

Foley, K. and Cooley, L. (1998). Apoptosis in late stage Drosophila nurse cells does not require genes within the H99 deficiency. *Development* **125**, 1075–1082.

Forbes, a J., Lin, H., Ingham, P. W. and Spradling, a C. (1996). hedgehog is required for the proliferation and specification of ovarian somatic cells prior to egg chamber formation in Drosophila. *Development* **122**, 1125–1135.

Fox, D. T., Morris, L. X., Nystul, T. and Spradling, A. C. (2008). Lineage analysis of stem cells. In *StemBook*, .

Frolov, M. V., Stevaux, O., Moon, N. S., Dimova, D., Kwon, E. J., Morris, E. J. and Dyson, N. J. (2003). G1 cyclin-dependent kinases are insufficient to reverse dE2F2-

mediated repression. *Genes Dev.* **17**, 723–728.

Fuller, M. (1993) Spermatogenesis. In: The Development of Drosophila Melanogaster Volume I. Cold Spring Harbor Laboratory Press, U.S.A, p.71-147.

Gemberling, M., Bailey, T. J., Hyde, D. R. and Poss, K. D. (2013). The zebrafish as a model for complex tissue regeneration. *Trends Genet.* **29**, 611–620.

Gönczy, P. and DiNardo, S. (1996). The germ line regulates somatic cyst cell proliferation and fate during Drosophila spermatogenesis. *Development* **122**, 2437–2447.

Goriely, A. and Wilkie, A. O. M. (2012). Paternal age effect mutations and selfish spermatogonial selection: Causes and consequences for human disease. *Am. J. Hum. Genet.* **90**, 175–200.

Greaves, L. C., Preston, S. L., Tadrous, P. J., Taylor, R. W., Barron, M. J., Oukrif, D., Leedham, S. J., Deheragoda, M., Sasieni, P., Novelli, M. R., et al. (2006). Mitochondrial DNA mutations are established in human colonic stem cells, and mutated clones expand by crypt fission. *Proc. Natl. Acad. Sci.* **103**, 714–719.

Greenspan, L. J. and Matunis, E. L. (2017). Live imaging of the drosophila testis stem cell niche. In *Methods in Molecular Biology*, pp. 63–74.

Greenspan, L. J., de Cuevas, M. and Matunis, E. (2015). Genetics of Gonadal Stem Cell Renewal. *Annu. Rev. Cell Dev. Biol.* **31**, 291–315.

Grisanti, L., Falciatori, I., Grasso, M., Dovere, L., Fera, S., Muciaccia, B., Fuso, A., Berno, V., Boitani, C., Stefanini, M., et al. (2009). Identification of spermatogonial stem cell subsets by morphological analysis and prospective isolation. *Stem Cells* **27**, 3043–3052.

Hanna, C. B. and Hennebold, J. D. (2014). Ovarian germline stem cells: An unlimited source of oocytes? *Fertil. Steril.* **101**, 20–30.

Hara, K., Nakagawa, T., Enomoto, H., Suzuki, M., Yamamoto, M., Simons, B. D. and Yoshida, S. (2014). Mouse spermatogenic stem cells continually interconvert between equipotent singly isolated and syncytial states. *Cell Stem Cell* **14**, 658–672.

Hardy, R. W., Tokuyasu, K. T., Lindsley, D. L. and Garavito, M. (1979). The germinal proliferation center in the testis of Drosophila melanogaster. *J. Ultrasructure Res.* **69**, 180–190.

Hariharan, I. K. and Serras, F. (2017). Imaginal disc regeneration takes flight. *Curr. Opin. Cell Biol.* **48**, 10–16.

Hartman, T. R., Zinshteyn, D., Schofield, H. K., Nicolas, E., Okada, A. and O'Reilly, A. M. (2010). Drosophila Boi limits hedgehog levels to suppress follicle stem cell proliferation. *J. Cell Biol.* **191**, 943–952.

Hasan, S., Hétié, P. and Matunis, E. L. (2015). Niche signaling promotes stem cell survival in the Drosophila testis via the JAK-STAT target DIAP1. *Dev. Biol.* **404**, 27–39.

Hasegawa, K. and Saga, Y. (2012). Retinoic acid signaling in Sertoli cells regulates organization of the blood-testis barrier through cyclical changes in gene expression. *Development* **139**, 4347–4355.

Hasegawa, K., Namekawa, S. H. and Saga, Y. (2013). MEK/ERK signaling directly and indirectly contributes to the cyclical self-renewal of spermatogonial stem cells. *Stem Cells* **31**, 2517–2527.

Hermann, B. P., Sukhwani, M., Hansel, M. C. and Orwig, K. E. (2010).

Spermatogonial stem cells in higher primates: Are there differences from those in rodents? *Reproduction* **139**, 479–493.

Hétié, P., de Cuevas, M. and Matunis, E. (2014). Conversion of Quiescent Niche Cells to Somatic Stem Cells Causes Ectopic Niche Formation in the Drosophila Testis. *Cell Rep.* **7**, 715–721.

Hu, Y.-C., de Rooij, D. G. and Page, D. C. (2013). Tumor suppressor gene Rb is required for self-renewal of spermatogonial stem cells in mice. *Proc. Natl. Acad. Sci.* **110**, 12685–12690.

Hudson, A. G., Parrott, B. B., Qian, Y. and Schulz, C. (2013). A Temporal Signature of Epidermal Growth Factor Signaling Regulates the Differentiation of Germline Cells in Testes of Drosophila melanogaster. *PLoS One* **8**, e70678.

Huynh, J. and St Johnston, D. (2000). The role of BicD, Egl, Orb and the microtubules in the restriction of meiosis to the Drosophila oocyte. *Development* 2785–2794.

Inaba, M., Yuan, H. and Yamashita, Y. M. (2011). String (Cdc25) regulates stem cell maintenance, proliferation and aging in Drosophila testis. *Development* **138**, 5079–5086.

Ishii, K., Kanatsu-Shinohara, M., Toyokuni, S. and Shinohara, T. (2012). FGF2 mediates mouse spermatogonial stem cell self-renewal via upregulation of Etv5 and Bcl6b through MAP2K1 activation. *Development* **139**, 1734–1743.

Issigonis, M., Tulina, N., De Cuevas, M., Brawley, C., Sandler, L. and Matunist, E. (2009). JAK-STAT signal inhibition regulates competition in the drosophila testis stem cell niche. *Science (80-.).* **326**, 153–156.

Jin, Z., Kirilly, D., Weng, C., Kawase, E., Song, X., Smith, S., Schwartz, J. and Xie,

T. (2008). Differentiation-Defective Stem Cells Outcompete Normal Stem Cells for Niche Occupancy in the Drosophila Ovary. *Cell Stem Cell* **2**, 39–49.

Johnston, L. A. (2009). Competitive Interactions between Cells: Death, Growth, and Geography. *Science (80-.).* **324**, 1679–1682.

Johnston, A. P. W., Yuzwa, S. A., Carr, M. J., Mahmud, N., Storer, M. A., Krause, M. P., Jones, K., Paul, S., Kaplan, D. R. and Miller, F. D. (2016). Dedifferentiated Schwann Cell Precursors Secreting Paracrine Factors Are Required for Regeneration of the Mammalian Digit Tip. *Cell Stem Cell* **19**, 433–448.

Kai, T. and Spradling, A. (2003). An empty Drosophila stem cell niche reactivates the proliferation of ectopic cells. *Proc. Natl. Acad. Sci.* **100**, 4633–4638.

Kai, T. and Spradling, A. (2004). Differentiating germ cells can revert into functional stem cells in Drosophila melanogaster ovaries. *Nature* **428**, 564–569.

Kanatsu-Shinohara, M. and Shinohara, T. (2013). Spermatogonial Stem Cell Self-Renewal and Development. *Annu. Rev. Cell Dev. Biol.* **29**, 163–187.

Kanatsu-Shinohara, M., Takehashi, M., Takashima, S., Lee, J., Morimoto, H., Chuma, S., Raducanu, A., Nakatsuji, N., Fässler, R. and Shinohara, T. (2008). Homing of Mouse Spermatogonial Stem Cells to Germline Niche Depends on β1-Integrin. *Cell Stem Cell* **3**, 533–542.

Kanca, O., Caussinus, E., Denes, A. S., Percival-Smith, A. and Affolter, M. (2014). Raeppli: a whole-tissue labeling tool for live imaging of Drosophila development. *Development* **141**, 725–725.

Kawase, E. (2004). Gbb/Bmp signaling is essential for maintaining germline stem cells and for repressing bam transcription in the Drosophila testis. *Development* **131**,

1365–1375.

Kiger, A. A., White-Cooper, H. and Fuller, M. T. (2000). Somatic support cells restrict germline stem cell self-renewal and promote differentiation. *Nature* **407**, 750–754.

Kiger, A. A., Jones, D. L., Schulz, C., Rogers, M. B. and Fuller, M. T. (2001). Stem cell self-renewal specified by JAK-STAT activation in response to a support cell cue. *Science (80-.).* **294**, 2542–2545.

King, R. S. and Newmark, P. A. (2012). The cell biology of regeneration. *J. Cell Biol.* **196**, 553–562.

Kirilly, D., Spana, E. P., Perrimon, N., Padgett, R. W. and Xie, T. (2005). BMP signaling is required for controlling somatic stem cell self-renewal in the Drosophila ovary. *Dev. Cell* **9**, 651–662.

Kitadate, Y. and Kobayashi, S. (2010). Notch and Egfr signaling act antagonistically to regulate germ-line stem cell niche formation in Drosophila male embryonic gonads. *Proc. Natl. Acad. Sci.* **107**, 14241–14246.

Klein, A. M. and Simons, B. D. (2011). Universal patterns of stem cell fate in cycling adult tissues. *Development* **138**, 3103–3111.

Klein, A. M., Nakagawa, T., Ichikawa, R., Yoshida, S. and Simons, B. D. (2010). Mouse germ line stem cells undergo rapid and stochastic turnover. *Cell Stem Cell* **7**, 214–224.

Korenjak, M., Anderssen, E., Ramaswamy, S., Whetstine, J. R. and Dyson, N. J. (2012). RBF Binding to both Canonical E2F Targets and Noncanonical Targets Depends on Functional dE2F/dDP Complexes. *Mol. Cell. Biol.* **32**, 4375–4387.

Kronen, M. R., Schoenfelder, K. P., Klein, A. M. and Nystul, T. G. (2014).

Basolateral junction proteins regulate competition for the follicle stem cell niche in the drosophila ovary. *PLoS One* **9**,.

Kubota, H., Avarbock, M. R. and Brinster, R. L. (2004). Growth factors essential for self-renewal and expansion of mouse spermatogonial stem cells. *Proc. Natl. Acad. Sci.* **101**, 16489–16494.

Kumar, S. R., Patel, H. and Tomlinson, A. (2015). Wingless mediated apoptosis: How cone cells direct the death of peripheral ommatidia in the developing Drosophila eye. *Dev. Biol.* **407**, 183–194.

Lacerda, S. M. dos S. N., Costa, G. M. J. and de França, L. R. (2014). Biology and identity of fish spermatogonial stem cell. *Gen. Comp. Endocrinol.* **207**, 56–65.

Lai, A. G. and Aboobaker, A. A. (2018). EvoRegen in animals: Time to uncover deep conservation or convergence of adult stem cell evolution and regenerative processes. *Dev. Biol.* **433**, 118–131.

Le Bras, S. and Van Doren, M. (2006). Development of the male germline stem cell niche in Drosophila. *Dev. Biol.* **294**, 92–103.

Leatherman, J. L. and Di Nardo, S. (2008). Zfh-1 controls somatic stem cell self-renewal in the Drosophila testis and nonautonomously influences germline stem cell self-renewal. *Cell Stem Cell* **3**, 44–54.

Leatherman, J. L. and Dinardo, S. (2010). Germline self-renewal requires cyst stem cells and stat regulates niche adhesion in Drosophila testes. *Nat. Cell Biol.* **12**, 806–811.

Lee, S., Zhou, L., Kim, J., Kalbfleisch, S. and Schöck, F. (2008). Lasp anchors the Drosophila male stem cell niche and mediates spermatid individualization. *Mech.*

Dev. **125**, 768–776.

Lei, L. and Spradling, A. C. (2013). Female mice lack adult germ-line stem cells but sustain oogenesis using stable primordial follicles. *Proc. Natl. Acad. Sci.* **110**, 8585–8590.

Lenhart, K. F. and DiNardo, S. (2015). Somatic Cell Encystment Promotes Abscission in Germline Stem Cells following a Regulated Block in Cytokinesis. *Dev. Cell* **34**, 192–205.

Li, M. A., Alls, J. D., Avancini, R. M., Koo, K. and Godt, D. (2003). The large Maf factor traffic jam controls gonad morphogenesis in Drosophila. *Nat. Cell Biol.* **5**, 994–1000.

Li, Y., Minor, N. T., Park, J. K., McKearin, D. M. and Maines, J. Z. (2009). Bam and Bgcn antagonize Nanos-dependent germ-line stem cell maintenance. *Proc. Natl. Acad. Sci. U. S. A.* **106**, 9304–9.

Lim, J. G. Y. and Fuller, M. T. (2012). Somatic cell lineage is required for differentiation and not maintenance of germline stem cells in Drosophila testes. *Proc. Natl. Acad. Sci.* **109**, 18477–18481.

Lopez-Onieva, L., Fernandez-Minan, A. and Gonzalez-Reyes, A. (2008). Jak/Stat signalling in niche support cells regulates dpp transcription to control germline stem cell maintenance in the Drosophila ovary. *Development* **135**, 533–540.

Losick, R. and Desplan, C. (2008). Stochasticity and cell fate. *Science (80-.).* **320**, 65–68.

Lou, J., Megee, S. and Dobrinski, I. (2009). Asymmetric distribution of UCH-L1 in spermatogonia is associated with maintenance and differentiation of spermatogonial

stem cells. *J. Cell. Physiol.* **220**, 460–468.

Ma, Q., Wawersik, M. and Matunis, E. L. (2014). The Jak-STAT target chinmo prevents sex transformation of adult stem cells in the drosophila testis niche. *Dev. Cell* **31**, 474–486.

Martin, L. A., Assif, N., Gilbert, M., Wijewarnasuriya, D. and Seandel, M. (2014). Enhanced fitness of adult spermatogonial stem cells bearing a paternal age-associated FGFR2 mutation. *Stem Cell Reports* **3**, 219–226.

Marusyk, A. and Polyak, K. (2010). Tumor heterogeneity: Causes and consequences. *Biochim. Biophys. Acta - Rev. Cancer* **1805**, 105–117.

Maskens, A. P. and Dujardin-Loits, R. M. (1981). Kinetics of tissue proliferation in colorectal mucosa during post-natal growth. *Cell Prolif.* **14**, 467–477.

Masuyama, H., Yamada, M., Kamei, Y., Fujiwara-Ishikawa, T., Todo, T., Nagahama, Y. and Matsuda, M. (2012). Dmrt1 mutation causes a male-to-female sex reversal after the sex determination by Dmy in the medaka. *Chromosom. Res.* **20**, 163–176.

Matson, C. K., Murphy, M. W., Sarver, A. L., Griswold, M. D., Bardwell, V. J. and Zarkower, D. (2011). DMRT1 prevents female reprogramming in the postnatal mammalian testis. *Nature* **476**, 101–105.

Matunis, E., Tran, J., Gönczy, P., Caldwell, K. and DiNardo, S. (1997). Punt and Schnurri Regulate a Somatically Derived Signal That Restricts Proliferation of Committed Progenitors in the Germline. *Development* **124**, 4383–4391.

Matunis, E. L., Stine, R. R. and de Cuevas, M. (2012). Recent advances in Drosophila male germline stem cell biology. *Spermatogenesis* **2**, 137–144.

McCall, K. and Steller, H. (1998). Requirement for DCP-1 caspase during Drosophila oogenesis. *Science (80-.).* **279**, 230–234.

Meng, X., Lindahl, M., Hyvönen, M. E., Parvinen, M., De Rooij, D. G., Hess, M. W., Raatikainen-Ahokas, A., Sainio, K., Rauvala, H., Lakso, M., et al. (2000). Regulation of cell fate decision of undifferentiated spermatogonia by GDNF. *Science (80-.).* **287**, 1489–1493.

Michel, M., Raabe, I., Kupinski, A. P., Pérez-Palencia, R. and Bökel, C. (2011). Local BMP receptor activation at adherens junctions in the Drosophila germline stem cell niche. *Nat. Commun.* **2**, 415.

Michel, M., Kupinski, A. P., Raabe, I. and Bokel, C. (2012). Hh signalling is essential for somatic stem cell maintenance in the Drosophila testis niche. *Development* **139**, 2663–2669.

Mohler, J., Mahaffey, J. W., Deutsch, E. and Vani, K. (1995). Control of Drosophila head segment identity by the bZIP homeotic gene cnc. *Development* **121**, 237–247.

Morris, L. X. and Spradling, A. C. (2011). Long-term live imaging provides new insight into stem cell regulation and germline-soma coordination in the Drosophila ovary. *Development* **138**, 2207–2215.

Morrissey, E. R. and Vermeulen, L. (2014). Stem cell competition: how speeding mutants beat the rest. *EMBO J.* **33**, 2277 LP-2278.

Mullaney, B. P. and Skinner, M. K. (1992). Basic fibroblast growth factor (bFGF) gene expression and protein production during pubertal development of the seminiferous tubule: Follicle-stimulating hormone-induced sertoli cell bFGF expression. *Endocrinology* **131**, 2928–2934.

Nakagawa, T., Nabeshima, Y. ichi and Yoshida, S. (2007). Functional Identification of the Actual and Potential Stem Cell Compartments in Mouse Spermatogenesis. *Dev. Cell* **12**, 195–206.

Naughton, C. K., Jain, S., Strickland, A. M., Gupta, A. and Milbrandt, J. (2006). Glial Cell-Line Derived Neurotrophic Factor-Mediated RET Signaling Regulates Spermatogonial Stem Cell Fate1. *Biol. Reprod.* **74**, 314–321.

Nicholson, L., Singh, G. K., Osterwalder, T., Roman, G. W., Davis, R. L. and Keshishian, H. (2008). Spatial and temporal control of gene expression in drosophila using the inducible geneSwitch GAL4 system. I. Screen for larval nervous system drivers. *Genetics* **178**, 215–234.

Noll, J. E., Williams, S. A., Purton, L. E. and Zannettino, A. C. W. (2012). Tug of war in the haematopoietic stem cell niche: Do myeloma plasma cells compete for the HSC niche? *Blood Cancer J.* **2**, e91.

Oatley, J. M. and Brinster, R. L. (2012). The Germline Stem Cell Niche Unit in Mammalian Testes. *Physiol. Rev.* **92**, 577–595.

Oatley, J. M., Avarbock, M. R., Telaranta, A. I., Fearon, D. T. and Brinster, R. L. (2006). Identifying genes important for spermatogonial stem cell self-renewal and survival. *Proc. Natl. Acad. Sci.* **103**, 9524–9529.

Oatley, J. M., Oatley, M. J., Avarbock, M. R., Tobias, J. W. and Brinster, R. L. (2009). Colony stimulating factor 1 is an extrinsic stimulator of mouse spermatogonial stem cell self-renewal. *Development* **136**, 1191–1199.

Ohlstein, B., Kai, T., Decotto, E. and Spradling, A. (2004). The stem cell niche: Theme and variations. *Curr. Opin. Cell Biol.* **16**, 693–699.

Okegbe, T. C. and DiNardo, S. (2011). The endoderm specifies the mesodermal niche for the germline in Drosophila via Delta-Notch signaling. *Development* **138**, 1259–1267.

Patel, T., Tursun, B., Rahe, D. P. and Hobert, O. (2012). Removal of Polycomb Repressive Complex 2 Makes C. elegans Germ Cells Susceptible to Direct Conversion into Specific Somatic Cell Types. *Cell Rep.* **2**, 1178–1186.

Prasad, M. and Montell, D. J. (2007). Cellular and Molecular Mechanisms of Border Cell Migration Analyzed Using Time-Lapse Live-Cell Imaging. *Dev. Cell* **12**, 997–1005.

Prasad, M., Jang, A. C. C., Starz-Gaiano, M., Melani, M. and Montell, D. J. (2007). A protocol for culturing drosophila melanogaster stage 9 egg chambers for live imaging. *Nat. Protoc.* **2**, 2467–2473.

Resende, L. P. F., Boyle, M., Tran, D., Fellner, T. and Jones, D. L. (2013). Headcase Promotes Cell Survival and Niche Maintenance in the Drosophila Testis. *PLoS One* **8**,.

Rhiner, C., Diaz, B., Portela, M., Poyatos, J. F., Fernandez-Ruiz, I., Lopez-Gay, J. M., Gerlitz, O. and Moreno, E. (2009). Persistent competition among stem cells and their daughters in the Drosophila ovary germline niche. *Development* **136**, 995–1006.

Riparbelli, M. G. and Callaini, G. (2011). Male gametogenesis without centrioles. *Dev. Biol.* **349**, 427–439.

Rotgers, E., Rivero-Müller, A., Nurmio, M., Parvinen, M., Guillou, F., Huhtaniemi, I., Kotaja, N., Bourguiba-Hachemi, S. and Toppari, J. (2014). Retinoblastoma

protein (RB) interacts with E2F3 to control terminal differentiation of Sertoli cells. *Cell Death Dis.* **5**, e1274.

Russell, L. D. (1978). The blood-testis barrier and its formation relative to spermatocyte maturation in the adult rat: a lanthanum tracer study. *Anat. Rec.* **190**, 99–111.

Ryu, B.-Y., Orwig, K. E., Oatley, J. M., Avarbock, M. R. and Brinster, R. L. (2006). Effects of Aging and Niche Microenvironment on Spermatogonial Stem Cell Self-Renewal. *Stem Cells* **24**, 1505–1511.

Sahai-Hernandez, P., Castanieto, A. and Nystul, T. G. (2012). Drosophila models of epithelial stem cells and their niches. *Wiley Interdiscip. Rev. Dev. Biol.* **1**, 447–457.

Salzmann, V., Inaba, M., Cheng, J. and Yamashita, Y. M. (2013). Lineage tracing quantification reveals symmetric stem cell division in drosophila male germline stem cells. *Cell. Mol. Bioeng.* **6**, 441–448.

Sánchez Alvarado, A. and Yamanaka, S. (2014). Rethinking differentiation: Stem cells, regeneration, and plasticity. *Cell* **157**, 110–119.

Sano, H., Renault, A. D. and Lehmann, R. (2005). Control of lateral migration and germ cell elimination by the Drosophila melanogaster lipid phosphate phosphatases Wunen and Wunen 2. *J. Cell Biol.* **171**, 675–683.

Sanson, B., White, P. and Vincent, J. P. (1996). Uncoupling cadherin-based adhesion from Wingless signalling in Drosophila. *Nature* **383**, 627–630.

Sarkar, A., Parikh, N., Hearn, S. A., Fuller, M. T., Tazuke, S. I. and Schulz, C. (2007). Antagonistic Roles of Rac and Rho in Organizing the Germ Cell Microenvironment. *Curr. Biol.* **17**, 1253–1258.

Schindelin, J., Arganda-Carreras, I., Frise, E., Kaynig, V., Longair, M., Pietzsch, T.,

Preibisch, S., Rueden, C., Saalfeld, S., Schmid, B., et al. (2012). Fiji: An open-source platform for biological-image analysis. *Nat. Methods* **9**, 676–682.

Schulz, C., Wood, C. G., Jones, D. L., Tazuke, S. I. and Fuller, M. T. (2002). Signaling from germ cells mediated by the rhomboid homolog stet organizes encapsulation by somatic support cells. *Development* **129**, 4523–4534.

Sheng, X. R. and Matunis, E. (2011). Live imaging of the Drosophila spermatogonial stem cell niche reveals novel mechanisms regulating germline stem cell output. *Development* **138**, 3367–76.

Sheng, X. R., Brawley, C. M. and Matunis, E. L. (2009). Dedifferentiating Spermatogonia Outcompete Somatic Stem Cells for Niche Occupancy in the Drosophila Testis. *Cell Stem Cell* **5**, 191–203.

Shilo, B. Z. (2014). The regulation and functions of MAPK pathways in Drosophila. *Methods* **68**, 151–159.

Shinohara, T., Avarbock, M. R. and Brinster, R. L. (1999). beta1- and alpha6-integrin are surface markers on mouse spermatogonial stem cells. *Proc. Natl. Acad. Sci.* **96**, 5504–5509.

Simon, L., Ekman, G. C., Tyagi, G., Hess, R. A., Murphy, K. M. and Cooke, P. S. (2007). Common and distinct factors regulate expression of mRNA for ETV5 and GDNF, Sertoli cell proteins essential for spermatogonial stem cell maintenance. *Exp. Cell Res.* **313**, 3090–3099.

Singh, S. R., Zheng, Z., Wang, H., Oh, S. W., Chen, X. and Hou, S. X. (2010). Competitiveness for the niche and mutual dependence of the germline and somatic stem cells in the Drosophila testis are regulated by the JAK/STAT signaling. *J. Cell.*

Physiol. **223**, 500–510.

Singh, S. R., Liu, Y., Zhao, J., Zeng, X. and Hou, S. X. (2016). The novel tumour suppressor Madm regulates stem cell competition in the Drosophila testis. *Nat. Commun.* **7**, 10473.

Slaidina, M. and Lehmann, R. (2014). Translational control in germline stem cell development. *J. Cell Biol.* **207**, 13–21.

Smith-Berdan, S., Nguyen, A., Hassanein, D., Zimmer, M., Ugarte, F., Ciriza, J., Li, D., García-Ojeda, M. E., Hinck, L. and Forsberg, E. C. (2011). Robo4 cooperates with Cxcr4 to specify hematopoietic stem cell localization to bone marrow niches. *Cell Stem Cell* **8**, 72–83.

Snippert, H. J., van der Flier, L. G., Sato, T., van Es, J. H., van den Born, M., Kroon-Veenboer, C., Barker, N., Klein, A. M., van Rheenen, J., Simons, B. D., et al. (2010). Intestinal crypt homeostasis results from neutral competition between symmetrically dividing Lgr5 stem cells. *Cell* **143**, 134–144.

Song, X. (2003). wingless signaling regulates the maintenance of ovarian somatic stem cells in Drosophila. *Development* **130**, 3259–3268.

Song, X. (2004). Bmp signals from niche cells directly repress transcription of a differentiation-promoting gene, bag of marbles, in germline stem cells in the Drosophila ovary. *Development* **131**, 1353–1364.

Song, X. and Xie, T. (2002). DE-cadherin-mediated cell adhesion is essential for maintaining somatic stem cells in the Drosophila ovary. *Proc. Natl. Acad. Sci. U. S. A.* **99**, 14813–8.

Song, X., Zhu, C. H., Doan, C. and Xie, T. (2002). Germline stem cells anchored by

adherens junctions in the Drosophila ovary niches. *Science (80-.).* **296**, 1855–1857.

Spradling, A., Fuller, M. T., Braun, R. E. and Yoshida, S. (2011). Germline stem cells. *Cold Spring Harb. Perspect. Biol.* **3**, a002642.

Stine, R. R. and Matunis, E. L. (2013). Stem cell competition: Finding balance in the niche. *Trends Cell Biol.* **23**, 357–364.

Stine, R. R., Greenspan, L. J., Ramachandran, K. V. and Matunis, E. L. (2014). Coordinate Regulation of Stem Cell Competition by Slit-Robo and JAK-STAT Signaling in the Drosophila Testis. *PLoS Genet.* **10**, e1004713.

Sutcliffe, J. E., Korenjak, M. and Brehm, A. (2003). Tumour suppressors - A fly's perspective. *Eur. J. Cancer* **39**, 1355–1362.

Suzuki, H., Sada, A., Yoshida, S. and Saga, Y. (2009). The heterogeneity of spermatogonia is revealed by their topology and expression of marker proteins including the germ cell-specific proteins Nanos2 and Nanos3. *Dev. Biol.* **336**, 222–231.

Tadokoro, Y., Yomogida, K., Ohta, H., Tohda, A. and Nishimune, Y. (2002). Homeostatic regulation of germinal stem cell proliferation by the GDNF/FSH pathway. *Mech. Dev.* **113**, 29–39.

Takatsu, K., Miyaoku, K., Roy, S. R., Murono, Y., Sago, T., Itagaki, H., Nakamura, M. and Tokumoto, T. (2013). Induction of female-to-male sex change in adult zebrafish by aromatase inhibitor treatment. *Sci. Rep.* **3**, 3400.

Tanaka-Matakatsu, M., Uemura, T., Oda, H., Takeichi, M. and Hayashi, S. (1996). Cadherin-mediated cell adhesion and cell motility in Drosophila trachea regulated by the transcription factor Escargot. *Development* **122**, 3697–3705.

Tanaka-Matakatsu, M., Xu, J., Cheng, L. and Du, W. (2009). Regulation of apoptosis of rbf mutant cells during Drosophila development. *Dev. Biol.* **326**, 347–356.

Tanaka, E. M. and Reddien, P. W. (2011). The Cellular Basis for Animal Regeneration. *Dev. Cell* **21**, 172–185.

Tanentzapf, G., Devenport, D., Godt, D. and Brown, N. H. (2007). Integrin-dependent anchoring of a stem-cell niche. *Nat. Cell Biol.* **9**, 1413–1418.

Teixeira, V. H., Nadarajan, P., Graham, T. A., Pipinikas, C. P., Brown, J. M., Falzon, M., Nye, E., Poulsom, R., Lawrence, D., Wright, N. A., et al. (2013). Stochastic homeostasis in human airway epithelium is achieved by neutral competition of basal cell progenitors. *Elife* **2013**,.

Thomas, D. M., Carty, S. A., Piscopo, D. M., Lee, J. S., Wang, W. F., Forrester, W. C. and Hinds, P. W. (2001). The retinoblastoma protein acts as a transcriptional coactivator required for osteogenic differentiation. *Mol. Cell* **8**, 303–316.

Thorel, F., Népote, V., Avril, I., Kohno, K., Desgraz, R., Chera, S. and Herrera, P. L. (2010). Conversion of adult pancreatic α-cells to B-cells after extreme B-cell loss. *Nature* **464**, 1149–1154.

Tran, J., Brenner, T. J. and DiNardo, S. (2000). Somatic control over the germline stem cell lineage during Drosophila spermatogenesis. *Nature* **407**, 754–757.

Tran, V., Lim, C., Xie, J. and Chen, X. (2012). Asymmetric division of Drosophila male germline stem cell shows asymmetric histone distribution. *Science (80-.).* **338**, 679–682.

Tulina, N. and Matunis, E. (2001). Control of stem cell self-renewal in Drosophila spermatogenesis by JAK-STAT signaling. *Science (80-.).* **294**, 2546–2549.

Tursun, B., Patel, T., Kratsios, P. and Hobert, O. (2011). Direct conversion of C. elegans germ cells into specific neuron types. *Science (80-.).* **331**, 304–308.

Uhlenhaut, N. H., Jakob, S., Anlag, K., Eisenberger, T., Sekido, R., Kress, J., Treier, A. C., Klugmann, C., Klasen, C., Holter, N. I., et al. (2009). Somatic Sex Reprogramming of Adult Ovaries to Testes by FOXL2 Ablation. *Cell* **139**, 1130–1142.

Vermeulen, L., Morrissey, E., Van Der Heijden, M., Nicholson, A. M., Sottoriva, A., Buczacki, S., Kemp, R., Tavaré, S. and Winton, D. J. (2013). Defining stem cell dynamics in models of intestinal tumor initiation. *Science (80-.).* **342**, 995–998.

Voog, J., D'Alterio, C. and Jones, D. L. (2008). Multipotent somatic stem cells contribute to the stem cell niche in the Drosophila testis. *Nature* **454**, 1132–1136.

Voog, J., Sandall, S. L., Hime, G. R., Resende, L. P. F., Loza-Coll, M., Aslanian, A., Yates, J. R., Hunter, T., Fuller, M. T. and Jones, D. L. (2014). Escargot Restricts Niche Cell to Stem Cell Conversion in the Drosophila Testis. *Cell Rep.* **7**, 722–734.

Wang, L., Li, Z. and Cai, Y. (2008). The JAK/STAT pathway positively regulates DPP signaling in the *Drosophila* germline stem cell niche. *J. Cell Biol.* **180**, 721–728.

Wasan, H. S., Park, H. S., Liu, K. C., Mandir, N. K., Winnett, A., Sasieni, P., Bodmer, W. F., Goodlad, R. A. and Wright, N. A. (1998). APC in the regulation of intestinal crypt fission. *J. Pathol.* **185**, 246–255.

Wee, P. and Wang, Z. (2017). Epidermal growth factor receptor cell proliferation signaling pathways. *Cancers (Basel).* **9**, E52.

Wing, J. P., Zhou, L., Schwartz, L. M. and Nambu, J. R. (1998). Distinct cell killing properties of the Drosophila reaper, head involution defective, and grim genes. *Cell*

Death Differ. **5**, 930–939.

Withers, H. R. and Elkind, M. M. (1970). Microcolony survival assay for cells of mouse intestinal mucosa exposed to radiation. *Int. J. Radiat. Biol.* **17**, 261–267.

Wright, N. A. and Al-Nafussi, A. (1982). The kinetics of villus cell populations in the mouse small intestine: II. Studies on growth control after death of proliferative cells induced by cytosine arabinoside, with special reference to negative feedback mechanisms. *Cell Prolif.* **15**, 611–621.

Wu, X., Oatley, J. M., Oatley, M. J., Kaucher, A. V., Avarbock, M. R. and Brinster, R. L. (2010). The POU Domain Transcription Factor POU3F1 Is an Important Intrinsic Regulator of GDNF-Induced Survival and Self-Renewal of Mouse Spermatogonial Stem Cells1. *Biol. Reprod.* **82**, 1103–1111.

Yacobi-Sharon, K., Namdar, Y. and Arama, E. (2013). Alternative germ cell death pathway in drosophila involves HtrA2/Omi, lysosomes, and a caspase-9 counterpart. *Dev. Cell* **25**, 29–42.

Yadlapalli, S. and Yamashita, Y. M. (2013). Chromosome-specific nonrandom sister chromatid segregation during stem-cell division. *Nature* **498**, 251–254.

Yamashita, Y. M. and Fuller, M. T. (2008). Asymmetric centrosome behavior and the mechanisms of stem cell division. *J. Cell Biol.* **180**, 261–266.

Yamashita, Y. M., Jones, D. L. and Fuller, M. T. (2003). Orientation of asymmetric stem cell division by the APC tumor suppressor and centrosome. *Science (80-.).* **301**, 1547–1550.

Yamashita, Y. M., Mahowald, A. P., Perlin, J. R. and Fuller, M. T. (2007). Asymmetric inheritance of mother versus daughter centrosome in stem cell division.

Science (80-.). **315**, 518–521.

Yan, D., Neumüller, R. A., Buckner, M., Ayers, K., Li, H., Hu, Y., Yang-Zhou, D., Pan, L., Wang, X., Kelley, C., et al. (2014). A regulatory network of Drosophila germline stem cell self-renewal. *Dev. Cell* **28**, 459–473.

Yoshida, S. (2012). Elucidating the identity and behavior of spermatogenic stem cells in the mouse testis. *Reproduction* **144**, 293–302.

Zhang, H., Zheng, W., Shen, Y., Adhikari, D., Ueno, H. and Liu, K. (2012). Experimental evidence showing that no mitotically active female germline progenitors exist in postnatal mouse ovaries. *Proc. Natl. Acad. Sci.* **109**, 12580–12585.

Zhang, Z., Lv, X., Jiang, J., Zhang, L. and Zhao, Y. (2013). Dual roles of Hh signaling in the regulation of somatic stem cell self-renewal and germline stem cell maintenance in Drosophila testis. *Cell Res.* **23**, 573–576.

Zhang, Q., Shalaby, N. A. and Buszczak, M. (2014). Changes in rRNA transcription influence proliferation and cell fate within a stem cell lineage. *Science (80-.)*. **343**, 298–301.

Zhou, Q., Brown, J., Kanarek, A., Rajagopal, J. and Melton, D. A. (2008). In vivo reprogramming of adult pancreatic exocrine cells to β-cells. *Nature* **455**, 627–632.

Zielke, N., Korzelius, J., VanStraaten, M., Bender, K., Schuhknecht, G. F. P., Dutta, D., Xiang, J. and Edgar, B. A. (2014). Fly-FUCCI: A Versatile Tool for Studying Cell Proliferation in Complex Tissues. *Cell Rep.* **7**, 588–598.

Zoller, R. and Schulz, C. (2012). The Drosophila cyst stem cell lineage. *Spermatogenesis* **2**, 145–157.

CURRICULUM VITAE

The Johns Hopkins University School of Medicine

Leah Joy Greenspan **June 28th, 2018**

Born: May 31st, 1986 in New York, USA

Educational History

Ph.D Expected	2018	Program in Biochemistry, Cellular and Molecular Biology Mentor: Erika Matunis, PhD	The Johns Hopkins University, School of Medicine, Baltimore, MD
B.S.	2008	Biological Sciences	Cornell University, Ithaca, NY

Professional Experience

Advances in Stem Cell Biology Course	2016 - 2016	Pasteur Institute, Paris, France
Practical Genomics: From Biology to Biostatistics Workshop	2015 - 2015	Carnegie Institution of Science, Baltimore, MD
IMARIS Training Workshop	2015 - 2015	John Hopkins University, School of Medicine, Baltimore, MD
Research Rotation	2013 -	Lab of Andrew Ewald, PhD, Johns Hopkins

	2013	University, Baltimore, MD
Research Rotation	2013 -	Lab of Geraldine Seydoux, PhD, Johns Hopkins
	2013	University, Baltimore, MD
Research Technician	2009 -	Lab of Jennifer Zallen, PhD, Memorial Sloan
	2012	Kettering Cancer Center, NY, NY
Undergraduate	2006 -	Lab of Andrew Clark, PhD, Cornell University,
Research Assistant	2008	Ithaca, NY

Scholarships and Fellowships

National Research	2016 -	Awarded by the National Institutes of Health, Institute
Service Award (NRSA)	2018	of Child Health and Human Development. Award #:
Predoctoral Fellowship		5F31HD85748-2. Includes stipend, graduate school dues, and health insurance.
Hay Fellowship	2015 -	Awarded by the Department of Cell Biology, Johns
	2016	Hopkins University, School of Medicine. Includes stipend, graduate school dues, and health insurance.

Academic and other honors

2018	David Yue Award	Young Investigator's Day Program, Johns Hopkins University, School of Medicine
2013	First Prize Poster	BCMB Retreat, Johns Hopkins University, School of Medicine

2008	*Magna Cum Laude*	Cornell University, College of Agriculture and Life Sciences
2008	Distinction in Research	Cornell University, College of Agriculture and Life Sciences Cornell

Publications

Greenspan LJ, and Matunis EL. (2018). Retinoblastoma Intrinsically Regulates Niche Cell Quiescence, Identity, and Niche Number in the Adult *Drosophila* Testis. Cell Rep., under revision.

Greenspan LJ and Matunis E. (2017). Live Imaging of the *Drosophila* Testis Stem Cell Niche. Methods Mol Biol. 1463:63-74.

Greenspan LJ, de Cuevas M, Matunis E. (2015). Genetics of Gonadal Stem Cell Renewal. Annu Rev Cell Dev Biol. 31: 291-315. PMCID: PMC4659427

Stine R, **Greenspan LJ**, Ramachandran K, and Matunis E. (2014). Coordinate regulation of stem cell competition by Slit-Robo and JAK-STAT signaling in the *Drosophila* testis. PLoS Genet. 10 (11): e1004713. PMCID: PMC4222695

Greenspan L and Clark AG. (2011). Associations between variation in X Chromosome male reproductive genes and sperm competitive ability in *Drosophila melanogaster*. Int J Evol Biol. 2011: 214280. PMCID: PMC3119407

Posters and Abstracts

Greenspan L, and Matunis E. Rbf intrinsically regulates niche cell quiescence, identity, and niche number in the adult *Drosophila* testis. Society for Developmental Biology Mid-Atlantic Regional Meeting, Baltimore, MD; Spring 2017.

Greenspan L, and Matunis E. Regulation of niche cell plasticity in the *Drosophila* testis. 57th Annual *Drosophila* Research Conference, Orlando, FL; Summer 2016.

Greenspan L and Matunis E. The tumor suppressor homolog Rbf maintains hub cell quiescence and identity, and prevents ectopic niche formation. **Platform presentation**, 56th Annual *Drosophila* Research Conference, Chicago, IL; March 2015.

Greenspan L, de Cuevas M, Hétié P, and Matunis E. Cellular and molecular regulation of stem cell niche quiescence. Society for Developmental Biology Mid-Atlantic Regional Meeting, Baltimore, MD; Spring 2014.

Greenspan L, Hétié P, and Matunis E. Cellular and molecular regulation of stem cell niche quiescence. 55th Annual *Drosophila* Research Conference, San Diego, CA; Spring 2014.

Greenspan L and Matunis E. Cellular and molecular regulation of stem cell niche quiescence. Oral Presentation. BCMB Retreat, Johns Hopkins University, School of Medicine, MD; Fall 2014.

Greenspan L, Hétié P, and Matunis E, Cellular and molecular signals maintaining niche cell quiescence. BCMB Retreat. Johns Hopkins University, School of Medicine, MD; Fall 2013.

Greenspan L and Zallen J. The Search for Molecular Mechanisms Involved in Axis Elongation. Developmental Biology Colloquium. Memorial Sloan Kettering Cancer Center, NY; June 2012.

Greenspan L and Clark A. Sperm competition in *Drosophila melanogaster* and its association with male reproductive genes on the X Chromosome. Honors Thesis Presentation. Cornell University, NY; May 2008.

Service and Leadership

2013 - 2018	Scientific mentor for two graduate rotation students, three Johns Hopkins undergrads, and two local Baltimore high school students.
2016 - 2018	EVOLVE co-founder and developer: developed an interactive online platform for pre-session content used to facilitate active classroom learning in the 1st year graduate genetics course
2017	Class session leader for Comparison Genetics in the 1st year graduate genetics course
2014, 2016	Course teaching assistant in the 1st year graduate genetics course
2014 - 2015	Tutorial teacher for the 1st year graduate genetics course

2013 - 2015 High school day of science organizer: organized three events for local Baltimore high school students to visit Johns Hopkins University, School of Medicine and participate in a day of scientific experiments.